**Division of Materials, Mechanics and Structures**

**Faculty of Engineering**

# THE USE OF SORBITOL-INITIATED POLYLACTIC ACID AS A COUPLING AGENT IN RESORBABLE PHOSPHATE GLASS FIBRE REINFORCED POLYLACTIC ACID COMPOSITES

## Madhavie S. Perera (MEng)

Thesis Submitted to the University of Nottingham for the degree of Doctor of Philosophy

**March 2015**

*To my grandmother, a woman who epitomized strength,*
*courage and integrity.*
*Leticia Ellen Gunasekera Perera, this is for you.*
*I miss you.*


*For showing me that success is not measured by scores and*
*accolades, but by dedication and hard work,*
*Mom and Dad, this is yours, too.*

# ABSTRACT

Resorbable phosphate glass fibre (PGF) reinforced polymer composites have been investigated for use as fracture fixation plates. While demonstrating impressive initial properties, these composites have shown poor retention of mechanical properties after immersion in a hydrolytic environment. Existing commercially available coupling agents for conventional glass composites have been of limited value and so novel coupling agents have been created specifically for PGF/ Poly (lactide) composites. Previous work on sorbitol-initiated poly (lactide) (S-PLA) oligomers has shown potential both in single fibre and full body composites. This thesis investigates chain length and concentration optimisation of S-PLA based coupling agents on the interfacial properties of PGF reinforced composites, both as manufactured and throughout degradation.

S-PLA was synthesised to three different chain lengths: S-PLA_s, S-PLA_m and S-PLA_l where s is short, m – medium and l – long. The oligomers were characterised via NMR, GPC, DSC and FTIR. $40P_2O_5$-$24MgO$-$16CaO$-$16Na_2O$-$4Fe_2O_3$ (P40) PGF fibres were produced and coated with S-PLA_s, S-PLA_m and S-PLA_l oligomers. It was found that the optimum coating concentration depended on the chain length of the oligomer. Initial tensile strength of the coated fibres increased compared to control though the increase was only significant for S-PLA_s coated fibres. A subsequent degradation study of the fibres in phosphate buffered saline (PBS) at 37 °C for 7 days showed that the tensile strength of the coated fibres decreased significantly compared to that of the control uncoated fibres. S-PLA_l coated fibres had better retention of the tensile strength than the medium and short chain coated fibres.

Initial IFSS of embedded S-PLA coated fibres increased significantly compared to that of control but did not differ significantly from each other. A

degradation study was conducted for single fibre composites with embedded control and coated fibres immersed in PBS at 37 °C for 7 days. Uncertainty in the true fibre strength during degradation made the IFSS of degraded single fibre composites inconclusive. Full-body composite studies were undertaken to investigate further.

Two different methods of application of S-PLA_s on to UD fibre mats were considered: dip coating and spray coating. Composite longitudinal and transverse flexural properties were assessed prior to and after degradation in PBS at 37 °C. The coupling agent improved initial flexural properties and was effective in retaining composite properties for up to 14 days. S-PLA spray coated UD composite samples was more effective in retaining interfacial properties.

Water uptake and wet mass change in longitudinal and transverse samples were stable up to 14 days after an initial increase seen at day 1. After day 14 a significant increase in water uptake and wet mass was observed for control composite samples compared to S-PLA coated samples. SEM micrographs and an increase in acidity observed at these time points show advanced fibre dissolution. XRD analysis for composite samples showed a crystallization peak at ~16.5° that did not increase in intensity throughout the degradation period indicating that the crystalline phase did not change during the study.

The chain length of S-PLA did not appear to affect the IFSS if the appropriate coating concentration was selected. S-PLA_s was selected due to ease of manufacture however the effect of the other chain lengths on macroscopic composite properties needs to be investigated. The method of coupling agent application onto fibre mats did not appear to make a difference in initial mechanical properties; however the spray coating method shows potential in retarding degradation. This requires further investigation.

# ACKNOWLEDGEMENTS

Much love and gratitude to the University of Nottingham Taekwondo Club, for the laughs, for the road trips and for the memories. Thank you for teaching me the value of perseverance and for helping me to unleash my potential.

To Simon and Adam I can't imagine anyone else I would have rather travelled the road of a postgraduate degree with. You are both true friends.

I would also like to take this opportunity to express my sincere gratitude and appreciation for the University of Nottingham. You have been my home for 8 years and I have treasured every bit of it. I am honoured to be among those who graduated from this university, twice. *Sapientia urbs conditur.*

Finally I would like to thank my family for supporting me and believing in me no matter what. Mom and Dad, you are my foundation and my strength. All that I am is because of you. Akki, you have more courage than anyone I know. I know that I can do anything I choose because of all you have achieved. My baby brother, thank you for reminding me every day that wishes and dreams can come true. I love you all.

"I have not failed. I've just found 10,000 ways that won't work."

*-Thomas A. Edison*

# ABBREVIATIONS

APS         3-aminopropyltriethoxy Silane

BS          British Standards

DC          Dip-Coating

DCM         Dichloromethane

DSC         Differential Scanning Calorimetry

FTIR        Fourier Transform Infrared Spectroscopy

GPC         Gel Permeation Chromatography

HA          Hydroxyapatite

IFSS        Interfacial Shear Stress

ISO         International Standards Organisation

$M_n$       Number Average Molecular Weight

$M_p$       Peak Molecular Weight

NMR         Nuclear Magnetic Resonance

P40         $40P_2O_5$-$24MgO$-$16CaO$-$16Na_2O$-$4Fe_2O_5$ in mol%

P45         $45\ P_2O_5$-$24MgO$-$16CaO$-$11Na_2O$-$4Fe_2O_5$ in mol%

PDI         Polydispersity Index

PBG         Phosphate Based Glass

PBS         Phosphate Buffered Saline

PCL         Poly-$\varepsilon$-caprolactone

PGA         Poly(glycolic) acid

PGF         Phosphate Glass Fibre

PDLLA       Poly(D,L-lactide)

PLA         Poly(lactide)

PLGA        Poly(lactide-co-glycolide)

PLLA        Poly(L-lactide)

| | |
|---|---|
| ROM | Rule of Mixtures |
| ROP | Ring Opening Polymerisation |
| S-PLA | Sorbitol initiated Poly(lactide) |
| S-PLA_l | Long chain Sorbitol initiated Poly(lactide) Oligomer |
| S-PLA_m | Medium chain Sorbitol initiated Poly(lactide) Oligomer |
| S-PLA_s | Short chain Sorbitol initiated Poly(lactide) Oligomer |
| SEM | Scanning Electron Microscopy |
| SFC | Single Fibre Composite |
| SFFT | Single Fibre Fragmentation Test |
| SFTT | Single Fibre Tensile Test |
| SP | Spray Coating |
| RM | Discontinuous Random Fibre Mat |
| THF | Tetrahydrofuran |
| $T_g$ | Glass Transition Temperature |
| UD | Unidirectional continuous fibre mat |
| $V_f$ % | Fibre Volume Fraction |
| XRD | X-ray Diffraction |

# NOMENCLATURE

| | |
|---|---|
| $d$ | Fibre diameter |
| $E_f$ | Fibre modulus |
| $E_m$ | Matrix modulus |
| $\varepsilon_f$ | Fibre strain |
| $\varepsilon_m$ | Matrix strain |
| $L_0$ | Gauge length |
| $L_c$ | Critical fragment length |
| $L_f$ | Average fragment length |
| $m$ | Weibull shape parameter |
| $m_i$ | Mass of sample before degradation |
| $m_d$ | Mass of sample after drying |
| $M_L$ | Mass loss |
| $m_t$ | Mass of sample at time, $t$ |
| $N$ | Number of fragments in gauge length |
| $\sigma$ | Tensile strength |
| $\sigma_0$ | Weibull scale parameter |
| $\sigma_f$ | Fibre fragment strength |
| $\tau_i$ | Interfacial shear stress |
| $W$ | Water uptake |
| $W_m$ | Wet mass change |

# TABLE OF CONTENTS

# LIST OF FIGURES

# LIST OF TABLES

# CHAPTER 1

# INTRODUCTION AND OVERVIEW

## 1.1 OVERVIEW

Bone is a natural composite material that is made of an organic phase (collagen fibres), an inorganic mineral phase (hydroxyapatite crystals (calcium phosphate)) and water [1-3]. There are two main types of bone: cortical and cancellous [1-2, 4]. Cortical and cancellous bones have the same basic structure but cancellous bone is more porous and less dense (*see* Figure 1.1) [1-2, 4-5]. The mechanical properties of cortical and cancellous bones vary due factors such as the structure, the direction of loading, test conditions, location of bone in the skeletal system, age, sex and health (*see* Table 1.1) [6-8].
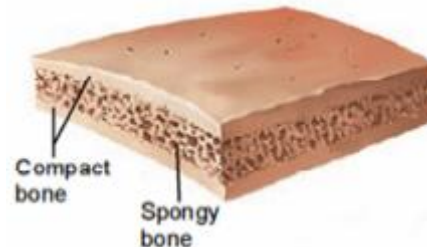


**Figure 1.1:** *The structure of flat bones in the human body with spongy cancellous bone lined on either side by a layer of cortical bone [4]*

**Table 1.1:** *Mechanical properties of human cortical and cancellous bone [5, 9-13]*

| Bone | Properties | | | | | |
|---|---|---|---|---|---|---|
| | Tensile | | Bending | | Shear | |
| | *Strength (MPa)* | *Modulus (GPa)* | *Strength (MPa)* | *Modulus (GPa)* | *Strength (MPa)* | *Modulus (GPa)* |
| **Cortical (longitudinal)** | 67-140 | 3-22 | 35-280 | 5-23 | 50-75 | 3.1-3.7 |
| **Cancellous** | 7-20 | 0.4 | 1-9 | 0.05-0.34 | - | - |

Wolff described bone as a dynamic material that adapts to the load applied [14]. When a bone fractures, fixation is required to stabilise the bone as

it heals. Fracture fixation can be internal or external depending on the severity of the injury. Metallic rigid fixation wires, pins, plates and screws have been used as internal fixation devices [15]. Unfortunately metallic implants induce a stress shielding effect due to the mismatch of mechanical properties between the implant and the bone. Stainless steel, for example, has strength and modulus values of 586 MPa and ~190 GPa [15]. The bone does not take the stress from the implant during healing and as a result has less density. It is, therefore, likely to refracture as the implant is removed after the bone has healed [15-17].

In order to diminish the stress shielding effect and eliminate the need for secondary surgery, materials such as resorbable phosphate glass fibre (PGF) reinforced polymer composites have been investigated [18]. Bioresorbable polymers such as poly (lactide) (PLA) and poly-ε-caprolactone (PCL) take between 24-72 months for complete resorption [19-20]. PGFs are fully resorbable, have high mechanical properties and are biocompatible [21-23]. In addition, the glass fibre formulation can be tailored to produce the desired mechanical properties and degradation profile [18].

Reinforcing PLA and PCL with PGF significantly improves the mechanical properties when compared to unreinforced bioresorbable polymers [18, 24-27]. The main challenge surrounding these composites is the inability to retain the mechanical properties for longer than a few days/weeks [26-27]. This lack of retention has been attributed to the loss of the interface between the fibre and matrix [26-28]. The need to improve the fibre-matrix interface has led to the development of novel coupling agents designed for use in a PLA matrix [29-30]. While all of the coupling agents increased the initial (i.e. prior to degradation) interfacial shear stress (IFSS) of PGF/PLA single fibre composites, sorbitol-

initiated PLA (S-PLA) had the largest increase (~23 MPa) [29]. The effect of the chain length of S-PLA on the IFSS however has not been investigated.

## 1.2 AIMS AND OBJECTIVES

The main aim of the work conducted in this thesis was to manufacture sorbitol initiated PLA (S-PLA) oligomers to three different chain lengths and investigate the consequent effect on the interfacial shear stress (IFSS) in phosphate glass fibre (PGF)/PLA composites. The objectives of this work are as follows:

- Synthesize S-PLA to three different chain lengths and characterise the oligomers using Gel Permeation Chromatography, Nuclear Magnetic Resonance, Differential Scanning Calorimetry and Fourier Transform Infrared Analysis

- Coat PGFs with S-PLA oligomers and prepare single fibre composites

- Assess the IFSS using an appropriate method and select a chain length to be used to coat fibre mats for full body composites

- Manufacture unidirectional fibre mats (UD) and investigate a method for coating UD fibres without losing fibre orientation

- Prepare fibre reinforced composites

- Investigate initial longitudinal and transverse flexural properties and retention of these properties.

- Investigate the degradation profile of control UD composites compared to coated UD composites after immersion in phosphate buffered saline (PBS) at 37°C.

This work is an extension of work done on novel coupling agents. To the author's knowledge there has not been an in depth study in the use of sorbitol initiated PLA as a coupling agent for PGF/PLA systems.

## 1.3 THESIS STRUCTURE

The layout of this thesis is as follows:

**Chapter 2** reviews the literature as it pertains to the need for resorbable fracture fixation devices to eliminate the stress shielding effect and removal surgery. Resorbable PGF reinforced composites are discussed in addition to the inability to retain mechanical properties during immersion in an aqueous environment due to loss of the fibre-matrix interface. The need for coupling agents for resorbable composites and the available methods to assess the fibre-matrix interface are also reviewed.

**Chapter 3** describes all the materials and methods used in this study including: manufacturing of glass fibres and composites; synthesis of oligomers; characterisation; fibre coating; mechanical testing; degradation study and statistical analysis.

**Chapter 4** looks at the synthesis and characterisation of S-PLA oligomers at three different chain lengths and the consequent IFSS study of embedded control and S-PLA coated fibres. The mechanical properties of $40P_2O_5$-$16CaO$-$16Na_2O$-$24MgO$-$4Fe_2O_3$ and $45P_2O_5$-$16CaO$-$11Na_2O$-$24MgO$-$4Fe_2O_3$ fibres are also investigated.

**Chapter 5** is an in depth analysis of control UD PGF/PLA composites and S-PLA coated UD PGF/PLA composites. Initial longitudinal and transverse flexural properties and the retention of these properties over time in phosphate buffer saline (PBS) at 37°C were investigated. The degradation profiles were also examined.

**Chapter 6** is a summary of the conclusions of this body of work and lists recommendations for future research with regards to the fibre-matrix interface of PGF/PLA composites

## 1.4 REFERENCES

1. J.A. McGeough, *Engineering of Human Joint Replacements*, John Wiley & Sons: Chichester, United Kingdom, 2013, pp. 14.

2. G.J. Tortora and B. Derrickson, *Introduction to the Human Body: The Essentials of Anatomy and Physiology*, John Wiley & Sons: United States of America, 2007.

3. R.B. Martin and D.L. Boardman, "The effects of collagen fibre orientation, porosity, density and mineralisation on bovine cortical bone bending properties", *Journal of Biomechanics*, vol. 26, no. 9, pp. 1047-1054, 1993.

4. P. Tate, *Seeley's Principles of Anatomy & Physiology*, Second edition: McGraw-Hill Science Engineering, New York, 2009, pp.129.

5. K.A. Athanasiou, C.F. Zhu, D.R. Lanctot, C.M. Agrawal, and X. Wang, "Fundamentals of Biomechanics in Tissue Engineering of Bone", *Tissue Engineering*, vol. 6, no. 4, pp. 361-381, 2000.

6. F.G. Evans, "Factors affecting the mechanical properties of bone", *Bulletin of the New York Academy of Medicine*, vol. 49, no.9, pp. 751-64, 1973.

7. Y. An and R. Draughn, *Mechanical Testing of Bone and the Bone-Implant Interface*, CRC Press: Boca Raton, Florida, 1999.

8. J. Black and G.W. Hastings, *Handbook of Biomaterials Properties*, London, U.K.: Chapman and Hall, 1998.

9. X.E. Guo, "Mechanical properties of cortical bone and cancellous bone tissue", In: S.C. Cowin, ed., *Bone Mechanics Handbook*, CRC Press: Boca Raton, Florida, 2001.

10. S.C. Cowin, ed., *Bone Mechanics*, CRC Press: Boca Raton, Florida, 1988.

11. J. C. Lotz, T.N. Gerhart and W.C. Hayes, "Mechanical properties of trabecular bone from the proximal femur: a quantitative CT study", *Journal of Computer Assisted Tomography*, vol. 14, no. 1, pp. 107-114, 1990.

12. D.T. Reilly and A.H. Burstein, "Review article: The mechanical properties of cortical bone", *Journal of Bone and Joint Surgery America*, vol. 56, no. 5, pp. 1001-1022, 1974.

13. Rho, J.-Y., L. Kuhn-Spearing, and P. Zioupos, "Mechanical properties and the hierarchical structure of bone", *Medical Engineering & Physics*, vol. 20, no. 2, pp. 92-102, 1998.

14. H.M. Frost, "Wolff's Law and bone's structural adaptations to mechanical usage: an overview for clinicians", *The Angle Orthodontist*, vol. 64, no. 3, pp. 175-188, 1994.

15. S. Ramakrishna, J. Mayer, E. Wintermantel and K.W. Leong, "Biomedical applications of polymer-composite materials: a review," *Composites Science and Technology*, vol. 61, no. 9, pp. 1189-1224, 2001.

16. A.J. Tonino, C.L. Davidson, P.J. Klopper and L.A. Linclau, "Protection from stress in bone and its effect", *Journal of Bone and Joint Surgery*, vol. 58-B, no. 1, pp. 107-113, 1976.

17. P. Christel, L. Claes, S.A. Brown, "Carbon reinforced composites in orthopaedic surgery", In : M. Szycher, ed., *High Performance Biomaterials: A Comprehensive Guide to Medical and Pharmaceutical Applications*, Lancaster, USA: Technomic, 1991, pp. 499-518.

18. A.J. Parsons, I. Ahmed, P. Haque, B. Fitzpatrick, M.I.K. Niazi, G.S. Walker and C.D. Rudd, "Phosphate glass fibre composites for bone repair", *Journal of Bionic Engineering*, vol. 6, no. 4, pp. 318-323, 2009.

19. J.C. Middleton and A.J. Tipton, "Synthetic biodegradable polymers as orthopaedic devices", *Biomaterials*, vol. 21, no. 23, pp. 2335-2346, 2000.

20. W.S. Pietrzak, D.R. Sarver and M.L. Verstynen, "Bioresorbable polymer science for the practicing surgeon", *Journal of Craniofacial Surgery*, vol. 8, no. 2, pp. 87-91, 1997.

21. E.A. Abou Neel, D.M. Pickup, S.P. Valappil, R.J. Newport and J.C. Knowles, "Bioactive functional materials: a perspective on phosphate-based glasses", *Journal of Materials Chemistry*, vol. 19, no. 6, pp. 690-701, 2009.

22. I. Ahmed, C.A. Collins, M.P. Lewis, I. Olsen and J.C. Knowles, "Processing, characterisation and biocompatibility of iron-phosphate glass fibres for tissue engineering", *Biomaterials*, vol. 25, no. 16, pp. 3223-3232, 2004.

23. N. Sharmin, A.J. Parsons, C.D. Rudd and I. Ahmed, "Effect of boron oxide addition on fibre drawing, mechanical properties and dissolution behavior of phosphate-based glass fibres with fixed 40, 45 and 50 mol% $P_2O_5$", *Journal of Biomaterial Applications*, vol. 0, no. 0, pp. 1-15, 2014.

24. S. Cozien-Cazuc, "Characterisation of resorbable phosphate glass fibres", University of Nottingham, 2006.

25. R.A. Khan, "Phosphate glass fibres and their interfaces in resorbable composites", University of Nottingham, 2006.

26. R.M. Felfel, I. Ahmed, A.J. Parsons, P. Haque, G.S. Walker, and C.D. Rudd, "Investigation of Crystallinity, Molecular Weight Change, and Mechanical Properties of PLA/PBG Bioresorbable Composites as Bone Fracture Fixation Plates", *Journal of Biomaterials Applications*, vol. 25, no. 7, pp. 765-789, 2012.

27. I. Ahmed, I.A. Jones, A.J. Parsons, J. Bernard, J. Farmer, C.A. Scotchford, G.S. Walker, and C.D. Rudd, "Composites for bone repair: phosphate glass fibre

reinforced PLA with varying fibre architecture", *Journal of materials science. Materials in medicine*, vol. 22, no. 8, pp. 1825-1834, 2011.

28. I. Ahmed, P.S. Cronin, E. Abou Neel, A. J. Parsons, J.C. Knowles, and C.D. Rudd, "Retention of mechanical properties and cytocompatibility of a phosphate-based glass fibre/polylactic acid composite", *Journal of biomedical materials research. Part B, Applied biomaterials*, vol. 89, no. 1, pp. 18-27, 2009.

29. P. Haque, I.A. Barker, A.J. Parsons, K.J. Thurecht, I. Ahmed, G.S. Walker, C.D. Rudd and D.J. Irvine, "Influence of compatibilizing agent molecular structure on the mechanical properties of phosphate glass fiber-reinforced PLA composites", *Journal of Polymer Science Part A: Polymer Chemistry*, vol. 48, no. 14, pp. 3082-3094, 2010.

30. P. Haque, A.J. Parsons, I.A. Barker, I. Ahmed, D.J. Irvine, G.S. Walker, and C.D. Rudd, "Interfacial properties of phosphate glass fibres/PLA composites: Effect of the end functionalities of oligomeric PLA coupling agents", *Composites Science and Technology*, vol. 70, pp. 1854-1860, 2010.

# CHAPTER 2

# LITERATURE REVIEW

## 2.1 INTRODUCTION

A biomaterial is a material that is intended for use in contact with a biological system to direct, supplement or to replace the functions of living tissues [1-3]. For centuries people have been replacing body parts such as eyes, teeth and limbs, and using materials such as linen, gold and cat gut for sutures [1, 4]. It was only about 60 years ago that synthetic materials were looked at for use in biomedical applications such as sutures, heart valves, vascular grafts, bone plates, joint replacements, dental implants, etc. [1, 4-11]. The development of these 'biomaterials' also involved ensuring that, once inserted in the body, they did not elicit an adverse reaction or inflammatory response, i.e. that they were biocompatible [4]. The biocompatibility of a material is important when selecting for specific biomedical applications and can be defined as "the ability of a material to perform with an appropriate host response in a specific application" [2, 12].

The biocompatibility of biomaterials can be explained further by distinguishing between the surface and the structural compatibility of an implant [13-14]. The surface compatibility of a biomaterial is its surface's chemical, biological and physical suitability to host tissues while the structural compatibility is the optimal adaptation to the mechanical behaviour of the host tissues [15]. The structural compatibility refers to an implant's mechanical properties (such as the elastic modulus and strength), implant design and the ideal load transmission at the implant-tissue interface. When the surface and structural compatibilities are combined together, the interaction between the

implant and the host will be optimised [15]. There are several factors listed by

Ramakrishna *et al.* that must be considered when selecting a material for use in a

biomedical application and these are replicated in Table 2.1.

*Table 2.1:* *Various factors of importance in material selection for biomedical applications [15]*

| Factors | Description | | |
|---|---|---|---|
| 1st Level material properties | Chemical/biological characteristics Chemical composition (bulk and surface) | Physical Characteristics Density | Mechanical/structural characteristics Elastic Modulus Poisson's Ratio Yield Strength Tensile Strength Compressive Strength |
| 2nd Level material properties | Adhesion | Surface topology (texture and roughness) | Hardness Shear Modulus Shear Strength Flexural Modulus Flexural Strength |
| Specific functional requirements (based on application) | Biofunctionality (non-thrombogenic, cell adhesion, etc) Bioinert (non-toxic, non-irritant, non-allergic, non-carcenogenic, etc) Bioactive Biostability (resistant to corrosion, hydrolysis, oxidation, etc.) Biogradation | Form (solid, porous, coating, film, fibre, mesh, powder) Geometry Coefficient of thermal expansion Electrical conductivity Colour, aesthetics Refractive index Opacity or translucency | Stiffness or rigidity Fracture Toughness Fatigue Strength Creep Resistance Friction and wear resistance Adhesion strength Impact Strength Proof Stress Abrasion resistance |
| Processing and Fabrication | Reproducibility, quality, sterilisability, packaging, secondary processability | | |
| Characteristics of host | Tissue, organ, species, age, sex, race, health condition, activity, systemic response | | |
| Medical/surgical procedure, period of application/usage | | | |
| Cost | | | |

Hench and Thompson grouped biomaterials into first, second and third generation biomaterials [16]. First generation biomaterials were developed in the 1960s and 1970s specifically for use inside the human body [16-17]. A common feature of these materials was biological 'inertness' and almost all of the materials used in the body were single phase materials. The aim of these materials was to "achieve a suitable combination of physical properties to match those of the replaced tissue with a minimal toxic response in the host". It was noted that this design principle is still valid today [16-17].

It was in the 1980s, when Professor Bonfield and his group identified the need for development of biomaterials which were bioactive, that the second generation of biomaterials were formed. The term 'bioactive' refers to materials that cause a controlled action and reaction in a physiological environment [16]. There were two categories of second generation biomaterials. The first was the development of two phase biocomposites materials that matched mechanical properties to the host tissue [18] and the second that developed these biocomposite materials to be broken down and resorbed into the body [16, 19].

There is a growing interest in third generation biomaterials that are being designed with the emphasis on a biological based method of repair, i.e. tissue regeneration [16]. These materials promote or inhibit certain cell activities as desired in addition to being bioresorbable [16, 20]. Phosphate based glasses (PBGs) have been shown to fit the criteria of third generation biomaterials. Studies showed that they are both bioresorbable and bioactive, and can be tailored to yield the desired properties for tissue engineering applications [21-24]. PBGs have properties that allow them to be used as hard tissue substitutes or as substrates for synthetic orthopaedic graft materials [21]. Additionally, PBGs have a similar composition to that of bone and can be doped

with metal oxides that can modify their physical properties such as dissolution rate [25]. Fujita *et al.* showed that the leaching of calcium ($Ca^{2+}$) ions from phosphate glasses promotes osteoblast-like cell proliferation and differentiation, whereas phosphate ions triggered the release of Cbfa-1 (an important bone marker) from bone cells [25].

PBGs can also be made into fibres to reinforce bioresorbable polymers such as Poly (lactic acid) (PLA) and Poly-ε-caprolactone (PCL) for use in internal fracture fixation devices or bone plates [8, 26-30]. This literature review will look at the development of materials for use in bone plates from metals to bioresorbable composites, including the development of resorbable phosphate glasses and fibres. A key factor in fibre reinforced composites is maintaining the interface between the fibre and the matrix [31]. Maintaining the interface will improve the ability of phosphate glass fibre (PGF) reinforced composites to retain mechanical properties for a longer period of time when immersed in an aqueous environment [8, 27, 32-33]. Preliminary improvements have been seen with novel coupling agents developed for PGF/PLA composites [33-35]. The single fibre fragmentation test (SFFT) was used to assess the interface in these studies. The SFFT and other methods used to assess the interfacial shear stress (IFSS) are also reviewed in this chapter.

## 2.2 METALS

Metals and metallic alloys such as stainless steel, cobalt-chromium, titanium and its alloys have been used for bone fracture fixation devices such as wires, pins, screws, plates and nails [36-38]. These rigid fixation devices provide good stability of the fracture, facilitate primary bone healing (without the formation of an external callous) and allow exercise of joints near fracture after operation

[15, 39]. There, however, are several drawbacks with the use of metallic implants [15].

The plate may be removed after the bone has healed (1-2 years post operation) and, when removed, bone atrophy can be found underneath [15]. Bone atrophy is the wasting of bone as a result of a loss of function [40]. This occurs as a result of the stress shielding effect that occurs due to the mismatch in elastic moduli between metals and bone [15]. According to Wolff's Law, bone remodels and adapts itself to the applied mechanical environment [41]. The difference in stiffness causes a majority of the stress to be transmitted by the plate. Therefore the bone under the plate experiences less stress particularly after the fracture has healed [42]. The bone adapts to this condition of low stress, becoming less dense, weak and low in strength. The removal of the plate can, consequently, cause the bone to refracture [43]. Table 2.2 shows a summary of mechanical properties for various metal alloys in comparison to bone.

Other complications with metallic implants include: corrosion of the implant over time and ion release may lead to allergic tissue reactions; lack of bioactivity; high density that results in elevated stresses on surrounding tissues; difficulty of examination with imaging techniques such as magnetic resonance imaging (MRI) and x-rays [36].

**Table 2.2:** *Mechanical properties of metallic biomaterials and cortical bone [1,12, 15, 44-48]*

| Material | Modulus (GPa) | Tensile strength (MPa) |
|---|---|---|
| Stainless Steel | 190-200 | 465-950 |
| Co-Cr Alloy | 210-240 | 655-1896 |
| Ti Alloy | 55-116 | 596-1100 |
| Cortical Bone | 3-22 | 67-140 |

**2.3 BIOPOLYMERS**

Polymers have been used as biomaterials for various biomedical applications due to their low cost, wide range of mechanical and physical properties and ease of manufacture into films, textiles, rods, fibres and gels [37, 49]. Polyethylene (PE), poly (methyl methacrylate) (PMMA), and polyetheretherketone (PEEK) are examples of biocompatible polymers that have been used in implants such as total hip replacements and dental implants [15]. Others such as polyacetal (PA), polytetrafluoroethylene (PTFE) and certain polyesters have been investigated for use as fracture fixation plates [15]. However, it was found that these polymers had insufficient stiffness and fatigue strength needed to withstand cyclic loads experienced at fracture sites [15]. Even if the mechanical properties could be matched, these bioinert polymers would also require removal after the fracture healed [10].

A fracture fixation plate with an elastic modulus closer to that of bone will reduce the stress shielding effect between the implant and the host tissue, i.e. the stress on the plate should decrease as the stress on the bone increases during healing [15]. Bioresorbable polymers have been studied to investigate the potential to achieve this.

**2.3.1 Bioresorbable Polymers**

Biodegradable polymers such as poly (lactic acid) (PLA), poly-ε-caprolactone (PCL), poly (glycolic acid) (PGA) and poly (lactic-co-glycolic acid) (PLGA) that would degrade in a physiological environment into products that can be absorbed into/ excreted from the body via natural pathways have been investigated [9-10, 50-51]. These polyesters have been used as plates, screws, sutures, dental implants and soft tissue applications [10, 52-54]. The ability to

degrade over time allows for the applied stress to be transferred to bone as it heals; diminishing stress shielding and bone atrophy seen in metal implants. It also eliminates the need for secondary surgery to remove the plate after healing is complete [10]. The easier, more cost-effective fabrication, the lack of need for removal surgery and the consequent reduced stay in hospitals when bioresorbable implants are used has been shown to decrease the cost of repairing fractures compared to the use of metallic implants [54-55].

The chemical composition of the bioresorbable polymer affects the end mechanical properties. PLA is synthesised from the cyclic dimer of lactic acid which exists as two isomers, D-lactide and L-lactide [52]. Changing the proportions of D-lactide to L-lactide can affect the mechanical properties and the resorption times of the synthesised polymer [9, 52, 56-57]. The same is true for copolymer blends like PLGA, i.e. the ratio of lactide to glycolide [9-10]. The mechanical properties of PLLA, PCL, PGA and PLGA, shown in Table 2.3, are less than that of cortical bone (Table 2.2) therefore they can be used in a limited number of applications [47]. The strength of cancellous bone, on the other hand, is an order of magnitude less than the strength of cortical bone and studies have been carried out on the use of poly (L-lactide) (PLLA) plates and screws for fixation of fractured maxillofacial and zygomatic bones [58-61]. Clinical studies have shown swelling at the site of implantation three years post operation and that the degradation rate of the PLLA bone plates was very low (after almost 6 years of implantation the degraded material had not been resorbed) [59-60].

The degradation time of a bioresorbable polymer (Table 2.3) affects the length of time an implant will maintain its mechanical strength. It is therefore necessary to understand the degradation mechanisms of these polymers in

addition to increasing the mechanical properties for use in fractures of cortical

bones.

**Table 2.3:** *Mechanical and thermal properties of bioresorbable polymers for orthopaedic applications. * Tensile or flexural modulus, ** the degradation time given is the time for complete resorption [12, 51-52, 56-57, 62-68].*

| Polymer | Tensile Strength (MPa) | Elastic Modulus* (GPa) | Melting Temperature, $T_m$ (°C) | Glass Transition Temperature, $T_g$ (°C) | Degradation Time** (months) |
|---------|------------------------|------------------------|---------------------------------|------------------------------------------|-----------------------------|
| PGA | 60-80 | 5-7 | 228 | 35-40 | 6-12 |
| PLLA | 80 | 3-6 | 173-178 | 60-65 | 24-72 |
| PCL | 20-40 | 0.4-0.6 | 58-63 | -60 | 24-48 |
| PLGA | 40-55 | 1-3 | Amorphous | 45-55 | 1-12 |

### 2.3.2 Degradation Mechanism for Bioresorbable Polymers

Bioresorbable polymers in an aqueous solution degrade via the hydrolysis (or

cleavage) of ester bonds in the polymer chain (Figure 2.1) [9-10, 52, 56-57, 69-

71]. This process is controlled by four parameters: the rate constant, the amount

of absorbed water, the diffusion coefficient of polymer chain fragments and the

solubility of degraded products [72]. Polyhydroxyacids like PLA and PGA

degrade to monomeric acids and then to carbon dioxide and water [57]. The

degradation profile for bioresorbable polymers typically occurs in two stages.

The first stage starts immediately after implantation when water molecules

attack the chemical bonds in the amorphous phase, converting the long chains

into shorter chains (oligomers) that are water soluble. As a result the molecular

weight of the polymer decreases, the absorbed water begins to fragment the

implant that leads to a decrease in mechanical properties (Figure 2.2). The

second stage is the enzymatic attack of the oligomer chains. The metabolised

fragments lead to a rapid loss in mass as shown in Figure 2.2 [9-10, 51, 73].

Fischer *et al.* saw the hydrolytic degradation of semi-crystalline PLLA in these

two stages. Further, the degree of crystallinity was found to increase over time [74].
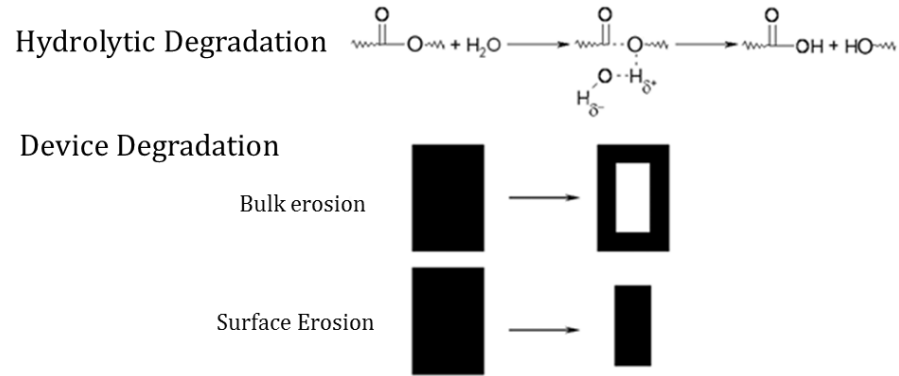


**Figure 2.1:** *Schematics of the hydrolysis mechanism of polyester and of the bulk and surface erosion of degradable polymeric devices [9].*
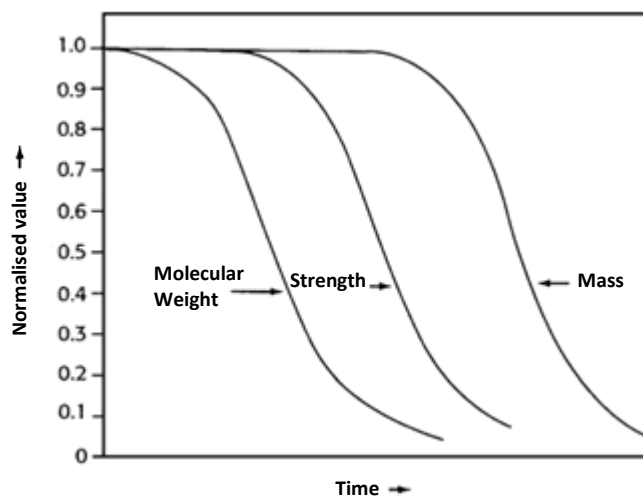


**Figure 2.2:** *Curves showing the sequence of reduction in molecular weight, strength and mass reduction over time during hydrolytic degradation [75].*

Figure 2.1 also shows the two main mechanisms for device degradation: 1) surface erosion and 2) bulk erosion. The erosion mechanisms are summarised in Table 2.4 [76-77]. It should be noted that all degradable polymers can erode via both methods when the conditions or implant geometry are selected correctly [46, 69-70, 77]. Hydrolytic degradation of bulk amorphous poly (D,L-lactic acid) (PDLA) devices were shown to be faster at the interior than the

surface due to the contribution of autocatalysis. The degradation caused an increase in the number of carboxylic acid chain ends as a result of ester cleavage and soluble oligomers close to the surface were leached out. The oligomers at the interior core of the polymer sample were trapped leading to an increase in acidity that led to an increase in degradation rate at the centre of the polymer compared to the degradation at the surface [70, 78]. This results in a high molecular weight distribution at the surface and a low distribution at the core that leads to a hollow structure [66, 79].

**Table 2.4:** *Differences between surface erosion and bulk erosion mechanisms in bioresorbable polymers [75-77].*

| Surface Erosion | Bulk Erosion |
|---|---|
| Heterogeneous | Homogeneous |
| Polymer degrades faster than water intrusion into bulk polymer | Water uptake is faster than polymer degradation |
| Degradation mainly in outermost layers | Entire system rapidly hydrated and polymer chains are cleaved |

The degradation of bioresorbable polymers is dependent on a number of factors: physical structure, polydispersity, chain orientation, crystallinity, applied load, and mass of the implant, to name a few [57, 80]. The degradation rate can be decreased by increasing molecular weight, degree of chain orientation, crystallinity and mass of the implant. Conversely, the degradation will be increased by stresses, high vascularisation of implant sites (i.e. more fluid exchange), porosity and exposed surface area [63, 70, 81-84]. Athanasiou *et al.* showed that poly (D,L-lactide-co-glycolide) implants with low porosity (0%) degrade faster than those with high porosity (75%) and suggested this was due to autocatalysis in the implants. Degraded acidic by-products were unable to leach out from the implants [81]. The effect of chain orientation on the degradation rate of PLLA fibres was investigated by Tsuji *et al.* [85]. It was found

that the mass loss of as-spun fibres increased by 50% compared that of drawn fibre with a draw ratio of ~1.4.

## 2.4 SELF-REINFORCED POLYMERS

Bioresorbable polymers can be reinforced in order to increase their mechanical properties. One way of doing this is 'self-reinforcing', i.e. a bioresorbable polymer matrix is reinforced with reinforcing fibrous elements of the same chemical composition as the matrix [55, 86]. These elements can be micro/macro fibrils, fibres, extended chain crystals, etc. [49]. Several studies have been conducted on self-reinforced (SR) PGA, SR-PLLA, SR-PDLLA and SR-PLGA composites [86-92]. A SR structure can be obtained using a solid state deformation method, sintering, hot compaction, compression moulding or injection moulding [55, 91, 93-94].

The advantages of SR polymer composites include ease of manufacturing, low cost, light weight and increased mechanical properties compared to unreinforced polymers [86, 95]. The chemical similarities between the matrix and the reinforcing elements meant that there is no need for adhesion promoters [87]. The mechanical properties of SR composites appear to be dependent on factors such as manufacturing method, molecular weight and draw ratio [55, 86].

Tormala *et al.* showed that sintering produced ultra-high-strength SR PGA composite rods with initial bending strengths and moduli ranging from 220-405 MPa and 8-15 GPa, respectively, for rods of diameter 1.5-4.5 mm [87]. *In vivo* tests of these rods showed that the smaller diameter rods lost ~50% of their bending properties within 2 weeks. The bending properties of larger diameter rods, on the other hand, decreased by ~50% after 3 weeks *in vivo*;

however the degradation rate decreased during the following weeks. Clinical trials of SR-PLLA and SR-PDLLA composites have shown positive results in the use of these materials for fracture fixation plates for maxillofacial fractures [86, 89]. However the mechanical properties of SR bioresorbable composites were still found to be too low for long bone applications [86-87].

Inflammation due to a collection of degraded products and limited ability to bond with bone and initiate new bone growth remain as disadvantages for SR polymers [96]. Seeding SR polymers with bioactive fillers was found to have an adverse effect on the mechanical properties during degradation. Poor matrix-filler adhesion and formation of a porous structure led to destabilisation of the composite [97-99]. Charles *et al.* coated PLLA fibres with hydroxyapatite (HA) and used these fibres to reinforce PLLA [90]. (HA is a synthetic calcium phosphate material that helps to promote bone adhesion [100]). The flexural modulus of SR-PLLA composites increased significantly to ~10 GPa, which is near the low range of the modulus for cortical bone. It was suggested that, as a result, SR-PLLA with HA coated fibres had the potential for long bone applications. However, no *in vitro* or *in vivo* studies have been conducted to show the retention of mechanical properties.

## 2.5 PHOSPHATE BASED GLASS

Phosphate based glasses (PBGs) have been used in many industrial applications including water treatment, pigment manufacturing and solid state lasers [101]. More recently, PBGs have been studied for use in biomedical applications, such as tissue engineering and as reinforcement in bioresorbable polymers for bone fracture fixation devices [22, 102-103]. PBGs have several advantages that make them a potential material for biomedical applications:

- they are totally soluble in an aqueous environment

- the dissolution rates can be controlled and predicted by altering the glass composition [104-105]

- the chemical composition of PBGs are similar to that of the mineral phase of bone (calcium phosphate)

- they are biocompatible and bioactive

- they can be formed into fibres [106]

- they have good mechanical properties when formed into fibres [8]

### 2.5.1 Structure

Phosphorus pentoxide ($P_2O5$) is a glass network former that has a tetrahedral phosphate unit ($PO_4^{3-}$) as the main building block (*see* Figure 2.3) [107]. Each unit is described in terms of $Q^i$ terminology, where *i* represents the number of bridging oxygens (BOs) per $PO_4^{3-}$ tetrahedron (Figure 2.4) [107-109]. $PO_4^{3-}$ units are polymeric in nature and the addition of modifiers (e.g. metal oxides) leads to the depolymerisation of the phosphate network by creating terminal oxygens in the place of a BO [105, 109-111]. Various oxides have been used as modifiers in PBGs to suit specific applications, e.g. sodium oxide ($Na_2O$), calcium oxide (CaO), magnesium oxide (MgO) and iron oxide ($Fe_2O_3$) [112].
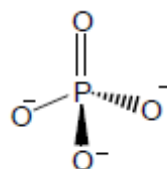


***Figure 2.3:*** *Chemical structure of the tetrahedral phosphate anion*
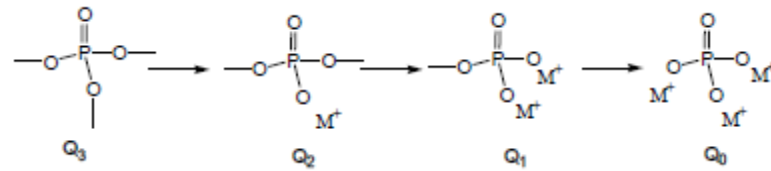
***Figure 2.4:*** *Four types of $Q^i$ species found in condensed phosphates (i is the number of bridging oxygens in a phosphate tetrahedron. Also shown is the effect of the addition of monovalent cation ($M^+$) on the Q structure of the $P_2O_5$ [107].*

PBGs can be classified into binary, ternary, quaternary and complex glass systems based on the number of modifying oxides in the glass composition. The Q structure of each classification of glass can be identified using techniques such as MAS NMR (Magic Angle Spinning Nuclear Magnetic Resonance) and Raman spectroscopy [113-115]. The occurrence of a particular Q species in glass is dependent on the oxygen:phosphorus (O:P) ratio which is consequently dependent on the addition of different metal oxides (MeO) [101]. As the ratio of MeO: P increases from 0 to 3, the phosphate structural groups go from $Q^3$ to $Q^0$ [116]. Table 2.5 shows a summary of the number of BOs, the O:P ratio and the Q species. PBGs that are dominated by $Q^1$ and $Q^0$ species are also known as invert glasses [109].

*Table 2.5:* *Summary of the type of phosphate associated with the number of bridging oxygens (BOs), the O:P ratio and the Q species [109].*

| Type of Phosphate | Number of BOs | O:P ratio | Q Species |
|---|---|---|---|
| Ultraphosphates | 3 | 2.5 | $Q^3$ – highly cross linked structure |
| Metaphosphates | 2 | 3 | $Q^2$ – infinitely long chains and/or rings |
| Polyphosphate | | >3 | $Q^2$ – chains terminated by $Q^1$ units |
| Pyrophosphates | 1 | 3.5 | $Q^1$ – phosphate dimers and chain terminators |
| Orthophosphates | 0 | 4 | $Q^0$ |

The Q species in a PBG is also dependent on the mol% of the modifying oxides added to the phosphate structure [22, 115, 117-123]. Binary sodium phosphate glasses with less than 50 mol% of $Na_2O$ found $Q^2$ and $Q^3$ tetrahedral sites to be dominant. With more than 50 mol% of $Na_2O$, the $Q^2$ and $Q^1$ tetrahedral sites in binary sodium phosphate glasses were found to be dominant [116]. A lot of work on ternary glass systems such as $P_2O_5$ – CaO – $Na_2O$ has been carried out [22, 106, 119, 121]. Ahmed *et al*. found that increasing the $P_2O_5$ content in ternary glass systems from 45 mol% to 50 mol% and 55 mol% increased the amount of $Q^2$ structures (identified as dimers in the 45 mol% system) and decreased the amount of $Q^1$ structures (suggested to be chain terminators in the 50 and 55 mol% glass systems) [22]. Similarly, in the quaternary glass system $P_2O_5$-CaO-$Na_2O$-MgO, Walter *et al.* reported that decreasing the mol% of $P_2O_5$ while simultaneously increasing the MgO content increased the content of $Q^1$ and $Q^0$ species, i.e. invert glasses [123]. Quinternary PBG systems have been investigated for structure, dissolution and biocompatibility by Sharmin *et al.*, Khan *et al.* and Haque *et al.* [26, 124-125]. However the structural information is limited.

### 2.5.2 Dissolution

The dissolution of PBGs takes place in two steps: 1. Hydration and 2. Network breakage (*see* Figure 2.5) [104, 126-127]. During hydration, the glass exchanges Na+ cations with hydrogen ions to form a hydroxyl group, typically at the outer layer of the glass. In the second stage, the hydrated layers on the glass surface are broken down via hydrolysis, leading to the cleavage of P-O-P bonds and a breakdown of the phosphate network structure. Phosphate chains of various lengths are then released into the degradation medium.
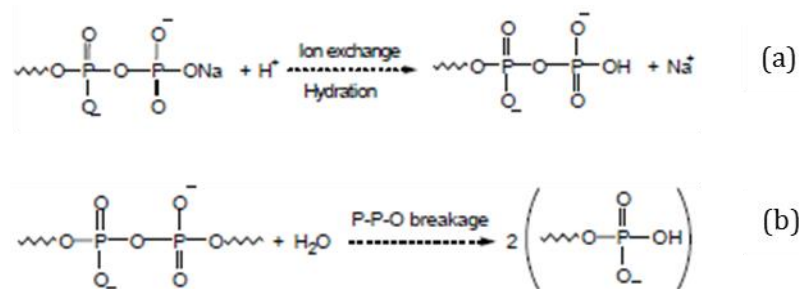


**Figure 2.5:** *Dissolution behaviour of phosphate based glasses in two stages (a) hydration reaction and (b) network breakage*

There are several factors that affect the dissolution of PBGs in addition to the glass composition such as: pH of degradation medium, temperature, thermal history and ratio of surface area to volume [126, 128]. The rate of dissolution in PBGs is sensitive to the glass composition and ranges between $10^{-4}$ to $10^{-9}$ g cm$^{-2}$ min$^{-1}$ [104]. Knowles *et al.* found fixing the content of CaO in a quaternary phosphate glass system and increasing the potassium oxide ($K_2O$) content in place of $Na_2O$ saw a decrease in glass solubility [129]. Ternary glass system $P_2O_5$ – CaO – $Na_2O$ had a decreased dissolution rate as Na+ was replaced by $Ca^{2+}$ [22, 130]. This was attributed to the increase in cross-linking between phosphate

chains. Adding oxides such as $Fe_2O_3$, $Ti_2O$ and $B_2O_3$ was shown to have a greater effect on the dissolution rate of phosphate glasses [24, 118, 124]. The phosphate network was strengthened due to the cross-linking of di- and tri-valent ions.

### 2.5.3 Biocompatibility

Gough *et al.* developed binary sodium phosphate glasses that showed good primary craniofacial osteoblast attachment. However over time it was shown that due to the high dissolution rate the cells found it difficult to remain attached to the glass surface [131-132]. Increasing the $P_2O_5$ content in the ternary glass system $P_2O_5 – CaO – Na_2O$ was shown to decrease the cytotoxicity effect in dental pulp cells. This was due to the increasing acidity of the medium with increasing $P_2O_5$ content [133]. Abou Neel *et al.* investigated the effect of the addition of $TiO_2$ to the glass system $P_2O_5 – CaO – Na_2O$. It was found that the addition of $TiO_2$ 3 and 5 mol% supported human osteosarcoma cell attachment and maintained cell viability for up to 7 days [24].

Bitar *et al.* studied the phosphate glass fibre (PGF) composition $(CaO)_{0.46}$-$(Na_2O)_n$-$(Fe_2O_3)_y$-$(P_2O_5)_{0.50}$ for use in 3D scaffolds for tissue engineering of the hard-soft tissue interface [23]. Human osteoblasts and fibroblasts that were seeded into the scaffold were maintained in culture for 21 days. Samples containing $Fe_2O_3$ at 2 and 3 mol% experienced an increase in cell numbers after 14 days in culture. Quinternary $P_2O_5$-$CaO$-$Na_2O$-$MgO$-$B_2O_3$ glass systems showed that the presence of $B_2O_3$ (up to 10 mol%) did not affect the cell metabolic activity and morphology [134]. Increasing the $P_2O_5$ content to 50 mol% however reduced the metabolic activity significantly. This was also observed by Hasan *et al.* and it was suggested that this was due to the increased amount of inorganic

phosphate ions released into the culture medium [135]. Excessive amounts of phosphate ions have been shown to be detrimental to cell functions [136].

## 2.6 PHOSPHATE GLASS FIBRE REINFORCED POLYMER COMPOSITES

Phosphate glass fibres (PGFs) can be drawn via the melt drawn method or a solid preform method [137-138]. Strong bonds within the molten glass are necessary to produce a continuous thread and they should be able to withstand the applied tensile stresses during the drawing process at high temperatures [139]. The ease of drawing fibres continuously has been shown to be dependent on the mol% of $P_2O_5$ in the PBG formulation, i.e. fibres with a mol% of 45 and higher were drawn continuously [106]. PGFs have shown high tensile strengths and moduli, varying from 321 – 1200 MPa and 44 – 74 GPa, depending on the glass formulation [8, 26, 32, 124-125, 134, 140-141]. Furthermore, a study by Ahmed *et al.* showed the PGF dissolution rate increased compared to that of bulk PBGs due to increased surface area [118].

PGF have been used to reinforce bioresorbable polymers such as PLA and PCL [26-30, 32-33, 140-142]. The glass composition, matrix material, fibre volume fraction ($V_f$) and fibre orientation have an effect on the mechanical and degradation properties of the end composite. Ahmed *et al.* studied the mechanical and degradation properties of binary calcium phosphate glass fibre/PCL composites where it was found that increasing the $V_f$ did not have a significant effect on the flexural strength (~25-30 MPa) of the random mat (RM) composites. This appears counterintuitive however the fibres may have been crushed during composite manufacture reducing the reinforcing effect. The RMs were made from fibres chopped to 10 mm in length. There was a significant increase found in the flexural modulus from ~0.5 GPa at 0% $V_f$ to 2.2 GPa at 18%

$V_f$ [141]. It was also found that the properties were increased slightly for fibres that were annealed. Increased mass loss was observed for the higher $V_f$ composites. The fibres were almost fully degraded by the end of the study.

In another study, Ahmed *et al.* compared RM $50P_2O_5$-$40CaO$-$5Na_2O$-$5Fe_2O_3$ (P50) PGF/PLA composites with unidirectional (UD) PGF/PLA composites and found that composites with fibres oriented in the same direction had higher flexural properties (~129 MPa where $V_f$ = ~24%) than RM composites (~121 MPa where $V_f$ = ~46%) [27]. A similar result was observed by Felfel *et al* for $40P_2O_5$-$16CaO$-$16Na_2O$-$24MgO$-$4Fe_2O_3$ PGF/PLA composites and Han *et al.* for $50P_2O_5$-$40CaO$-$5Na_2O$-$5Fe_2O_3$ [30, 32]. This was attributed to the increased reinforcing effect in UD composites due to loads being applied in same direction as the fibre axis. Ahmed *et al.* immersed composite samples in deionised water at 37°C and found an immediate decrease in mechanical properties in the first week. The decrease was more pronounced for UD composites due to wicking [143]. Wicking is a process by which water is absorbed by composites along the fibres. The discontinuous arrangement of fibres in RM composites is believed to slow down this process [143].

PGF/PLA composites have been looked at for use as fracture fixation plates and as intramedullary nails [27-30]. Felfel *et al.* found that PGF reinforced rods had a potential for use as intramedullary nails with initial properties similar to that of cortical bone [28]. Initial flexural, shear and compressive strengths were found to be 242, 82 and 400 MPa, respectively. Han *et al.* found that using a larger number of thinner UD fibre prepregs layers significantly improved composite mechanical properties by ~86% due to enhanced wet out and therefore better fibre dispersion in the PLA matrix [30].

The recurring scenario is a loss in mechanical properties within the first day(s) of study [27-30, 32, 140-141]. Various glass fibre formulations have been investigated in order to find a formulation to slow the dissolution rate further [124, 134]. However, it is widely believed that the fibre-matrix interface is attacked immediately during the wicking process [26, 32, 140]. The loss of interfacial adhesion leads to the loss of mechanical properties as the fibres are no longer acting as efficient reinforcement. It is therefore necessary to improve the interfacial properties of PGF reinforced bioresorbable polymer composites in order to retain the mechanical properties of composites in aqueous environments. This is vital if these composites are going to be used as fracture fixation implants.

## 2.7 FIBRE-MATRIX INTERFACE

Early assessment of the fibre-matrix interface assumed that interfacial bonding was "perfect", i.e. complete adhesion, no debonding, cracking or slipping. In reality, important processes take place at the interface, and stresses generated at the interfacial structure can promote plastic deformation of the matrix that can lead to material failure [144]. Examining interfacial characteristics and bonding mechanisms will aid in the understanding of the micromechanics at the PGF/ resorbable matrix interface.

The interface in fibre reinforced composites was initially thought of as a two-dimensional region where the fibre and matrix meet [145-146]. An ideal composite would have complete adhesion between fibre and matrix where loads applied to the composite would transfer from matrix to the fibre reinforcement [147]. However, the discovery of a three-dimensional region in between the fibre and the matrix called the interphase led to reassessment of the fibre-matrix

interface. The interphase has been defined as the region that extends from the fibre surface to where the properties of the bulk matrix begin to appear again (*see* Figure 2.6) [31, 148]. The structure and properties of the interphase are different to the other constituents of the composite [31]. Stress transfer from the matrix to the fibre has to pass through the interphase meaning that this region can be designed to improve the mechanical properties of the overall composite, particularly strength and fracture toughness [148].
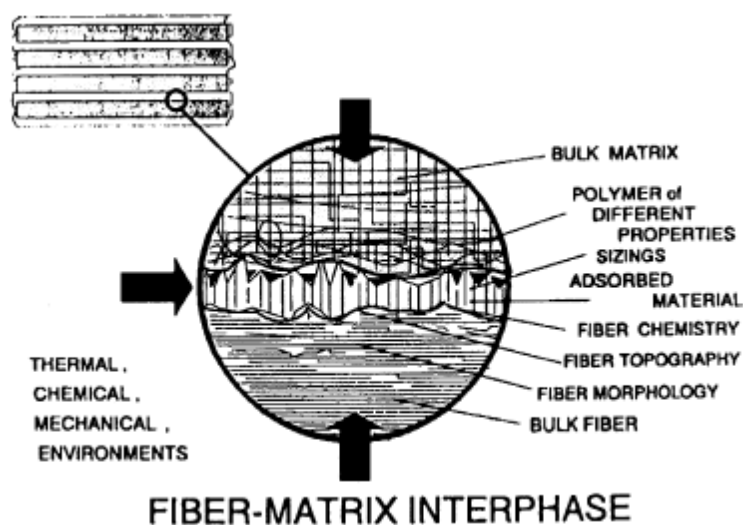


*Figure 2.6:* Image showing the interphase region in a polymer composite [31]

### 2.7.1 Interface Test Methods

There are three main methods used to investigate interfacial properties: single fibre fragmentation test (SFFT), pull-out/ microbond and micro-indentation test. There are many advantages and disadvantages for each test method and the debate on which method is most effective is ongoing [31, 149-153]. The selection process for the method appears to be dependent on the properties of fibre-matrix materials as will be shown in the subsequent sections.

*2.7.1.1Single Fibre Fragmentation Test (SFFT)*

The single fibre fragmentation test (SFFT) is one of the most frequently used methods for calculating interfacial shear stress (IFSS) [31, 149, 154]. A single fibre is embedded in a matrix in the shape of a dog bone and axially loaded as shown in Figure 2.7 [155]. Tensile stress from the matrix is transferred to the fibre during the tensile test. Fibre fragmentation begins when the tensile strain in the fibre exceeds the fibre failure strain and continues breaking the fibre into shorter and shorter lengths as the applied load increases. Shear stress at the fibre will increase until it is insufficient to cause further fibre fracture, known as fibre saturation [31, 149, 154, 156].
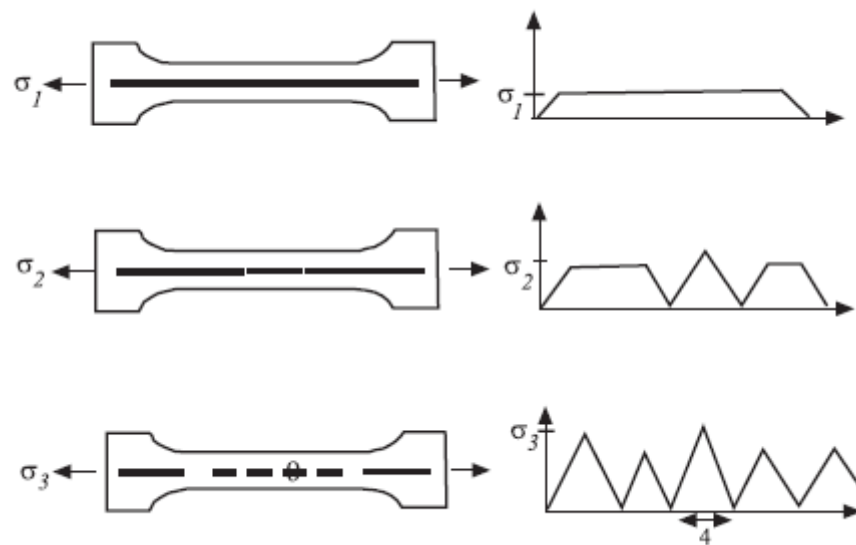


**Figure 2.7:** *A schematic representation of the single fibre fragmentation test (SFFT) [31]*

The shortest fragment length is known as the critical fibre length and is used to calculate the IFSS. The earliest model used to calculate the IFSS, $\tau_i$, was developed by Kelly-Tyson in 1965 [155]:

$$\tau_i = \frac{d\sigma_f}{2L_c}$$

*Equation 2.1*

where $\sigma_f$ is the fibre strength, d is the fibre diameter and $L_c$ is the critical fibre fragment length [155]. This model is also known as the constant shear stress model. The stress distribution along the fibre-matrix interface is assumed to be constant and the fibre strength assumed to have negligible variability [31, 151, 155]. The matrix strain needs to be at least three times that of the fibre strain which means that this method can only be used for certain fibre-matrix combinations [31, 34-35, 149, 154, 157]. A matrix which has a strain to failure that is at least three times larger than that of the fibre also helps to ensure that fibre saturation has been reached [31, 149, 154, 157-158].

The constant shear stress model considers the shear stress transfer as a result of friction due to interfacial debonding or shear yielding of the matrix [152]. However, studies have shown that interfacial debonding and matrix yielding can occur in the same sample [159-160]. Alternative models such as Cox's shear lag model (which is another stress-based scheme) have been used to analyse data from the SFFT [144, 161]. Energy-based schemes that calculate the energy required for the fibre to debond from the matrix in the elastic region have also been looked at as an alternative to the shear stress models and do not require fibre saturation [161-167].

As load is transferred from the matrix to the fibre, there are three main ways in which failure can occur at the interface leading to fibre fragmentation (Figure 2.8) [154, 155, 167-169]:

1. Matrix cracking (transverse)

2. Matrix cracking (conical)

3. Interfacial debonding of the fibre and the matrix

It has been shown that the level of adhesion at the fibre-matrix interface affects the interfacial failure [161]. At the highest level of adhesion failure occurs via radial matrix fracture (Figure 2.8 (a)), at the intermediate level by interfacial crack growth (Figure 2.8 (b)) and at the lowest level of adhesion via frictional debonding (Figure 2.8 (c)) [168-169].
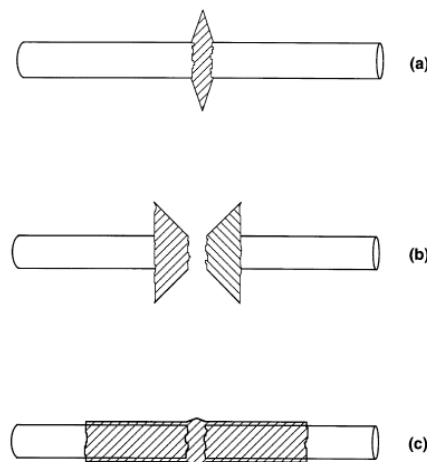


***Figure 2.8:*** *The three modes of fracture in a single fibre composite during a fragmentation experiment: (a) strong interface – the initial fibre break is followed by a disk shaped matrix crack; (b) strong interface but with a matrix that has relatively lower shear than tensile strength capability – the initial fibre break is followed by a double cone matrix crack; (c) weak interface – the initial fibre break is simultaneously accompanied by interfacial debonding [164, 167-169]*

A recent study by Johnson *et al.* shows that the fibre-matrix debonding and transverse matrix cracking can both occur in unsized E-glass (alumina-borosilicate glass) fibres in epoxy resin. Larger transverse matrix cracks and small conical cracks were observed in samples with a matrix of high yield strength (79.4 MPa) which was attributed to the lower energy absorbing capability of a high yield strength material. Matrices of decreasing yield strength (64.7 MPa and 43.7 MPa) show reduction of length in transverse matrix cracks and an increase in length of conical cracks. It was suggested that a matrix with a

lower modulus and yield strength helps to reduce the probability of the formation of transverse cracks and therefore increase the fracture toughness of the composite. The presence of conical matrix cracks, however, was attributed to plastic deformation of the matrix [168].

Haque *et al.* used the constant shear stress model to calculate IFSS for resorbable PGF/PLA systems. Single P40 fibres were embedded in between two 75 mm x 25 mm films of NatureWorks PLA and dog bones of 25 mm gauge length were then punched out using a cutter for tensile testing [34-35]. Pitkethly *et al.* and Zhou *et al.* have made the singe fibre composites in the shape of a dog bone, eliminating the punching out process [150, 170]. The fibres can be preloaded in the mould prior to adding the polymer matrix to ensure that the fibre fragments in the linear portion of the stress-strain curve [170]. It is necessary to note that where dog bone moulds were used the samples were 1 mm or 2 mm thick whereas the single fibre composites (SFCs) produced by Haque *et al.* were 0.2 mm thick. The thickness of the specimen has been shown by Drzal *et al.* to have an effect on the stress transfer from matrix to fibre and consequently the number of fragments produced [171]. Cozien-Cazuc has investigated the minimum thickness (0.2 mm) a SFC can be before there is insufficient matrix to embed fibre for a successful SFFT [172].

The SFFT produces a large amount of data and both IFSS and interfacial fracture toughness can be determined from this data. However, there is constant debate over the validity of the models used to obtain these values. Lodeiro *et al.* states a number of disadvantages of the SFFT including that sample preparation, data collection and analysis are time consuming [149]. Tripathi *et al.* argues that until a valid stress transfer model is developed the interfacial properties calculated from the SFFT will not be entirely accurate [154]. Piggott states that

the values for fibre fracture toughness rely heavily on the accuracy of the assumptions used to determine the coefficient of friction, μ, and the radial pressure and concludes that fibre fragmentation does not produce clear results for measurement of interfacial properties [151]. Even so, interfacial properties are still assessed by this method and much research has gone into developing an appropriate data reduction methods [31, 144, 161, 173, 175]. There is a general consensus that repeating results of SFFT from lab to lab is difficult, however, it is also agreed that an increase in interfacial properties from uncoated to coated fibres can be seen using the SFFT [150].

### 2.7.1.2 Pull-out/Microbond Test

The pull-out test, developed in the early stages of composite research, is considered to be the most direct method to calculate IFSS. Unlike the SFFT, this method can be used with any fibre/matrix combination and has been used to assess interfacial properties (IFSS and interfacial fracture energy) for various fibre-polymer composite systems [31, 149]. A fibre is embedded in a matrix block of known geometry that is held in place while a force is applied to the fibre to pull it from the matrix (Figure 2.9 (a)). The load and displacement are monitored until the fibre is pulled out of the matrix or the fibre breaks. The maximum load recorded is defined as the debonding force in the cases where the fibre is pulled from the matrix. The IFSS is calculated using the following equation [149]:

$$\tau_i = \frac{F}{\pi d l_e}$$
*Equation 2.2*

where F is the debonding load, d is the fibre diameter and $l_e$ is the fibre embedded length. The IFSS for pull-out has also been stated in literature in a similar form to the Kelly-Tyson model for SFFT:

$$\tau_i = \frac{d\sigma_f}{2L}$$

*Equation 2.3*

where L, in this case, is the fibre embedded length and $\sigma_f$ is the fibre strength . The assumption that the shear stress is constant along the embedded length is applied here as well.
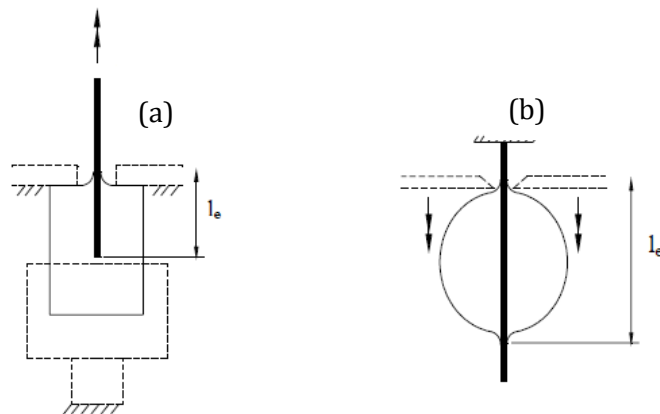


***Figure 2.9:*** *Schematic showing a) Pull-out test from a block of matrix and b) Microbond test with polymer droplet [145]*

The microbond method is specific type of pull-out test where the matrix geometry is in the form of a droplet on the fibre (Figure 2.9 (b)). The IFSS can be calculated using Equation 2.3 and it is [again] assumed that the IFSS is uniformly distributed along the embedded length of the fibre [31, 149]. The sample preparation for this method is considered to be simpler than that for the pull-out technique and requires smaller amounts of material. One of the difficulties with this method is ensuring that the droplets of polymer are similar in size and that

the polymer droplet is more or less uniformly distributed around the fibre. This means that a large number of samples have to be prepared for testing which can be time consuming especially considering that any sample that fails at the meniscus cannot be included in the calculation. Another limiting factor of the pull-out and microbond interfacial tests is the allowed embedded length for fibres of small diameters. Drzal reported that for fibre diameters in the range 5-50 μm, the maximum allowed embedded length is in the range 0.05-1 mm [31].

Yang *et al.* compared the pull-out and microbond test method for interface strength in glass fibre embedded in polypropylene. Both the microbond and pull out samples were tested under the same conditions. SEM imaging of the tested samples showed two types of debonded surfaces: 1. Residual resin on the pulled out fibre and 2. Clean debonded surface. The authors reported that there was no residual resin on the tested samples for the fibre pull-out test. Constant interfacial debonding was not observed for all samples and this was attributed to the variation in matrix properties that develop during sample manufacture [176].

In a study by Le Duigou *et al.*, the interfacial bonding of flax fibre/poly (l-Lactide) (PLLA) composites was investigated using the microbond method. The droplets were prepared by tying a knot of PLLA around a flax fibre and then placing it in an oven at 150°C for 15 min. The temperature was increased to 175°C and samples were left for 5 min before cooling at 10°C/min. The thermal treatment was selected to ensure that the droplet formed was symmetrical [177]. Both stress-based models and energy-based models can be used to analyse the data from the pull-out test and the microbond test to obtain interfacial properties [167, 177].

*2.7.1.3 Microindentation*

The microindentation test method is the only direct method for obtaining the IFSS that requires the manufacture of a high volume fraction composite and is also the least commonly used [31, 149]. The composite is typically made in the shape of a circular rod with the fibres aligned UD parallel to the axis of the rod. A small section of the rod is cut perpendicular to the fibres polished to optical smoothness and can be mounted on a light microscope or in a SEM [170]. The section is moved so a single fibre is placed directly under an indenter with a flat/rounded end. The indenter pushes on the fibre with an applied load that is continuously monitored along with the depth of indentation until debonding and/or fibre slippage occurs [149, 170]. The fibre debonding can be monitored by unloading and observing the fibre optically or by monitoring using acoustic emission sensors. The IFSS is calculated using the following equation:

$$\tau_i = \frac{nF}{2\pi r^2} \qquad\qquad \textbf{\textit{Equation 2.4}}$$

where F is the debonding load, n is the volume fraction and r is the fibre radius. It is common for the IFSS in microindentation tests to be calculated using Finite Element Analysis (FEA) so that the effects of the surrounding fibres can be included [178]. Unlike the other methods, the microindentation technique is considered to be an *in situ* interface tests that can be comparable to real composites with the added advantage of producing similar processing conditions [31, 149].

Zhou *et al.* compared interfacial properties of E-glass/epoxy composites measured by the microindentation test (called push-out in this study) and the SFFT [170]. Both the IFSS and the interfacial energy were calculated for the

push-out test and the SFFT and fibres with and without coupling agent γ-APS were tested. Table 2.6 shows a summary of these results.

**Table 2.6:** *IFSS and Interfacial Energy results measured by push-out and fragmentation for E-glass/epoxy composites [170]*

| Fibre Treatment | IFSS (MPa) | | Interfacial Energy (J/m²) | |
|---|---|---|---|---|
| | **Push-out** | **Fragmentation** | **Push-out** | **Fragmentation** |
| None | 43 ± 15 | 30 ± 7 | 73 ± 19 | 571 ± 162 |
| γ-APS | 73 ± 18 | 43 ± 11 | 139 ± 64 | 957 ± 216 |

Even though the results show increased values for IFSS for the microindentation test (Table 2.6), there are a number of disadvantages with this method [31, 149]:

- Difficult to detect debonding load

- Failure criterion is subjective and arbitrary

- Fibre damage during indentation process

- Failure mode cannot be observed

- Assumes a uniform stress state, like the other test methods, when the reality is a very complex, non-uniform stress state at interface

- Does not take the other fibres present in the sample into account

It is clear that each of the interface test methods available have advantages and disadvantages. The SFFT can only be used for materials where the matrix strain is 3 times greater than the fibre strain. It also provides a significant amount of information of fibre behaviour in a composite [31, 149, 154]. The pull-out and microbond tests can be used for any fibre-matrix combination however a large number of samples need to be manufactured as failure can occur at the meniscus (Figure 2.9) and not due to debonding. The embedded fibre length is also very small increasing the difficulty in sample

preparation [31]. The microindentation method was developed in an effort to produce an *in situ* interface test for real composites [31, 179]. Assuming a uniform stress state is too simplistic and an accurate shear stress distribution can only be assessed using computational methods [31, 178].

When selecting a test method to assess the fibre-matrix interface the following was considered: ease of manufacture, reproducibility of data and direct comparison with IFSS already conducted for PGF/PLA composites [34-35].

### 2.7.2 Improving the Interface

The bond between the fibre and matrix is important in maintaining the interface and for obtaining optimum composite mechanical properties [31]. Interfacial adhesion can be divided into three categories: chemical adhesion (chemical bonding between the fibre and matrix), physical adhesion (bonding due to the surface energies of the fibre and matrix) and mechanical adhesion (mechanical interlocking between the fibre and the matrix due to the surface roughness of the fibre and the wetting ability of the matrix) [144, 180-182]. Without chemical or physical coating, glass fibres have a smooth surface and rely on polymer wetting to create adhesion between the fibre and matrix. Insufficient wetting during composite manufacture can lead to the presence of voids (areas where the fibre and matrix are not in contact) [144, 181].

#### 2.7.2.1 Coupling Agents

Chemical adhesion, with the assistance of a coupling agent, is the most prominent method that has been used to improve the resistance of composite materials to water at the fibre-matrix interface [183]. To do this, carbon fibres

and E-glass fibres are produced with custom coatings that are made up of several components: lubricant, antistat, binder, and a coupling agent. The first three components are added to aid in the processing of the fibres and to protect the fibres when being handled. In commercially produced fibres, the exact composition of the fibre coating is regarded as proprietary information so is not fully detailed. However, the coupling agent is typically an organofunctional silane and so several studies have been conducted using various organofunctional silanes to define the ideal coupling agent for a given fibre-matrix combination [181, 183-185].

Silane coupling agents are able to form a bond between organic and inorganic materials. The chemical structure of a silane is shown in Figure 2.10. On one end of an organofunctional silane is a hydrolysable group ($X_3$). After hydrolysis a reactive silanol group is formed which condenses with other silanol groups. It then forms a hydrogen bond to the substrate surface (such as glass fibre). The other chain end is a non-hydrolysable organofunctional group (R) that bonds covalently to the polymer resin [186]. Therefore, the type of polymer used as a matrix will impact the choice of silane coupling agent. Unlike in thermoset materials, it is often difficult to promote fibre-matrix adhesion with silane coupling agents for thermoplastic matrices [186]. The silanes have to react with the polymer and not the monomeric precursors. This limits the avenues for coupling and leads to problems in thermal properties during composite formation [186].

$$R - (CH_2)_n - Si - X_3$$

Organofunctional group    Linker    Silicon atom    Hydrolysable group
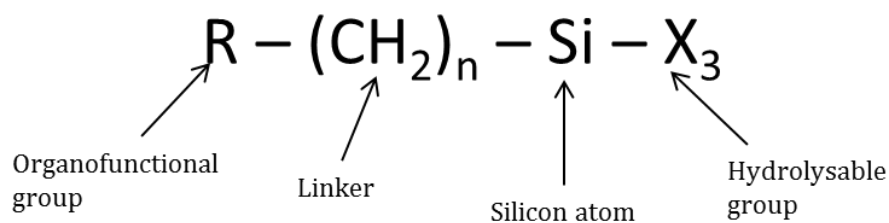
***Figure 2.10:*** *Chemical structure of a typical silane coupling agent*

*2.7.2.2 Interface of Resorbable PGF Reinforced Polymer Composites*

Selected silanes and other commercially available coupling agents have also been used in single fibre studies involving resorbable phosphate glass fibre reinforced polymer composites [34-35, 172, 187]. In an interfacial shear stress (IFSS) study conducted by Khan *et al.* on Poly ε-caprolactone (PCL) reinforced with $40P_2O_5$-$24MgO$-$16CaO$-$20Na_2O$ phosphate glass fibres, the fibres were coated with one of four silanes: 3-Aminopropyl triethoxy silane (APS), [3-(2-Aminoethyl amino) propyl] trimethoxy silane (AAPS), Trimethoxy[3-(phenylamino) propyl] silane (TPPS), Methyl trimethoxy silane (MS) [187]. Novel coupling agents were developed by Haque *et al.* for use in a PGF/PLA composite system [34-35]. The authors' added sodium (PLA-Na) and acid (PLA-Acid) end groups onto a PLA chain [34]. In a separate study hydroxyls such as sorbitol (S-PLA), ethylene glycol (EG-PLA) and glycerol (G-PLA) were added to a PLA chain [35]. The IFSS of these coupling agents were investigated via the SFFT to see if there was an improvement to the interface [34-35]. A summary of these results can be seen in the table below. All of the IFSS values shown were obtained via the SFFT. It is also evident that the novel PLA oligomers developed by Haque *et al.* increase the IFSS compared to silane coupling agents [34-35].

*Table 2.7:* *Summary of IFSS for selected compression moulded resorbable PGF reinforced polymer single fibre composite systems. * denotes manufacture of single fibre composites via in situ polymerization*

| Matrix | Glass Fibre (mol%) | Coupling Agent | IFSS (MPa) | Ref. |
|---|---|---|---|---|
| PCL | $40P_2O_5$-$20Na_2O$-$24MgO$-$16CaO$ | - | 12.9 | [172]* |
| | | 1% APS | 12.7 | |
| PCL | $40P_2O_5$-$20Na_2O$-$24MgO$-$16CaO$ | - | 1.7 | [187] |
| | | 1% APS | 3.8 | |
| | | 1% AAPS | 2.3 | |
| | | 1% TPPS | 2.6 | |
| | | 1% MS | 2.8 | |
| PLA | $40P_2O_5$-$24MgO$-$16CaO$-$16Na_2O$-$4Fe_2O_3$ | - | 9.0 | [34] |
| | | APS | 8.4 | |
| | | PLA-Na | 12.1 | |
| | | PLA-Acid | 13.3 | |
| PLA | $40P_2O_5$-$24MgO$-$16CaO$-$16Na_2O$-$4Fe_2O_3$ | - | 14 | [35] |
| | | EG-PLA | 9 | |
| | | G-PLA | 16 | |
| | | S-PLA | 23 | |

*2.7.2.3 Mechanical Properties of Full-Body Composites*

S-PLA has been used to coat UD fibre mats by Haque and Hasan *et al.*, albeit at two different concentrations [33, 188]. The flexural strength and modulus in both studies increased significantly when compared to uncoated UD composites. However, after immersion in PBS at 37°C, the flexural properties decreased significantly. The flexural strength in Haque's study decreased to that of the uncoated UD composites after 7 days of immersion [33]. Hasan *et al.* saw 68% decrease in flexural strength for S-PLA UD composites after 7 days, which was much more than the uncoated UD composites (35% decrease) [188].

Drzal *et al.* states that the most effective way to observe the interfacial properties in a composite system is to measure the off-axis properties such as transverse tensile and flexural, in-plane shear and short beam shear [31, 169]. Haque tested the in-plane shear of uncoated and S-PLA coated UD composites and found that the in-plane shear strength of the S-PLA composites (42 MPa)

was significantly higher than that for control (32 MPa). After 7 days immersion in PBS at 37°C, the in-plane shear strength of S-PLA composites was still 50% greater than that of control even though it had decreased by ~25% during degradation [33].

The literature has shown that S-PLA oligomer improves the interfacial properties in full-body composites [33, 188]. This work focusses on the in depth study of S-PLA, specifically the effect of the oligomer chain length and the coating concentration on the IFSS. Furthermore a detailed *in vitro* study comparing on-axis and off-axis properties of UD composites was conducted.

## 2.8 REFERENCES

1.  B.D. Ratner, A.S. Hoffman, F.J. Schoen and J.E. Lemons, *Biomaterials Science: An Introduction to Materials in Medicine*, New York: Academic Press, 2012.

2.  D.F. Williams, *The Williams Dictionary of Biomaterials*, Liverpool University Press, 1991.

3.  M. Pavlovic, *Bioengineering*, Springer International Publishing: Switzerland, 2015, pp. 229.

4.  L.A. Pruitt and A.M. Chakravartula, *Mechanics of Biomaterials – Fundamental Principles for Implant Design*, University Press: Cambridge, U.K., 2011, pp. 4.

5.  J.J. Blaker, S.N. Nazhat and A.R. Boccaccini, "Development and characterisation of silver-doped bioactive glass-coated sutures for tissue engineering and wound healing applications", *Biomaterials*, vol. 25, no. 7-8, pp. 1319-1329, 2004.

6.    M. Blazewicz. "Carbon materials in the treatment of soft and hard tissue injuries", *European Cells and Materials*, vol. 2, pp. 21-29, 2001

7.    S.A. Brown, R.S. Hastings, J.J. Mason and A. Moet, "Characterisation of short-fibre reinforced thermoplastics for fracture fixation devices", *Biomaterials*, vol. 11, no. 8, pp. 541-547, 1990.

8.    A.J. Parsons, I. Ahmed, P. Haque, B. Fitzpatrick, M.I.K. Niazi, G.S. Walker and C.D. Rudd, "Phosphate glass fibre composites for bone repair", *Journal of Bionic Engineering*, vol. 6, no. 4, pp. 318-323, 2009.

9.    D. Eglin and M. Alini, "Degradable polymeric materials for osteosynthesis: tutorial", *European Cell and Materials*, vol. 16, pp. 80-91, 2008.

10.   L. Tan, X. Yu, P. Wan and K. Yang, "Biodegradable materials for bone repairs: A review", *Journal of Materials Science and Technology*, vol. 29, no. 6, pp. 503-513, 2013.

11.   N. Sykaras, A.M. Iacopino, V.A. Marker, R.G. Triplett and R.D. Woody, "Implant materials designs and surface topographies: their effect on osseointegration: A literature review", *The International Journal of Oral and Maxillofacial Implants*, vol. 15, no. 5, pp. 675-690, 2000.

12.   J. Black and G.W. Hastings, *Handbook of Biomaterials Properties*, London, U.K.: Chapman and Hall, 1998.

13.   E. Wintermantel and J. Mayer, "Anisotropic biomaterials strategies and developments for bone implants", In: D.L. Wise, D.J. Trantolo, D.E. Altobelli, J.D. Yaszemiski, J.D. Gresser and E.R. Schwartz, ed., *Encyclopedic Handbook of Biomaterials and Bioengineering, Part B-1*, Marcel Dekker: New York, 1995, pp. 3-42.

14.   E. Wintermantel and S.W. Ha, *Biokompatible Werkstoffe und Bauweisen: Implantate fur Medizin und Umwelt*, Berlin, Germany: Springer-Verlag, 1998.

15. S. Ramakrishna, J. Mayer, E. Wintermantel and K.W. Leong, "Biomedical applications of polymer-composite materials: a review," *Composites Science and Technology*, vol. 61, no. 9, pp. 1189-1224, 2001.

16. L.L. Hench and I. Thompson, "Twenty-first century challenges for biomaterials", *Journal of the Royal Society Interface*, vol. 7, Suppl. 4, pp. S379-S391, 2010.

17. L.L. Hench and J.M. Polak, "Third-generation biomedical materials", *Science*, vol. 295, no. 5557, pp. 1014-1017, 2002.

18. S.M. Bea and W. Bonfield, "Biocomposites for medical applications*", Journal of the Australian Ceramic Society*, vol. 40, no. 1, pp. 43-57, 2004.

19. L. Hench, "Biomaterials", *Science*, vol. 208, no. 4446, pp. 826-831, 1980.

20. R. Narayan, "The next generation of biomaterial development", *Philisophical Transactions of the Royal Society A*, vol. 368, no. 1917, pp. 1831-1837, 2010.

21. E.A. Abou Neel, D.M. Pickup, S.P. Valappil, R.J. Newport and J.C. Knowles, "Bioactive functional materials: a perspective on phosphate-based glasses", *Journal of Materials Chemistry*, vol. 19, no. 6, pp. 690-701, 2009.

22. I. Ahmed, M. Lewis, I. Olsen and J.C. Knowles, "Phosphate glasses for tissue engineering: Part 1. Processing and characterisation of a ternary based $P_2O_5$-CaO-$Na_2O$ glass system", *Biomaterials*, vol. 25, no. 3, pp. 491-499, 2004.

23. M. Bitar, J.C. Knowles, M.P. Lewis and V. Salih, "Soluble phosphate glass fibres for bone–ligament interface", *Journal of Materials Science: Materials in Medicine*, vol. 16, no. 12, pp. 1131-1136, 2005.

24. E.A. Abou Neel and J.C. Knowles, "Physical and biocompatibility studies of novel titanium dioxide doped phosphate-based glasses for bone tissue

engineering applications", *Journal of Material Science: Mareials in Medicine*, vol. 19, no. 1, pp. 377-386, 2007.

25. T. Fujita, N. Izumo, R. Fukuyama, T. Meguro, H. Nakamuta, T. Kohno and M. Koida, "Phosphate provides an extracellular signal that drives nuclear export of Runx2/Cbfa1 in bone cells", *Biochemical and Biophysical Research Communications*, vol. 280, no. 1, pp. 348-352, 2001

26. R.A. Khan, A.J. Parsons, I.A. Jones, G.S. Walker, C.D. Rudd, "Degradation and Interfacial Properties of Iron Phosphate Glass Fibre-Reinforced PCL-Based Composite for Synthetic Bone Replacement Materials", *Polymer-Plastics Technology and Engineering*, vol. 49, no. 12, pp. 1265-1274, 2010.

27. I. Ahmed, I.A. Jones, A.J. Parsons, J. Bernard, J. Farmer, C.A. Scotchford, G.S. Walker, and C.D. Rudd, "Composites for bone repair: phosphate glass fibre reinforced PLA with varying fibre architecture", *Journal of materials science. Materials in medicine*, vol. 22, no. 8, pp. 1825-1834, 2011.

28. R. Felfel, I. Ahmed, A.J. Parsons, L.T. Harper and C.D. Rudd, "Initial mechanical properties of phosphate-glass fibre- reinforce rods for use as resorbable intramedullary nails", *Journal of Materials Science*, vol. 47, no. 12, pp. 4884-4894, 2012.

29. R.M. Felfel, I. Ahmed, A.J. Parsons, G.S. Walker and C.D. Rudd, "In vitro degradation, flexural, compressive and shear properties of fully bioresorbable composite rods", *Journal of the Mechanical Behaviour of Biomedical Materials*, vol. 4, no. 7, pp. 1462-1472, 2011.

30. N. Han, I. Ahmed, A.J. Parsons, L. Harper, C.A. Scotchford, B.E. Scammell and C.D. Rudd, "Influence of screw holes and gamma sterilization on properties of phosphate glass fibre-reinforced composite bone plates", *Journal of Biomaterials Applications*, vol. 27, no. 8, pp. 990-1002, 2011.

31. L.T. Drzal, P.J. Herrera-Franco and H. Ho, "Fibre-matrix interface tests", *Comprehensive Composite Materials: Test Methods, Nondestructive Evaluation and Smart Materials*, vol. 5, pp.71-111, 2000.

32. R.M. Felfel, I. Ahmed, A.J. Parsons, P. Haque, G.S. Walker, and C.D. Rudd, "Investigation of Crystallinity, Molecular Weight Change, and Mechanical Properties of PLA/PBG Bioresorbable Composites as Bone Fracture Fixation Plates", *Journal of Biomaterials Applications*, vol. 25, no. 7, pp. 765-789, 2012.

33. P. Haque, "Oligomeric PLA coupling agents for phosphate glass/PLA composites", University of Nottingham, 2011.

34. P. Haque, I.A. Barker, A.J. Parsons, K.J. Thurecht, I. Ahmed, G.S. Walker, C.D. Rudd and D.J. Irvine, "Influence of compatibilizing agent molecular structure on the mechanical properties of phosphate glass fiber-reinforced PLA composites", *Journal of Polymer Science Part A: Polymer Chemistry*, vol. 48, no. 14, pp. 3082-3094, 2010.

35. P. Haque, A.J. Parsons, I.A. Barker, I. Ahmed, D.J. Irvine, G.S. Walker, and C.D. Rudd, "Interfacial properties of phosphate glass fibres/PLA composites: Effect of the end functionalities of oligomeric PLA coupling agents", *Composites Science and Technology*, vol. 70, no. 13, pp. 1854-1860, 2010.

36. S.H. Teoh, *Engineering materials for biomedical applications*, Singapore, Hackensack, NJ: World Scientific Pub, 2004.

37. J.B. Park and R.S. Lakes, *Biomaterials: an Introduction*, New York: Springer, 2007.

38. M. Niinomi, "Metallic Biomaterials", *Journal of Artificial Organs*, vol. 11, no. 3, pp. 105-110, 2008.

39. G.A. Graves and B.K. Jr, "Bioresorbable Glass Fibres of Bioresorbablbe Polymers for Bone Fixation Devices and Artificial Ligaments in United States", Patent 1986, University of Dayton.

40. Bone atrophy. (n.d.) *Mosby's Dental Dictionary, 2nd edition*. (2008). Retrieved February 23 2015 from http://medical-dictionary.thefreedictionary.com/bone+atrophy

41. H.M. Frost, "Wolff's Law and bone's structural adaptations to mechanical usage: an overview for clinicians", *The Angle Orthodontist*, vol. 64, no. 3, pp. 175-188, 1994.

42. A.J. Tonino, C.L. Davidson, P.J. Klopper and L.A. Linclau, "Protection from stress in bone and its effect", *Journal of Bone and Joint Surgery*, vol. 58-B, no. 1, pp. 107-113, 1976.

43. P. Christel, L. Claes, S.A. Brown, "Carbon reinforced composites in orthopaedic surgery", In : M. Szycher, ed., *High Performance Biomaterials: A Comprehensive Guide to Medical and Pharmaceutical Applications*, Lancaster, USA: Technomic, 1991, pp. 499-518.

44. M. Geetha, A.K. Singh, R. Asokamani and A.K. Gogia, "Ti based biomaterials, the ultimate choice for orthopaedic implants – A review", *Progress in Materials Science*, vol. 54, no. 3, pp. 397-425, 2009.

45. M. Long and H.J. Rack, "Titanium alloys in total joint replacement- a materials science perspective", *Biomaterials*, vol. 19, no. 18, pp. 1621-1639, 1998.

46. J.A. Davidson and F.S. Georgette, "State of the Art Materials for orthopaedic Prosthetic Devices: on Implant Manufacturing and Material Technology", *Proceedings of the Society of Manufacturing Engineering*, Itasca, Italy, 1987.

47. M. Navarro, A. Michiardi, O. Castano and J.A. PLanell, "Biomaterials in orthopedics", *Journal of the Royal Society Interface*, vol. 5, no. 27, pp. 1137-1158, 2008.

48. S.C. Cowin, ed., *Bone Mechanics*, CRC Press: Boca Raton, Florida, 2001.

49. A. Mahapatro and A.S. Kulshrestha, American Chemical Society Meeting, American Chemical Society, Division of Polymeric Materials and Engineering, *Polymers for Biomedical Applications*, Washington, DC: American Chemical Society, Distributed by Oxford University Press, 2008.

50. Y. Onuma and P.W. Surreys, "Bioresorbable Scaffold: the advent of a new era in percutaneous coronary and peripheral revascularization?", *Circulation*, vol. 123, no. 7. pp. 779-797, 2011.

51. W.S. Pietrzak, D.R. Sarver and M.L. Verstynen, "Bioresorbable polymer science for the practicing surgeon", *Journal of Craniofacial Surgery*, vol. 8, no. 2, pp. 87-91, 1997.

52. J.C. Middleton and A.J. Tipton, "Synthetic biodegradable polymers as orthopedic devices", *Biomaterials*, vol. 21, no. 23, pp. 2335-2346, 2000.

53. B. Gupta, N. Revagade, and J. Hilborn, "Poly(lactic acid) fiber: An overview", *Progress in Polymer Science*, vol. 32, no. 4, pp. 455-482, 2007.

54. T. Juutilainen, H. Pätiälä, M. Ruuskanen, and P. Rokkanen, "Comparison of costs in ankle fractures treated with absorbable or metallic fixation devices", *Archives of Orthopaedic and Trauma Surgery*, vol. 116, no. 4, pp. 204-208, 1997.

55. P. Törmälä, T. Pohjonen and P. Rokkanen, "Bioabsorbable polymers: materials technology and surgical applications", *Proceedings of the Institution of Mechanical Engineers, Part H: Journal of Engineering in Medicine*, vol. 212, no. 2, pp.101-111, 1998.

56. P.A. Gunatillake and R. Adhikari, "Biodegradable synthetic polymers for tissue engineering", *European Cells and Materials*, vol. 5, pp.1-16, 2003.

57. S. Gogowalski, "Bioresorbable polymers in trauma and bone surgery", *Injury*, vol. 31, Suppl. 4, pp. 28-52, 2000.

58. J.L. Stone, G.S. Beaupre and W.C. Hayes, "Multiaxial strength characteristic of trabecular bone", *Journal of Biomechanics*, vol. 16, no. 9, pp. 743-752, 1983.

59. E.J. Bergsma, F.R. Rozema, R.R.M. Bos and W.C. De Bruijn, "Foreign body reactions to resorbable poly (L-lactide) bone plates and screws used for the fixation of unstable zygomatic fractures", *Journal of Oral and Maxillofacial Surgery*, vol. 51, no. 6, pp. 666-670, 1993.

60. E.J. Bergsma, W.C. De Bruijn, F.R. Rozema, R.R.M. Bos and G. Boering, "Late degradation tissue response to poly (L-lactide) bone plates and screws", *Biomaterials*, vol. 18, no. 1, pp. 25-31, 1995.

61. R. Suuronen, M.J. Manninen, T. Pohjonen, O. Laitinen and C. Lindqvist, "Mandibular osteomy fixed with biodegradable plates and screws: an animal study", *British Journal of Oral and Maxillofacial Surgery*, vol. 35, no. 5, pp. 341-348, 1997.

62. P.B. Maurus and C.C. Kaeding, "Bioabsorbable implant material review", *Operative Techniques in Sports Medicine*, vol. 12, no. 3, pp. 158-160, 2004.

63. A. Nathan and J. Kohn, "Amino acid derived polymers", In: S.W. Shalaby, ed., *Biomedical polymers designed to degrade systems*, New York: Hanser, 1994, pp.117-151.

64. Birmingham Polymers, Inc. Corporate Literature Brochure #11-001-B 1999.

65. I. Armentano, M. Dottori, E. Fortunati, S. Mattioli and J.M. Kenny, "Biodegradable polymer matrix nanocomposites for tissue engineering: A

review", *Polymer Degradation and Stability*, vol. 95, no. 11, pp. 2126-2146, 2010.

66. M.A. Woodruff and D.W. Hutmacher, "The return of a forgotten polymer – Polycaprolactone in the 21st century", *Progress in Polymer Science*, vol. 35, no. 10, pp. 1217–1256, 2010.

67. A.U. Daniels, M.K.O. Chang, K.P. Andriano, and J. Heller, "Mechanical properties of biodegradable polymers and composites proposed for internal fixation of bone", *Journal of Applied Biomaterials*, vol. 1, no. 1, pp. 57-78, 1990.

68. K. Van de Velde and P. Kiekens, "Biopolymers: overview of several properties and consequences on their applications", *Polymer Testing,* vol. 21, no. 4, pp. 433-442, 2002.

69. D.E. Henton, P. Gruber, J. Lunt and J. Randall, "Polylactic Acid Technology", In: A.K. Mohanty, M. Misra and L.T. Drzal, ed., *Natural fibres, biopolymers and biocomposites*, Taylor and Francis: Boca Raton, Florida, 2005, pp. 527-577.

70. C.S. Proikakis, N.J. Mamouzelos, P.A. Tarantili and A.G. Andreopoulos, "Swelling and hydrolytic degradation of poly (D,L-lactic acid) in aqueous solutions", *Polymer Degradation and Stability*, vol. 91, no. 3, pp. 614-619, 2006.

71. M. Kiremitci-Gumusderelioglu and G. Deniz, "Synthesis, characterisation and in vitro degradation of poly (DL-lactide-co-glycolide) films", *Turkish Journal of Chemistry*, vol. 23, pp. 153-161, 1999.

72. G. Schliecker, C. Schmidt, St. Fuchs and T. Kissel, "Characterisation of a homologous series of D,L-lactic acid oligomers: a mechanistic study on the degradation kinetics in vitro", *Biomaterials*, vol. 24, no. 21, pp. 3835-3844, 2003.

73. W.S. Pietrzak, B.S. Verstynen and D.R. Sarver, "Bioabsorbable fixation devices: status for craniomaxillofacial surgeon", *Journal of Craniofacial Surgery*, vol. 8, no. 2, pp. 92-96, 1997.

74. E.W. Fischer, H.J. Sterzel and G. Wegner, "Investigation of structure of solution grown crystals of lactide copolymers by means of chemical reactions", *Colloid and Polymer Science*, vol. 251, no. 11, pp. 980-990, 1973.

75. J. Siepmann and A. Gopferich, "Mathematical modelling of bioerodible, polymeric drug delivery systems", *Advanced Drug Delivery Reviews*, vol. 48, no. 2-3, pp. 229-247, 2001.

76. J. Kohn and R. Langer, "Bioresorbable and bioerodible materials", In: B.D. Ratner, A.S. Hoffman, F.J. Schoen and J.E. Lemons, *Biomaterials Science: An Introduction to Materials in Medicine*, New York: Academic Press, 1996, pp. 64-72.

77. I. Grizzi, H. Garreau, S. Li and M.Vert, "Hydrolytic degradation of devices based on poly (D,L-lactic acid) size dependence", *Biomaterials*, vol. 16, no. 4, pp. 305-311, 1995.

78. S.J. de Jong, E.R. Arias, D.T.S. Rijkers, C.F. van Nostrum, J.J. Kettenes-van den Bosch and W.E. Hennick, "New insights into hydrolytic degradation of poly (lactic acid): participation of the alcohol terminus", *Polymer*, vol. 42, no. 7, pp. 2795-2802, 2001.

79. R. Smith, *Biodegradable polymers for industrial applications*, Woodhead, 2005.

80. S. Gogolewski, "Resorbable polymers for internal fixation", *Clinical Materials*, vol. 10, no. 1-2, pp. 13-20, 1992.

81. K.A. Athanasiou, J.B. Schmitz and C.M. Agrawal, "The effects porosity on *in vitro* degradation of polylactic acid – polyglycolic acid implants used in

repair of articular cartilage", *Tissue Engineering*, vol. 4, no. 1, pp. 53-63, 1998.

82.    J. Mauduit, E. Perouse and M. Vert, "Hydrolytic degradation of films prepared from blends of high and low molecular weight poly(D,L-lactic acids)", *Journal of Biomedical Materials Research*, vol. 30, no. 2, pp. 201-207, 1996.

83.    S. Hyon, K. Jamashidi and Y. Ikada, "Effects of residual monomer on the degradation of D,L-lactide polymer", *Polymer International*, vol. 46, no. 3, pp. 196-202, 1998.

84.    H. Tsuji and K. Nakahara, "Poly (L-lactide). IX. Hydrolysis in acid media", *Journal of Applied Polymer Science*, vol. 86, no. 1, pp. 186-194, 2002.

85.    H. Tsuji, Y. Kidokoro and M. Mochizuki, "Enzymatic degradation of poly (L-lactic acid) fibers: Effects of small drawing", *Journal of Applied Polymer Science*, vol. 103, no. 3, pp. 2064-2071, 2007.

86.    N. Ashammakhi, H. Peltoniemi, W. Waris, R. Suuronen, W. Serlo, M. Kellomaki, P. Törmälä and T. Waris, "Developments in craniomaxillofacial surgery: use of self-reinforced bioresorbable osteofixation devices", *Plastic and Reconstructive Surgery*, vol. 108, no. 1, pp. 167-180, 2001.

87.    P. Törmälä, J. Vasenius, S. Vainionpaa, J. Laiho, T. Pohjonen and P. Rokkanen, "Ultra-high-strength absorbable self-reinforced polyglycolide (SR-PGA) composite rods for internal fixation in bone fractures: in vitro and in vivo study", *Journal of Biomedical Materials Research*, vol. 25, no. 1, pp. 1-22, 1991.

88.    D.D. Wright-Charlesworth, D.M. Miller, I. Miskioglu and J.A. King, "Nanoindentation of injection molded PLA and self-reinforced composite PLA after *in vitro* conditioning for three months", *Journal of Biomedical Materials Research Part A*, vol. 74, no. 3, pp. 388-396, 2005.

89. L. Ylikontiola, K. Sunqvuist, G.K.B. Sandor, P. Tormala and N. Ashammakhi, "Self-reinforced bioresorbable poly-L/DL-Lactide [SR-P(L/DL)LA] 70/30 miniplates and miniscrews are reliable for fixation of anterior mandibular fractures: a pilot study", *Oral Surgery, Oral Medicine, Oral Pathology, Oral Radiology and Endodontology*, vol. 97, no. 3, pp. 312-317, 2004.

90. L.F. Charles, E.R. Kramer, M.T. Shaw, J.R. Olson and M Wei, "Self-reinforced composites of hydroxyapatite-coated PLLA fibres: Fabrication and mechanical characterisation", *Journal of the Mechanical Behaviour of Biomedical Materials*, vol. 17, pp. 269-277, 2013.

91. P. Törmälä, "Ultra-high strength, self-reinforced absorbable polymeric composites for applications in different disciplines of surgery", *Clinical Materials*, vol. 13, no. 1-4, pp. 35-40, 1993

92. H. Pihlajamaki, O. Bostman, E. Hirvensalo, P. Rokkanen and P. Tormala, "Absorbable pins of self-reinforced poly-L-lactic acid for fixation of fractures and osteomies", *Journal of Bone and Joint Surgery*, vol. 74, no. 6, pp. 853-857, 1992.

93. P. Törmälä, "Biodegradable self-reinforced composite materials: Manufacturing structure and mechanical properties", *Clinical Materials*, vol. 10, no. 1-2, pp.29-34, 1992.

94. R.J. Yan, P.J. Hine, I.M. Ward, R.H. Olley and D.C. Bassett, "The hot compaction of spectra gel-spun polyethylene fibres", *Journal of Materials Science*, vol. 32, no. 18, pp.4821-4831, 1997.

95. P. Törmälä, T. Pohjonen, and P. Rokkanen, "Ultra-high-strength self-reinforced polylactide composites and their surgical applications", *Macromolecular Symposia*, vol. 123**,** no. 1, pp. 123-131, 1997.

96. G.E. Wnek and G.L. Bowlin, *Encyclopedia of Biomaterials and Biomedical Engineering*, Second Edition (Four-Volume Set): Informa Healthcare, 2008.

97.  H. Niiranen, T. Pyhältö, P. Rokkanen, M. Kellomäki, and P. Törmälä, "In vitro and in vivo behavior of self-reinforced bioabsorbable polymer and self-reinforced bioabsorbable polymer/bioactive glass composites", *Journal of Biomedical Materials Research Part A*, vol. 69A, no. 4, pp. 699-708, 2004.

98.  T. Niemela, "Effect of Î²-tricalcium phosphate addition on the in vitro degradation of self-reinforced poly-l,d-lactide", *Polymer Degradation and Stability*, vol. 89, no. 3, pp. 492-500, 2005.

99.  T. Niemela, D.B. Aydogan, M. Hannula, J. Hyttinen, and M. Kellomaki, "Determination of bioceramic filler distribution and porosity of self-reinforced bioabsorbable composites using micro-computed tomography", *Composites Part A: Applied Science and Manufacturing*, vol. 42, no. 5, pp. 534-542, 2011.

100. H.H.K. Xu, J.B. Quinn, S. Takagi, L.C. Chow, F.C. Eichmiller, "Strong and macroporous calcium phosphate cement: Effects of porosity and fiber reinforcement on mechanical properties", *Journal of Biomedical Materials Research*, vol. 57, no. 3, pp. 457–466, 2001.

101. J.R. Van Wazer, *Phosphorus and its Compounds: Vol. 1*, Interscience, New York, 1958.

102. V. Rajendran, A.V. Gayathri Devi, M. Azooz and F.H. El-Batal, "Physicochemical studies of phosphate based $P_2O_5$-$Na_2O$-$CaO$-$TiO_2$ glasses for biomedical applications", *Journal of Non-Crystalline Solids*, vol. 353, no. 1, pp. 77-84, 2007.

103. A. Saranti, I. Kotselas and M.A. Karakassides, "Bioactive glasses in the system $CaO$-$B_2O_3$-$P_2O_5$: Preparation, structural study and in vitro evaluation", *Journal of Non-Crystalline Solids*, vol. 352, no. 5, pp. 390-398, 2006.

104. B.C. Bunker, G.W. Arnold, and J.A. Wilder, "Phosphate glass dissolution in aqueous solutions", *Journal of Non-Crystalline Solids*, vol. 64, no. 3, pp. 291-316, 1984.

105. R.C. Ropp, *Inorganic polymeric glasses*, Elsevier, 1992.

106. I. Ahmed, M. Lewis, I. Olsen and J.C. Knowles, "Phosphate glasses for tissue engineering: Part 2. Processing and characterisation of a ternary based $P_2O_5$-CaO-$Na_2O$ glass fibre system", *Biomaterials*, vol. 25, no. 3, pp. 501-507, 2004.

107. J.C. Knowles, "Phosphate based glasses for biomedical applications", *The Royal Society of Chemistry*, vol. 13, no. 10, pp. 2395-2401, 2003.

108. U. Hoppe, "A structural model for phosphate glasses", *Journal of Non-Crystalline Solids*, vol. 195, no. 1-2, pp. 138-147, 1996.

109. R.K. Brow, "Review: the structure of simple phosphate glasses", *Journal of Non-Crystalline Solids*, vol. 263-264, pp. 1-28, 2000.

110. N.H. Ray, "The structure and properties of inorganic polymeric phosphates", *British Polymer Journal*, vol. 11, no. 4, pp. 163-177, 1979.

111. J.U. Otaigbe, and G.H. Beal, "Inorganic phosphate glasses as polymers", *Trends in Polymer Science*, vol. 5, no. 11, pp. 369-379, 1997.

112. E.A. Abou Neel, W. Chrzanowski, D.M. Pickup, L.A. O'Dell, N.J. Mordan, R.J. Newport, M.E. Smith, and J.C. Knowles, "Structure and properties of strontium doped phosphate-based glasses", *Journal of The Royal Society Interface*, vol. 6, no. 34, pp. 435-446, 2009.

113. R.J Kirk Patrick and R.K. Brow, "Nuclear magnetic resonance investigation of the structures of phosphate and phosphate containing glasses: a review", *Solid State Nuclear Magnetic Resonance*, vol. 5, no. 1, pp. 9-21, 1995.

114. K.P. Joseph, M. Amarendra, G. Govindan, K.V. Kutty, C.S. Sundar and P.R. Vasudeva Rao, "Structure of cesium loaded iron phosphate glasses: an infrared and Raman spectroscopy study", *Journal of Nuclear Materials*, vol. 420, no. 1-3, pp. 49-53, 2012.

115. D. Qiu, P. Guerry, I. Ahmed, D.M. Pickup, D. Carta, J.C. Knowles, M.E. Smith and R.J. Newport, "A high-energy X-ray diffraction, P and B solid state NMR study of the structure of aged sodium borophosphate glasses", *Materials Chemistry and Physics*, vol. 111, no. 2-3, pp. 455-462, 2008.

116. S.W. Martin, "Review of the structures of phosphate glasses", *European Journal of Solid State Inorganic Chemistry*, vol. 28, pp. 163-205, 1991.

117. R. Ciceo Lucacel, A.O. Hulpus, V. Simon and I. Ardelean, "Structural characterisation of phosphate glasses doped with silver", *Journal of Non-Crystalline Solids*, vol. 355, no. 7, pp. 425-429, 2009.

118. I. Ahmed, C.A. Collins, M.P. Lewis, I. Olsen and J.C. Knowles, "Processing, characterisation and biocompatibility of iron-phosphate glass fibres for tissue engineering", *Biomaterials*, vol. 25, no. 16, pp. 3223-3232, 2004.

119. D.M. Pickup, I. Ahmed, P. Guerry, J.C. Knowles, M.E. Smith and R.J. Newport, "The structure of phosphate glass biomaterials from neutron diffraction and P nuclear magnetic resonance data", *Journal of Physics: Condensed Matter*, vol. 19, no. 41, 2007, DOI:10.1088/0953-8984/19/41/415116.

120. E.A. Abou Neel, L.A. O'Dell, W. Chrzanowski, M.E. Smith and J.C. Knowles, "Control of surface free energy with titanium doped phosphate based glasses by co-doping with zinc", *Journal of Biomedical Materials Research Part B: Applied Biomaterials*, vol. 89, no. 2, pp. 392-407, 2009.

121. D. Carta, D. Qiu, P. Guerry, I. Ahmed, E.A. Abou Neel, J.C. Knowles, M.E. Smith and R.J. Newport, "The effect of composition on the structure of

sodium borophosphate glasses", *Journal of Non-Crystalline Solids*, vol. 354, no. 31, pp. 3671-3677, 2008.

122. R.K. Brow, D.R. Tallant, JJ. Hudgens, S.W. Martin and A.D. Irwin, "The short-range structure of sodium ultraphosphate glasses", *Journal of Non-Crystalline Solids*, vol. 177, pp. 221-228, 1994.

123. G. Walter, J. Vogel, U. Hoppe and P. Hartmann, "The structure of CaO-Na$_2$O-MgO- P$_2$O$_5$ invert glass", *Journal of Non-Crystalline Solids*, vol. 296, no. 3, pp. 212-223, 2001.

124. N. Sharmin, A.J. Parsons, C.D. Rudd and I. Ahmed, "Effect of boron oxide addition on fibre drawing, mechanical properties and dissolution behavior of phosphate-based glass fibres with fixed 40, 45 and 50 mol% P$_2$O$_5$", *Journal of Biomaterial Applications*, vol. 0, no. 0, pp. 1-15, 2014.

125. P. Haque, I. Ahmed, A. Parsons, R. Felfel, G. Walker and C. Rudd, "Degradation properties and microstructural analysis of 40P$_2$O$_5$-24MgO-16CaO-16Na$_2$O-4Fe$_2$O$_3$ phosphate glass fibres", *Journal of Non-Crystalline Solids*, vol. 375, pp. 99-109, 2013.

126. H. Gao, T. Tan, and D. Wang, "Dissolution mechanism and release kinetics of phosphate controlled release glasses in aqueous medium", *Journal of Controlled Release*, vol. 96, no. 1, pp. 29-36, 2004.

127. F. Delahaye, L. Montagne, G.R. Palavit, J. Claude Touray, and P. Baillif, "Acid dissolution of sodium-calcium metaphosphate glasses" *Journal of Non-Crystalline Solids*, vol. 242, no. 1, pp. 25-32, 1998.

128. H. Gao, T. Tan, and D. Wang, "Effect of composition on the release kinetics of phosphate controlled release glasses in aqueous medium", *Journal of Controlled Release*, vol. 96, no. 1, pp. 21-28, 2004.

129. J.C. Knowles, K. Franks and I. Abraham, "Investigation of the solubility and ion release in the glass system $K_2O$-$Na_2O$-$CaO$-$P_2O_5$", *Biomaterials*, vol. 22, no. 23, pp. 3091-3096, 2001.

130. K. Franks, I. Abraham and J.C. Knowles, "Development of soluble glasses for biomedical use part I: in vitro solubility measurement", *Journal of Materials Science: Materials in Medicine*, vol. 11, no. 10, pp. 609-614, 2000.

131. J.E. Gough, P. Christian, C.A. Scotchford, C.D. Rudd and I.A. Jones, "Synthesis, degradation and in vitro cell responses of sodium phosphate glasses for craniofacial bone repair", *Journal of Biomedical Materials Research*, vol. 59, no. 3, pp. 481-489, 2002.

132. J.E. Gough, P. Christian, C.A. Scotchford and I.A. Jones, "Long-term craniofacial osteoblast culture on a sodium phosphate and a calcium/sodium phosphate glass", *Journal of Biomedical Materials Research*, vol. 66, no. 2, pp. 233-240, 2003.

133. M. Uo, M. Mizuno, Y. Kuboki, A. Makishima and F. Watari, "Properties and cytotoxicity of water soluble $Na_2O$-$CaO$-$P_2O_5$ glasses", *Biomaterials*, vol. 19, no. 24, pp. 2277-2284, 1998.

134. N. Sharmin, "Preparation and characterisation of phosphate based glasses, fibres and composites: effect of boron and iron oxide additions", University of Nottingham, 2014.

135. M.S. Hasan, I. Ahmed, A.J. Parsons, G.S. Walker and C.A. Scotchford, "Material characterisation and cytocompatibility assessment of quinternary phosphate glasses," *Journal of Materials Science: Materials in Medicine*, vol. 23, no. 10, pp. 2531-2541, 2012.

136. H.-J. Moon, K.-N. Kim, K.-M. Kim, S.-H. Choi, C.-K. Kim, K.-D. Kim, R. LeGeros and Y.-K. Les, "Effect of calcium phosphate glass on bone formation in

calvarial defects of Sprague-Dawley rats", *Journal of Materials Science: Materials in Medicine*, vol. 17, no. 9, pp. 807-813, 2006.

137. F.T. Wallenberger and N.E. Weston, "Glass fibres from high and low viscosity melts", *Materials Research Society Symposium Proceedings*, vol. 702, pp. 165-172, 2002.

138. K.L. Lowenstein, "The manufacture of continuous glass fibres", *Platinum Metal Review*, vol. 19, no. 3, pp. 82-87, 1975.

139. J.B. Murgatroyd, "The delayed elastic effect in glass fibres and the constitution of glass fibre form", *Journal of the Society of Glass Technology*, vol. 32, pp. 291-300, 1948.

140. I. Ahmed, P.S. Cronin, E. A. Abou Neel, A. J. Parsons, J.C. Knowles, and C.D. Rudd, "Retention of mechanical properties and cytocompatibility of a phosphate-based glass fibre/polylactic acid composite", *Journal of Biomedical Materials Research Part B: Applied Biomaterials*, vol. 89, no. 1, pp. 18-27, 2009.

141. I. Ahmed, A.J. Parsons, G. Palmer, J.C. Knowles, G.S. Walker and C.D. Rudd, "Weight loss, ion release and initial mechanical properties of a binary calcium phosphate glass fibre/ PCL composite", *Acta Biomaterialia*, vol. 4, no. 5, pp. 1307-1314, 2008.

142. X. Liu, D.M. Grant, G. Palmer, A.J. Parsons, C.D. Rudd and I. Ahmed, "Magnesium phosphate glass fibres for unidirectional reinforcement of Polycaprolactone composites", *Journal of Biomedical Materials Research Part B: Applied Biomaterials*, 2014, DOI: 10.1002/jbm.b.33324.

143. M.C. Zimmerman, H. Alexander, J.R. Parsons and P.K. Bajpai. "The design and analysis of laminated degradable composite bone plates for fracture fixation", In: T.L. Vigo, A.F. Turbak, editors. *High Tech Fibrous Materials. Washington: ACS Publications*, 1991. pp. 132-148.

144. D. Hull and T.W. Clyne, *An Introduction to Composite Materials*, Cambridge, UK: Cambridge University Press, 1996.

145. P.P Gohil and A.A. Shaikh, "Analytical investigation and comparative assessment of Interphase influence on elastic behaviour of Fibre reinforced composites", *Journal of reinforced plastics and composites*, vol. 29, no. 5, pp. 685-699, 2010.

146. J.L. Thomason, "Interfaces and Interfacial effects in glass reinforced thermoplastics", *Proceedings of the 28th Riso International Symposium on Materials Science: Interface Design of Polymer Matrix Composites – Mechanics, Chemistry, Modelling and Manufacturing*, pp. 75-92, 2007.

147. F.R. Jones, "The chemical aspects of fibre surfaces and composite interfaces and interphases and their influence on the mechanical behavioud of interfaces", *Proceedings of the 28th Riso International Symposium on Materials Science: Interface Design of Polymer Matrix Composites – Mechanics, Chemistry, Modelling and Manufacturing*, pp. 21-44, 2007.

148. S. Gao and E. Mäder, "Characterisation of interphase nanoscale property variations in glass fibre reinforced polypropylene and epoxy resin composites", *Composites: Part A*, vol. 33, no. 5, pp. 559-576, 2002

149. M.J. Lodeiro, S. Maudgal, L.N. McCartney, R. Morrell and B. Roebuck, "Critical review of interface testing methods for composites", Centre for Materials, Measurement and Technology, *National Physics Laboratory Report*, April 1998.

150. M.J. Pitkethly, J.P. Favre, U. Gaur, J. Jakubowski, S.F. Mudrich, D.L. Caldwell, L.T. Drzal, M. Nardin, H.D. Wagner, L. Di Landro, A. Hampe, J.P. Armistead, M. Desaeger and, I. Verpoest, "A round-robin programme on interfacial

test methods", *Composites Science and Technology*, vol. 48, no. 1-4, pp. 204-214, 1993.

151. M.R. Piggott, "Why interface testing by single-fibre methods can be misleading", Composites *Science and Technology*, vol. 57, no. 8, pp. 965-974, 1997.

152. D. Tripathi and F.R. Jones, "Measurement of the load bearing capability of the fibre/matrix interface by single-fibre fragmentation", *Compositess Science and Technology*, vol. 57, no. 8, pp. 925-935, 1997.

153. I. Verpoest, M. Desaeger and R. Keunings, "Critical review of direct micromechanical test methods for interfacial strength measurements in composites", In: H. Ishida, ed., *Controlled Interphases in Composite Materials*, Springer Netherlands, 1990, pp. 653-666.

154. D. Tripathi and F.R. Jones, "Review: Single fibre fragmentation test for assessing adhesion in fibre reinforced composites", *Journal of Material Science*, vol. 33, no. 1, pp. 1-16, 1998.

155. A. Kelly and W.R. Tyson, "Tensile properties of fibre-reinforced metals: copper/tungsten and copper molybdenum", *Journal of Mechanics and Physics of Solids*, vol. 13, no. 6, pp. 329-350, 1965.

156. F.A. Ramirez and L.A. Carlsson, "Modified single fibre fragmentation test procedure to study water degradation of the fibre/matrix interface toughness of glass/vinylester", *Journal of Material Science*, vol. 44, no. 12, pp. 3035-3042, 2009.

157. C.-Y. Hui, S.L. Phoenix and D. Shia, "The single-filament-composite test: A new statistical theory for estimating the interfacial shear strength and Weilbull parameters for fibre strength", *Composites Science and Technology*, vol. 57, no. 12, pp. 1707-1725, 1997.

158. D. Mendels, "Analysis of the single fibre fragmentation test", Centre for Materials, Measurement and Technology, *National Physics Laboratory Report*, 2001.

159. N. Melanitis, C. Galiotis, P.L. Tetlow and C.K.L. Davies, "Interfacial stress distribution in model composites: 2. Fragmentation studies on carbon fibre epoxy system", *Journal of Composite Materials*, vol. 26, no. 4, pp. 574-610, 1992.

160. C. Galiotis, "A study of mechanism of stress transfer in continuous- and discontinuous model composite by laser Raman spectroscopy", *Composite Science and Technology*, vol. 48, no. 1-4, pp. 15-28, 1993.

161. A.N. Netravali, R.B. Henstenburg, S.L. Phoenix and P. Schwartz, "Interfacial shear strength studies using the Single-Filament-Composite test I: Experiments on graphite fibres in epoxy", *Polymer Composites*, vol. 10, no. 4, pp. 226-241, 1989.

162. J.O. Outwater and M.C. Murphy, "Fracture energy of unidirectional laminates", *Modern Plastics*, vol. 71, pp.160-168, 1970.

163. J.V. Mullin, J.M. Berry and A. Gatti, "Some fundamental fracture mechanisms applicable to advanced filament reinforced composites", *Journal of Composite Materials*, vol. 2, no. 1, pp. 82-90, 1968.

164. J.V. Mullin and V.F. Mazzio, "Basic failure mechanisms in advanced composites", NASw2093, NASA, 1971.

165. A.T. DiBenedetto, "Measurement of thermomechanical stability of interphases", *Composite Science and Technology*, vol. 42, no. 1-3, pp. 103-115, 1991.

166. A.H. Nayfeh, "Thermomechanically induced interfacial stresses in fibrous composites", *Fibre Science and Technology*, vol. 10, no. 3, pp. 195-205, 1977.

167. X.-F Zhou, J.A. Nairn and H.D. Wagner, "Fibre-matrix adhesion from the single fibre composite test: nucleation of interfacial debonding", *Composites: Part A Applied Science and Manufacturing*, vol. 30, no. 12, pp. 1387-1400, 1999.

168. A.C. Johnson, S.A. Hayes and F.R. Jones, "The role of matrix cracks and fibre/matrix debonding on the stress transfer between fibre and matrix in a single fibre fragmentation test", *Composites: Part A*, vol. 43, no. 1, pp.65-72, 2012.

169. L.T. Drzal and M. Madhukar, "Fibre-matrix adhesion and its relationship to composite mechanical properties", *Journal of Materials Science*, vol. 28, no. 3, pp. 569-610, 1993.

170. X.-F Zhou, H.D. Wagner and S.R. Nutt, "Interfacial properties of polymer composites measured by push-out and fragmentation tests", *Composites: Part A*, vol. 32, no. 11, pp. 1543-1551, 2001.

171. L.T. Drzal, "The effect of polymeric matrix mechanical properties on the fibre-matrix interfacial shear strength", *Materials Science and Engineering*, vol. 126, no. 1-2, pp. 289-293, 1990.

172. S. Cozien-Cazuc, "Characterisation of resorbable phosphate glass fibres", University of Nottingham, 2006.

173. J.-M. Park, J.-W. Kong, J.-W. Kim and D.-J. Yoon, "Interfacial evaluation of electrodeposited single carbon fibre/ epoxy composites by fibre fracture source location using fragmentation test and acoustic emission", *Composites Science and Technology*, vol. 64, no. 7-8, pp. 983-999, 2004.

174. D. Tripathi, F. Chen and F.R. Jones. "The effect of matrix yield strain on the data reduction technique of the single-filament fragmentation test", *Composites Part A. Applied Science and Manufacturing*, vol. 27, no. 9, pp. 709-715, 1996.

175. A.C. Johnson, S.A. Hayes and F.R. Jones, "Data reduction methodologies for single fibre fragmentation test: Role of the interface and interphase", *Composites: Part A*, vol. 40, no. 4, pp. 449-454, 2009.

176. L. Yang and J.L. Thomason, Interface strength in glass fibre-polypropylebe measured using the fibre pull-out and microdebond methods", In: *17th International Conference on Composite Materials*, ICCM17, pp. 27-31, 2009.

177. A. Le Duigou, P. Davies and C. Baley, "Interfacial bonding of Flax fibre/Poly (L-Lactide) biocomposites", *Composites Science and Technology*, vol. 70, no. 2, pp. 231-239, 2010.

178. P. Herrera-Franco and L.T. Drzal, "Comparison of methods for the measurement of fibre/matrix adhesion in composites", *Composites*, vol. 23, no. 1, pp. 2-27, 1992.

179. J.F. Mandall, J.-H. Chen and F.J. McGarry, "A Microdebonding test for in-situ fibre-matrix bond and moisture effects", Proceedings of the 35th Conference on R.P./Composites Institute, *Society of the Plastics Industry*, Paper 26D, 1980b.

180. N.R. Sottos, R.L. McCullough and W.R. Scott, "The influence of interphase regions on local thermal displacements in composites", *Composites and Science Technology*, vol. 44, no. 4, 319-332, 1992.

181. E. Plueddemann, *Silane Coupling Agents*, New York City, New York: Plenum Press, 1991.

182. J.L. Thomason, "The interface region in glass fibre-reinforced epoxy resin composites: 1. Sample preparation, void content and interfacial strength", *Composites*, vol. 26, no. 7, pp. 467-475, 1995.

183. P. G. Pape and E. Plueddemann, "Methods for improving the performance of silane coupling agents", *Journal of Adhesion Science and Technology*, vol. 5, no. 10, pp. 831-842, 1991.

184. G. Tesoro and Y. Wu, "Silane coupling agents: the role of the organofunctional group", *Journal of Adhesion Science and Technology*, vol. 5, no. 10, pp. 771-784, 1991.

185. A. Bergeret, M.P. Bozec, C.-C. Quantin and A. Crespy, "Study of Interphase in glass fibre-reinforced poly (butylenes terephthalate) composites", *Polymer Composites,* vol. 25, no. 1, pp. 12-25, 2004.

186. B. Arkles and G. Larson, "Silicon compounds: silanes and silicones", 2nd ed., Gelest, Inc: Morrisville, Pennsylvannia, USA, 2008.

187. R.A. Khan, "Phosphate glass fibres and their interfaces in resorbable composites", University of Nottingham, 2006.

188. M.S. Hasan, I. Ahmed, A.J. Parsons, G.S. Walker and C.A. Scotchford, "The influence of coupling agents on mechanical property retention and long-term cytocompatibility of phosphate glass fibre reinforced PLA composites", *Journal of the Mechanical Behaviour of Biomedical Materials*, vol. 28, pp. 1-14, 2013.

# CHAPTER 3

# MATERIALS AND METHODOLOGY

## 3.1 SUMMARY

*This chapter details the materials and methods used to manufacture the oligomer Sorbitol-ended PLA (S-PLA) and phosphate glass fibres (PGF) investigated in this thesis. S-PLA was characterised using DSC, GPC, NMR and FTIR and the mechanical properties (tensile and modulus) of PGF were also obtained. The single fibre fragmentation test (SFFT) used to calculate the interfacial shear stress (IFSS) is also detailed here along with the preparation of single fibre composites (SFC) and unidirectional (UD) composites. The characterisation and imaging techniques used for SFC and UD composites are also described.*

## 3.2 MATERIAL MANUFACTURE

### 3.2.1 S-PLA Production

The following materials were used as purchased unless otherwise stated. High Molecular Weight Poly lactic acid (PLA) (Resin grade 6201-D, NatureWorks LLC, USA), 3,6-Dimethyl-1,4-dioxane-2,5-dione (DL Lactide) (Fisher Scientific, UK). Tin Octanoate, Chloroform, Sorbitol and Dichloromethane (DCM) were purchased from Sigma Aldrich (UK). HPLC grade Tetrahydrofuran (THF) was purchased from Fisher Scientific (UK).

The coupling agent sorbitol-initiated PLA (S-PLA) was selected due to positive results seen in the IFSS study conducted by Haque *et al.* [1]. It showed that of all the polymer-based coupling agents investigated by Haque *et al*., sorbitol ended PLA revealed a significantly enhanced improvement of IFSS.

Table 3.1 (below) shows the amount of each material (Lactide, sorbitol and tin octanoate) used for the three different chain lengths – **s**hort, **m**edium and **l**ong manufactured and characterised. Lactide and sorbitol were dried under a vacuum for 24 h prior to synthesis. The appropriate amount of dried Lactide, sorbitol and tin octanoate was placed in a round bottom flask with a magnetic stirrer and heated at 140°C under an inert atmosphere for 24 h. The polymer was then decanted onto aluminium foil and placed into a vacuum oven at 50°C for 1-2 days. The sample was collected and refrigerated until further use.

**Table 3.1:** *A list of codes for synthesised coupling agents and quantities of Lactide, sorbitol and tin octonoate used for each where 's' , 'm' and 'l' represent 'short', 'medium' and 'long', respectively.*

| Code | Lactide (g) | Sorbitol (g) | Tin Octonoate (g) |
|---|---|---|---|
| S-PLA_s | 15 | 2.184 | 0.972 |
| S-PLA_m | 15 | 0.546 | 0.243 |
| S-PLA_l | 25 | 0.0911 | 0.0405 |

### 3.2.2 Phosphate Glass Manufacture and Fibre Production

The phosphate glass formulations used were $40P_2O_5$-$24MgO$-$16CaO$-$16Na_2O$-$4Fe_2O_3$ (P40) and $45P_2O_5$-$24MgO$-$16CaO$-$11Na_2O$-$4Fe_2O_3$ (P45) (in mol%). The precursors used were sodium dihydrogen phosphate ($NaH_2PO_4$), calcium hydrogen phosphate ($CaHPO_4$), magnesium hydrogen phosphate trihydrate ($MgHPO_4.3H_2O$), iron phosphate dihydrate ($FePO_4.2H_2O$) and phosphorus pentoxide ($P_2O_5$) (Sigma Aldrich, UK). The salts were placed into a platinum crucible (5% Au/95% Pt, Birmingham Metal Company, UK) and heated to 350°C and held for 30 min. The crucible was then transferred to a melt furnace at 1100°C for 1.5 h and the resulting melt was poured onto a steel plate to cool to room temperature. The glass was then used to produce continuous fibres via a melt-draw spinning method using an in house fibre manufacturing facility (Figure 3.1). The fibres were stored in a desiccator prior to use.
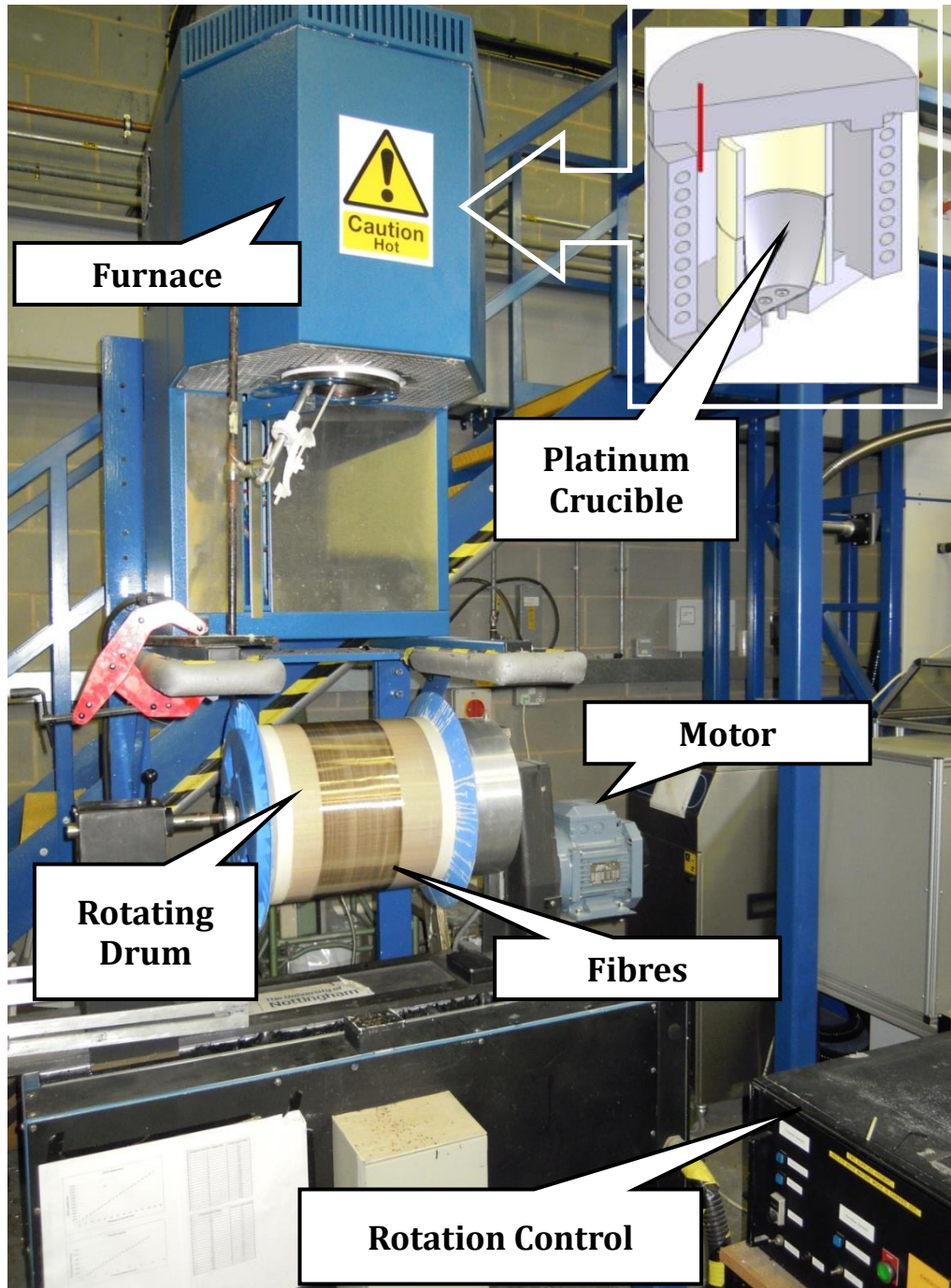
**Figure 3.1:** *In house fibre manufacturing rig with traversing drum*

## 3.3 CHARACTERISATION TECHNIQUES

### 3.3.1 Nuclear Magnetic Resonance (NMR)

A Bruker DPX300 (300MHz) spectrometer was used to obtain the $^1$H spectra for each of the coupling agents. Samples of each oligomer were dissolved in d-Chloroform CDCL$_3$. The chemical shifts were referenced against the residual solvent signal (7.26 ppm). The spectra were analysed using ACD Labs (Version 12.00, 2008) to determine the polymer to monomer conversion.

### 3.3.2 Gel Permeation Chromatography (GPC)

A refractive index (RI) detector with HPLC grade THF as the eluent was used to conduct GPC analysis, which was performed at 40°C with a flow rate of 1 ml/min through two PL gel Mixed-C columns. The columns were calibrated using Poly (styrene) (PS) and Poly (methyl methacrylate) (PMMA) standards. The calibration range set was 580 – 377,400 Da. The GPC equipment and standards were supplied from Polymer Laboratories (Varian Inc). Both PS and PMMA standards were used to assess the data obtained from the GPC. The data was analysed using the Cirrus GPC offline software (Version 3.0, 2006)

### 3.3.3 Differential Scanning Calorimetry (DSC)

A Thermal Analysis (TA) Q10 Differential Scanning Calorimeter (DSC) was used to find the glass transition temperature (T$_g$) of the synthesised coupling agents. Each oligomer was run from room temperature to 230°C at a ramp rate of 10°C/min for 2 cycles. Universal Analysis (TA) software was used to determine the T$_g$ values for each sample. The values shown in this report were taken from an average of three repeats.

### 3.3.4 Fourier Transform Infrared (FTIR)

Infrared spectroscopy of chopped fibres of around 1-2 mg was performed on a Bruker Tensor 27 spectrometer (Bruker Optics, Germany), operated in absorbance mode. Spectra were recorded in the region of 400 to 4000 wavenumbers using a Standard Pike ATR cell (Pike Technology, UK). The spectrum was analysed using OPUS software version 5.5.

### 3.3.5 X-Ray Diffraction (XRD)

XRD diffraction patterns of PLA were recorded using a D500 diffractometer (SIEMENS) operated at 40 kV and 25 mA, utilising a CuKα- radiation source ($\lambda$=0.154). The scans were controlled by the Diffrac-AC software program. For XRD analysis, samples were scanned using a step-scanning method with a step-size of 0.05° and 2 s intervals in the range from 2° to 50° of the diffraction angle (2θ).

### 3.3.6 Scanning Electron Microscopy (SEM)

Samples were coated with carbon or platinum and micrographs were taken using a Philips XL30 SEM (FEI, USA) at an accelerating voltage of 20 kV using SE (Secondary Electron) modes.

## 3.4 SINGLE FIBRE COMPOSITE (SFC)

### 3.4.1 Single Fibre Tensile Test

The mechanical properties of single fibres were conducted following the international standard BS ISO 11566 [2]. A Single Fibre Testing machine

(Rexvoth MiniTech and UV 1000 control unit) was used to measure the tensile strength and modulus of the fibres. The fibre diameter was measured and recorded using a Mituyoto Laser Scan Micrometer, LSM-6200. The tensile data was recorded and analysed using UVWin software. The Weibull shape and scale parameters for the fibre tensile strength were obtained using Minitab software (Version 16.1.0, 2010).

### 3.4.2 Single Fibre Composite (SFC) Production

Thin films of PLA were made using vacuum dried 6201D PLA pellets from NatureWorks. 5 g of PLA were placed between PTFE lined aluminium platens at 210°C and heated for 10 min after which they were pressed at 3-4 bar for 30 s. The films were cut into 75 x 25 mm rectangles and a single fibre was placed in between two films and held in place via adhesive tape. Prepared specimens were placed into a mould with 75 x 25 mm rectangular cut outs and heated at 210°C for ~10 min in a Daniels Heated Press (DHP) and pressed for a further 1-2 min at a load of 10 bar. The SFCs were then cooled to below $T_g$ at a rate of ~9°C/min by water flowing through the heated platens. A dog bone cutter with dimensions 65 x 10 x 2 mm was used to cut out coupons with a gauge length of 25 mm.
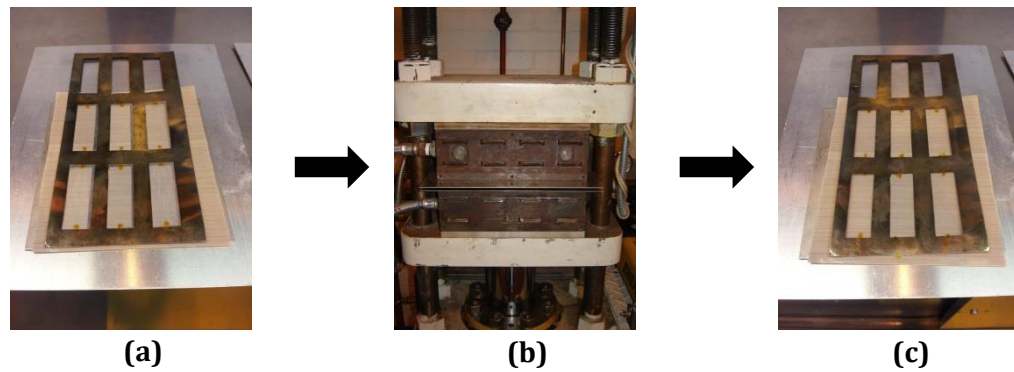
***Figure 3.2:*** *Single Fibre Composite preparation (a) single fibre composites and mould prior to compression moulding (b) compression moulding single fibre composites in Daniels Heated Press at 210°C and (c) single fibre composites ready for dog bone cutter*

### 3.4.3 Fibre Coating Process

The fibres were coated in a similar manner to that described in Haque *et al.* [1]. The sorbitol initiated PLA sizing solution was created using a sizing agent: solvent ratio which was varied for each of the coupling agents: S-PLA_s – 0.0064 moles: 100 ml; S-PLA_m – 0.0022 moles: 100 ml; S-PLA_l – 0.00013 moles: 100 ml. The fibre: sizing solution ratio used was 1.5 g: 100 ml. The solvent used was dichloromethane (DCM). Fibres were soaked in the sizing solution for 30 min and then dried at room temperature for 2 h. The fibres were then cured at 230°C for 3-4 h and dried at room temperature for 24 h. Excess S-PLA was removed by rinsing the fibres in solvent for 30 min before drying again at 120°C for 2 h.

### 3.4.4 Single Fibre Fragmentation Test

The IFSS for the specimens was obtained using the single fibre fragmentation test (SFFT). Dog bones were axially loaded in a Hounsfield Series S tensile testing machine using a 1 kN load cell and a crosshead speed of 1 mm/min.

### 3.4.5 Optical Microscopy

An optical microscope (Nikon Optiphot Microscope and Digital Camera DXM200F) was used to observe and count the number of fibre fragments in the gauge length of each of the specimen after testing. As it was difficult to see through the matrix in the prepared SFCs, the gauge length was cut and placed onto a microscope slide. It was softened to approximately 80°C on a hotplate for 5 min. A second slide was gently pressed on top of the softened matrix and allowed to cool to room temperature.

### 3.4.6 Interfacial Shear Stress Calculation

This was used to calculate the IFSS using the Kelly-Tyson model for the SFFT (Equation 3.1). The average IFSS value was taken from 10-15 repeat samples.

$$\tau_i = \frac{\sigma_f d}{2L_c}$$  *Equation 3.1*

$\tau_i$ is the IFSS; $\sigma_f$ is the fibre fragment strength; $L_c$ is the critical fragment length; d is the diameter of the fibre. $L_c$ is calculated using Equation 3.2 and 3.3 as follows.

$$L_f = \frac{L_0}{N}$$  *Equation 3.2*

$$L_c = L_f \frac{4}{3}$$  *Equation 3.3*

$L_f$ is the average fragment length; $L_0$ is the gauge length; N is the number of fragments. $\sigma_f$ is calculated from Weibull shape and scale parameters obtained from the fibre tensile data (Section 3.7.1)

$$\sigma_f = \sigma_0 \left( \frac{L_c}{L_0} \right)^{-1/m}$$

**Equation 3.4**

$\sigma_0$ is the scale parameter and m is the shape parameter. $\sigma_f$ and $L_c$ can now be put into Equation 3.1 to obtain IFSS, $\tau_i$.

## 3.5 UNIDIRECTIONAL (UD) COMPOSITES

### 3.5.1 UD Mat Production

Continuous P45 fibres were drawn via melt-draw spinning at ~1220°C and ~1500 rpm using a dedicated in house facility. The diameter of the fibres pulled at this speed was ~25 μm. The UD mats were drawn on a traversing drum for ~20 min yielding a mass of ~30 g of fibres per drum pulled. (*See* Figure 3.3)
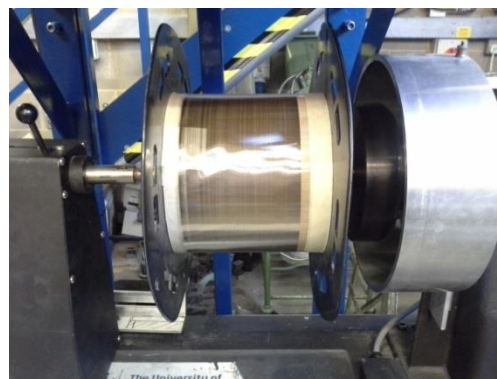


***Figure 3.3:*** *Unidirectional (UD) Mat of P45 fibres on drum after 20 minutes of continuous drawing.*

### 3.5.2 UD Mat Coating Process

UD mats for control composite production were sprayed with a 2.5% (wt/v) solution of NatureWorks PLA in chloroform to bind them together and left to dry overnight. The mats were removed from the drum and cut into 140 x 128 mm sections (Figure 3.4 (a)). S-PLA_s oligomer was made in 50 g batches as detailed in Section 3.2.1 and all individually characterised via GPC, NMR and DSC. The batches were then mixed together and characterised again. The GPC results obtained from the mixed batch was used to make the sizing solution for UD mat coating.

Two of the UD mats were sprayed with the sizing solution similar to control UD mats. The mats were left to dry for 2 h at room temperature, removed from the drum and cut as stated above. The mats were cured following the process described in Section 3.4.3. (*See* Figure 3.4 (b))

The coating process as described in Section 3.4.3 was scaled up for dipping a UD fibre mat in the sizing solution. A stainless steel tray of 650 x 200 x 30 mm tray was filled with the solution. The UD fibre mat was taped onto a PTFE sheet covering a steel mesh and placed in the tray. After the drying process described in Section 3.4.3 the mats were cut into 140 x 128 mm sections to produce dip coated S-PLA_s fibre mats (Figure 3.4 (c)).
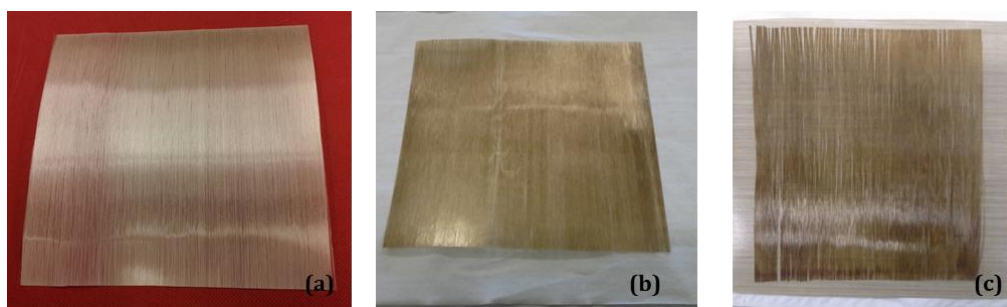


***Figure 3.4:*** *UD mats for (a) control P45 fibre sprayed with PLA (b) P45 fibre sprayed with S-PLA_s and (c) P45 fibre dip coated with S-PLA_s*

### 3.5.3 UD Composite Production

UD composites were prepared via a laminate film stacking process. PLA films were prepared by compression moulding as stated in Section 3.4.2 and were stacked alternately with UD mats in a mould cavity with dimensions 140 x 128 x 2 mm (Figure 3.5 (a)) between two metallic plates. The stack was then heated in the DHP for 10 min at 180°C and pressed for 10 min at 40 bar. The composite was cooled at a rate of ~10°C/min to below $T_g$ of PLA (~58°C). The resulting laminated composites were cut into 40 x 15 mm samples using a band saw with the fibres oriented longitudinally and transversely. The fibre volume and mass fractions of the composites were obtained using the matrix burn off method, according to the standard test method ASTM D2584-94.
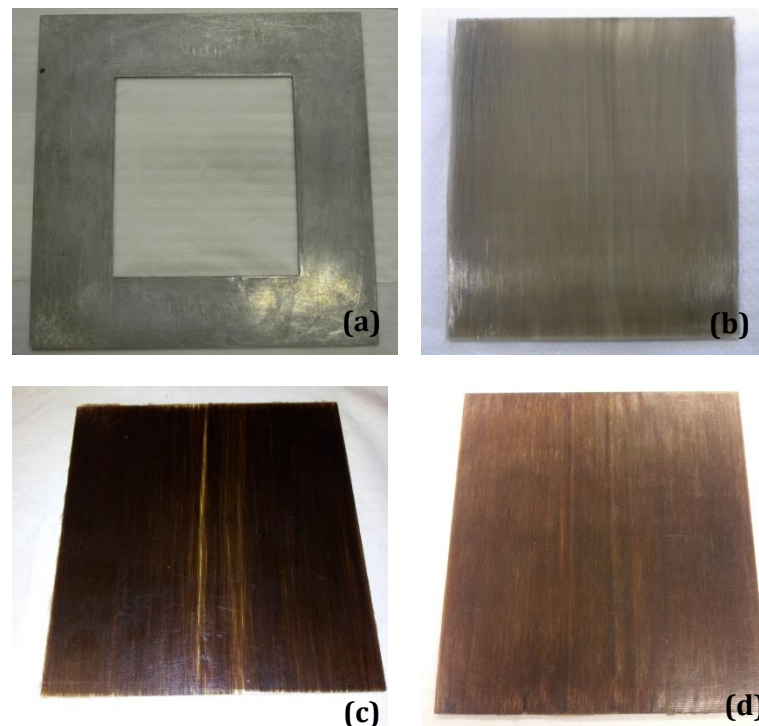


*Figure 3.5:* *(a) Composite mould used for composite manufacture (b) Control UD composite after removal from mould (c) S-PLA_s dip coated UD composite and (d) S-PLA_s spray coated UD composite*

### 3.5.4 Mechanical Properties

The initial flexural strength and modulus were evaluated by flexural (three-point bending) tests using a Hounsfield Series S testing machine. These measurements were done according to the standards BS EN ISO 14125:1998 [3]. A crosshead speed of 1 mm/min and a 1 kN load cell was used. The measurements were conducted on wet samples (i.e. samples were removed from degradation medium, pat dried and tested immediately) because a) to simulate mechanical properties of the composite within *in-vitro* conditions [4], b) drying of wet samples rapidly destroys their structure leading to a decrease of strength in measurement conditions [5] and c) drying wet samples can cause partial restoration of ionic bonds that could lead to misleading results [6]. The measurements were carried out in triplicate.

The mechanical testing was conducted according to the standards utilising the minimum number of replicates (n = 3). The reason for using this minimum number of samples was mainly due to lack of large quantities of PBG fibres to manufacture more composite specimens for all of the tests conducted. In addition, the spread of error between the replicates was considered sufficiently small that n = 3 were deemed suitable for the tests conducted.

### 3.5.4 Pycnometry

The density of specimens was measured using a Micrometrics AccuPyc 1330 helium pycnometer (Norcross, GA, USA). During the test, the helium pressure was set to 21 psi with a purging time of approximately 15 min. The measurements were conducted at room temperature and a relative humidity of 50%. Triplicate specimens were run for each sample

**3.6 DEGRADATION STUDY**

### 3.6.1 Single Fibre Composites

Degradation tests were carried out on fibres and on dog bone samples with embedded control fibres and S-PLA_s, S-PLA_m and S-PLA_l coated fibres. 0.2 - 0.3 g of each fibre batch were immersed in 30 ml of phosphate buffered solution (PBS) at 37°C for 1, 3 and 7 days. At each time point, at least 20 samples from each batch of fibre were tensile tested. For each batch of fibre, 30 single fibre composite dog bone samples were made as described in Section 3.4.2 and degraded in 30 ml of PBS at 37°C for 1, 3 and 7 days. At each time point, 10 samples were tensile tested and the corresponding fibre fragments counted for IFSS calculations.

### 3.6.2 UD Composites

UD composites were cut into samples of 40 x 15 x 2 mm – 24 were cut with the fibres oriented longitudinally and 24 were cut with the fibres oriented transversely. Each of the samples were immersed in 30 ml of PBS at 37°C for 1, 3, 7, 10, 14, 21 and 28 days (with the exception of spray coated S-PLA PGF/ PLA composites which were immersed for 1, 3, 7, 10 and 14 due to a limited number of composites available). At each time point 3 samples were tested for flexural modulus and strength. The study was conducted following the standard BS EN ISO 10993-13:2010 [7].

### 3.6.3 Water Uptake, Mass Loss and Wet Mass Change

The samples were taken out at each time point and blot dried before weight measurements were obtained. The mass of the samples was taken prior to

immersion, $m_i$. The mass of the sample at time, $t$, is denoted as $m$. The samples were then dried for two days at 50°C and the dry mass was measured, $m_d$. Equations 3.5 – 3.7 show how the water uptake (W), mass loss ($M_L$) and wet mass change ($W_m$) were calculated.

$$W = \frac{m - m_d}{m_d} \times 100$$

*Equation 3.5*

$$M_L = \frac{m_d - m_i}{m_i} \times 100$$

*Equation 3.6*

$$W_m = \frac{m - m_i}{m_i} \times 100$$

*Equation 3.7*

### 3.6.4 pH measurements

The pH of the PBS was measured before sample immersion and at each time point during the degradation study. Measurements were taken using Hanna Instruments pH 211 Microprocessor pH meter.

## 3.7 STATISTICAL ANALYSIS

### 3.7.1 Weibull Analysis

A two-parameter Weibull distribution was used to characterise the failure mode of brittle fibres such as PGF. Weibull parameters were obtained from the tensile strength data calculated using Minitab® 16 (version 16.2.2).

### 3.7.2 Analysis of Variance test

Analysis of Variance (ANOVA) tests were conducted to identify if there was a statistical difference between the means of two sets of data. A one-way ANOVA

test followed by Tukey's multiple comparison tests was used to conduct a statistical analysis on the values for IFSS, fibre strengths and moduli and flexural strength and moduli for UD composites. The ANOVA test was conducted using GraphPad Prism software (v. 5). To interpret the test, a $p$-value was considered with a 95% confidence interval and the value of significance level 0.05. The difference was accepted as significant when $p < 0.05$. All data are expressed as mean ± standard error.

## 3.8 REFERENCES

1. P. Haque, A.J. Parsons, I.A. Barker, I. Ahmed, D.J. Irvine, G.S. Walker, and C.D. Rudd, "Interfacial properties of phosphate glass fibres/PLA composites: Effect of the end functionalities of oligomeric PLA coupling agents", *Composites Science and Technology*, vol. 70, no. 13, pp. 1854-1860, 2010.

2. BS ISO 11566 (1996). "Carbon Fiber – Determination of the Tensile Properties of Single-filament Specimens, Geneva, Switzerland. International Standard".

3. BS EN ISO 14125 (1998). "Fiber Reinforced Plastic Composites— Determination of Flexural Properties, Geneva, Switzerland, International Standard".

4. R.M. Felfel, I. Ahmed, A.J. Parsons, P. Haque, G.S. Walker, and C.D. Rudd, "Investigation of Crystallinity, Molecular Weight Change, and Mechanical Properties of PLA/PBG Bioresorbable Composites as Bone Fracture Fixation Plates," *Journal of biomaterials applications*, vol. 25, no. 7, pp. 765-789, 2012.

5. P. Törmälä, J. Vasenius, S. Vainionpää, J. Laiho, T. Pohjonen, and P. Rokkanen, "Ultra-high-strength absorbable self-reinforced polyglycolide

(SR-PGA) composite rods for internal fixation of bone fractures: In vitro and in vivo study", *Journal of Biomedical Materials Research*, vol. 25, no. 1, pp. 1-22, 1991.

6.  S. Ramsay, R. Pilliar, L. Yang, and J. Santerre, "Calcium Polyphosphate/Polyvinyl acid-carbonate Copolymer Based Composites for use in Biodegradable Load-bearing Composites for Orthopaedic Implant Fabrication", *Key Engineering Materials*, vol. 284-286, pp. 787-790, 2005.

7.  BS EN ISO 10993-13:2010, "Biological evaluation of medical devices. Identification and quantification of degradation products from polymeric medical devices".

# CHAPTER 4

# INTERFACIAL SHEAR STRESS OF PHOSPHATE GLASS FIBRE REINFORCED POLY (LACTIDE) (PGF/PLA) SINGLE FIBRE COMPOSITES

## 4.1 SUMMARY

*This chapter reports the synthesis and characterisation of short (s), medium (m) and long (l) chain Sorbitol-ended Polylactic acid (S-PLA). All samples were synthesized to 100% conversion and characterised using Nuclear Magnetic Resonance (NMR), Gel Permeation Chromatography (GPC), Differential Scanning Calorimetry (DSC) and Fourier-transform Infrared (FTIR). It was determined that sorbitol was not bonded to the end of a single PLA chain as previously thought but rather it had two PLA chains bonded to two OH groups in the sorbitol structure.*

*The effects of S-PLA_s, S-PLA_m and S-PLA_l on the IFSS of $40P_2O_5$-$24MgO$-$16CaO$-$16Na_2O$-$4Fe_2O_3$ (P40) glass fibres embedded in a PLA matrix are also investigated. The coating concentration was found to be dependent on the molecular weight of the coupling agent. Optimising the coating concentration for S-PLA_s showed the optimum concentration to be 0.0064 moles with an IFSS value of $24 \pm 5$ MPa compared to the control IFSS value of $12 \pm 2$ MPa. The IFSS values for S-PLA_m and S-PLA_l single fibre composites (SFC) were also found to be significantly different to that of the uncoated control prior to degradation. Degradation studies on single fibre composites embedded with S-PLA_s, S-PLA_m and S-PLA_l coated fibres over 1, 3 and 7 days showed a 50-60% increase in IFSS over time compared to the control with uncorrected Weibull parameters. With corrected Weibull parameters, obtained from degrading the fibres over 7 days, the*

*IFSS was shown to decrease by 48% after 7 days respectively compared to the degraded control.*

*Single fibre fragmentation tests (SFFT) were carried out on $45P_2O_5$-$24MgO$-$16CaO$-$11Na_2O$-$4Fe_2O_3$ (P45) glass fibres (control and coated with S-PLA_s), to ensure that changing the glass formulation did not have an effect on the IFSS. P45 fibres yielded statistically similar IFSS values for both coated and uncoated fibres to those of P40 fibres when embedded in PLA. P45 fibres are easier to draw continuously than P40 fibres aiding in the manufacture of unidirectional mats.*

## 4.2 INTRODUCTION

Resorbable phosphate glass fibre (PGF) reinforced polymer composites are currently being investigated for bone repair applications. Fracture fixation plates are currently made from metals such as titanium alloys, stainless steel, nickel and cobalt-chrome [1-2]. Due to the difference in mechanical properties between the metals (Modulus: 55-240 GPa [1, 3-4]) and bone, the implants support the majority of the applied load, which can cause stress shielding effects (*see* Chapter 2 Section 2.2) [3, 5]. This, in addition to inflammatory responses or failure of the implant, can require secondary surgery for the device to be removed [6-7]. A material that has similar properties to bone and degrades at a predetermined rate whilst maintaining its mechanical integrity is attractive as it will exclude the need for secondary surgery and diminish the stress shielding effects, i.e. the bone will gradually take the load from the implant as it heals.

### 4.2.1 Macroscopic Composite Properties

The initial mechanical properties of resorbable fibre reinforced composites have been found to be similar to that of cortical bone (modulus: 3 – 22 GPa and tensile strength: 67 – 140 MPa [8-11]). Studies conducted (for the last ten years) show that a number of factors affect the mechanical properties of the composite including the chemical composition of the phosphate glass fibres, the polymer matrix used and the orientation of the fibres in the composite [12-14].

A study by Ahmed *et al.* showed the initial flexural strength and modulus of $50P_2O_5$-$40CaO$-$5Na_2O$-$5Fe_2O_3$ resorbable fibre reinforced PLA composites were dependent on the orientation of the fibre mats and on the fibre volume fraction ($V_f$). Composites with unidirectional (UD) mats had a higher initial flexural strength and modulus (~129 MPa and ~11.5 GPa, respectively) than the random (RM) mat composites (30% $V_f$: 105 MPa, 8.4 GPa; 40% $V_f$: 121 MPa, 9.4 GPa). After immersion in deionised water at 37°C for 6 weeks, UD and RM composites had flexural strength and modulus values of: UD ~30 MPa and 2 GPa; 30% $V_f$ random: 40-50 MPa and 2.5 GPa; 40% $V_f$ random: 40-50 MPa and 1.5 GPa, respectively [12].

Felfel *et al.* made resorbable fibre composite plates with both RM and UD mat $40P_2O_5$-$24MgO$-$16CaO$-$16Na_2O$-$4Fe_2O_3$ fibres embedded in PLA. The initial flexural strength and modulus for RM composites was 106 MPa and 6.8 GPa. The flexural strength and modulus for UD composites was 115 MPa and 9 GPa. The composites were degraded in phosphate buffered saline (PBS) solution at 37°C and after 95 days immersion the flexural strength and modulus had decreased to ~50 MPa and ~4.5 GPa for RM composites. For UD composites the flexural strength had decreased to ~50 MPa after 95 days while the flexural modulus

increased to ~11.5 GPa after the first week and after 2 weeks plateaued to ~10 GPa for the rest of the study [13].

The lack of retention of mechanical properties has been attributed to the loss of the bond between the fibre and the matrix during degradation due to hydrolysis taking place at the interface [15-17]. Maintaining this interface between the fibre and the matrix in fibre reinforced polymer composites has proven to be essential in order to retain the mechanical properties of the composite over time especially if the material is placed in a hydrolytic environment [15-19].

### 4.2.2 Interfacial properties

There are several methods by which the fibre and matrix can bond to each other: chemical reaction, molecular entanglement of polymer chains following interdiffusion, electrostatic attraction and mechanical keying, to name a few. The majority of polymer composites currently used in the automotive and aerospace industries are made with fibres (carbon, E-glass) that can be coated with commercially available coupling agents (such as silanes). [20-22]

There are three common methods used to assess the interfacial properties between the fibre and matrix in composite materials: pull-out/ microbond test, microindentation and the single fibre fragmentation test (SFFT) [23-24]. The advantages and disadvantages of these tests have been debated for years (*see* Chapter 2 Section 2.7.1) [25-29]. A study conducted by Pitkethly *et al*. demonstrated that the same interfacial test conducted with the same fibre-matrix combination in different labs yielded completely different results [26]. The SFFT method has been widely used to assess the interfacial shear stress (IFSS) and has been considered to provide a great deal of information about the

interface [23-24, 29-31]. It has also been successfully used to assess the IFSS of resorbable single PGF polymer composites [30, 32-34].

Cozien-Cazuc investigated the interfacial shear stress (IFSS) of single $40P_2O_5$-$20Na_2O$-$16CaO$-$24MgO$ fibres embedded in a PCL matrix. Some of the embedded fibres were sized with 3-aminopropyl triethoxy silane (APS). The IFSS of the sized and unsized fibres were ~13 MPa prior to degradation. After 1 day of immersion in deionised water, the unsized and sized fibres yielded an IFSS of ~24 MPa and ~22MPa, respectively. Cozien-Cazuc did not continue the study for the sized fibres however the unsized fibres had an IFSS of ~23 MPa and ~65 MPa after 3 and 7 days of immersion, respectively. The increase in the IFSS was noted as counter-intuitive and suggested that mechanical keying was taking place between the degraded fibre surface and the matrix improving the IFSS [32].

Haque *et al.* developed PLA-based coupling agents such as sodium ended PLA (PLA-Na) and acid ended PLA (PLA-acid) compared to commercially available coatings such as APS, Phosphonic acid and Hydroxy Ethyl Methacrylate (HEMA) to coat resorbable $40P_2O_5$-$24MgO$-$16CaO$-$16Na_2O$-$4Fe_2O_3$ (P40) fibres. The aim of synthesising such oligomers was so the acidic or sodium salt end groups would interact with hydroxyl groups present on the glass fibre surface, whilst the oligomeric (PLA) chain would interact well with the matrix polymer with the same structure [31]. Single fibres coated with coupling agents were embedded in a PLA matrix to give IFSS values of up to 15 MPa, whereas embedded control P40 fibres had an IFSS of ~9 MPa [33].

In a consequent study, Haque *et al*. studied the effects of synthesizing a PLA oligomer with hydroxyl groups as a chain end namely, ethylene glycol (EG-PLA), glycerol (G-PLA) and sorbitol (S-PLA). EG, G and S each have 1, 2 and 5

hydroxyl groups, respectively. The authors suggested that the number of hydroxyl groups on the functional chain end had a vital role in the ability of the oligomer to bond to the PGF surface. It was found that the multi-hydroxyl end group sorbitol yielded the largest increase in IFSS (23.2 ± 10.3 MPa) for P40/PLA composites compared to the control (uncoated) fibres (14.3 ± 6.1 MPa) [34].

In both studies by Haque *et al.* gel permeation chromatography (GPC), matrix assisted laser desorption ionization time of flight mass spectroscopy (MALDI-TOF MS), nuclear magnetic resonance (NMR) and differential scanning calorimetry (DSC) were all used to characterize the synthesized PLA oligomers. Additionally, thermogravimetric analysis (TGA), XPS and SEM were used to confirm that the oligomers were on the glass fibre surfaces [33-34].

This chapter builds on this prior work. S-PLA was synthesised to different chain lengths to determine the effect on chain length upon the quality of the bond achieved between the fibre and the matrix in a system containing PLA matrix polymer and a degradable PGF. The synthesis of S-PLA was taken to 100% conversion and NMR, GPC, DSC and FTIR techniques were used to confirm the conversion, molecular weight, glass transition temperature and the presence of the sorbitol chain end. The SFFT was used in the studies conducted by both Cozien-Cazuc and Haque *et al.* This method has been used in this study to assess the IFSS of fibres coated with sorbitol-initiated PLA (S-PLA) of three varying chain lengths designated short (S-PLA_s), medium (S-PLA_m) and long (S-PLA_l). In addition to having the capability to conduct this test, the SFFT allowed for a direct comparison with work done by Haque *et al.* and Cozien-Cazuc. The coating concentration of S-PLA_s was optimised to find the concentration that would obtain the highest IFSS value. A degradation study of the single fibre composites

with embedded coated fibres and control fibres was conducted to investigate the resulting effect on the IFSS. One-way ANOVA tests were conducted to identify statistical difference between the data sets. The difference was accepted as significant when $p < 0.05$ (*See* Chapter 3 Section 3.7.2).

## 4.3 RESULTS AND DISCUSSIONS

### 4.3.1 Synthesis of Sorbitol-ended PLA from Dilactide

A previous study of sorbitol-initiated Polylactic acid (S-PLA) synthesised these oligomer via degradation of NatureWorks (NW) Ingeo PLA 3251D [34]. However, this strategy was proved an unacceptable method for using in this study as it allowed insufficient control of the molecular weight of the resulting oligomer. S-PLA was therefore synthesised *via* direct polymerisation of the dilactide monomer as described in Chapter 3 section 3.3.1 and by Barker *et al.* [35].

In this method, sorbitol was used as an initiator for a ring opening polymerisation of a cyclic dilactide monomer and tin octanoate was used as the pre-catalyst as shown in Figure 4.1.
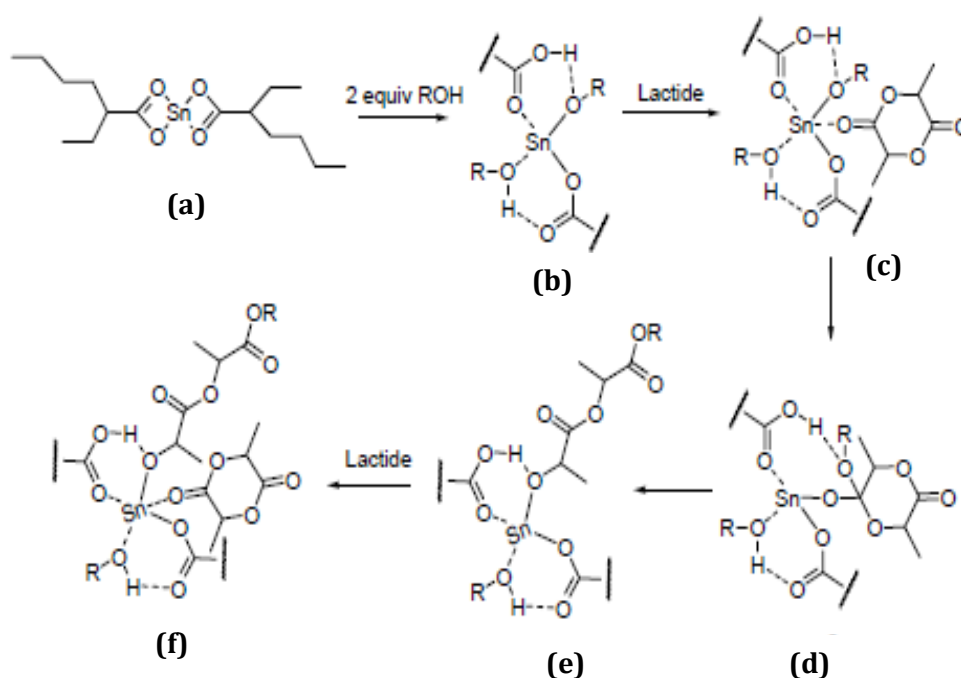
***Figure 4.1:*** *Coordination-insertion mechanism of tin (II) octanoate (Sn(Oct)₂) catalysed polymerisation of L-lactide: (a) Sn(Oct)₂, (b) Alcohol initiator exchange with octoate ligands, (c) Coordination of lactide to metal centre, (d) Insertion of the alcohol, (e) Ring Opening and (f) Generation of Linear monomer and beginning of propagation [36].*

In this reaction, sorbitol reacts with the tin octanoate to form the true catalytic species [34, 37]. Barker *et al.* stated that the mechanism for the catalyst to be formed requires both octanoate ligands to be replaced by hydroxyl species, i.e. two molecules of sorbitol bonds to become a ligand [35]. This consequently triggered the coordination-insertion mechanism ring opening polymerisation (ROP) of the dilactide monomer that started the chain growth of the PLA oligomer. Figure 4.1 shows a general coordination-insertion mechanism for polymerisation of L-lactide [36]. Tin octanoate is a preferred catalyst in the polymerisation of PLA due to high reaction rates, high conversion rates and the ability to yield high molecular weight polymers [36, 38]. It is also the most industrially applied catalyst for commercial manufacture of PLA polymers and is FDA approved.

The resulting S-PLA oligomer was initially assumed to have a sorbitol chain end. However, it is now thought that two PLA chains were formed off the

primary hydroxyls of sorbitol. The chemical structures of D,L lactide, sorbitol, PLA and the proposed structure of S-PLA are shown in Figure 4.2. Figure 4.2 (b) shows the chemical structure of sorbitol. The carbons that carry the hydroxyl groups ($CH_2OH$) are attached one alkyl group, in this case CH. These are the two primary hydroxyl groups that the PLA chains are formed off of (Figure 4.2 (d)). The 4 remaining hydroxyl groups in sorbitol are identified as secondary hydroxyls (as the carbon with the hydroxyl (CHOH) is joined to two alkyl groups.

It should be noted that the final oligomers (S-PLA_s, S-PLA_m and S-PLA_l) were not purified.
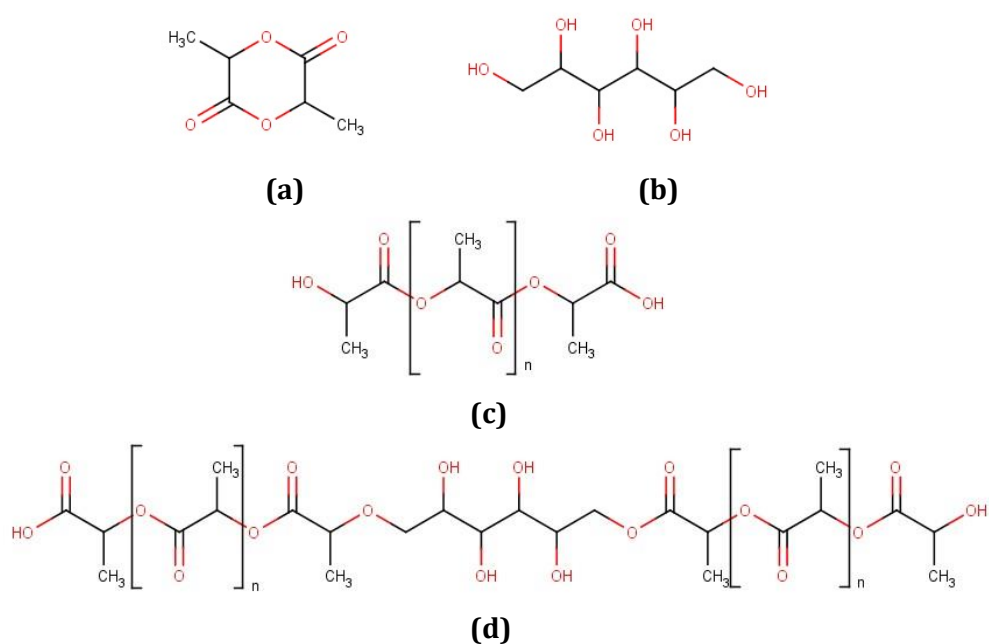


**Figure 4.2:** *Chemical structures of (a) D,L Lactide (b) Sorbitol (c) PLA and (d) S-PLA*

### 4.3.2 Nuclear Magnetic Resonance (NMR) Analysis

The NMR analysis was conducted as detailed in Chapter 3 Section 3.2.1. Figures 4.3-4.5 shows the ^{1}H-NMR spectra for S-PLA_s, S-PLA_m and S-PLA_l, respectively.
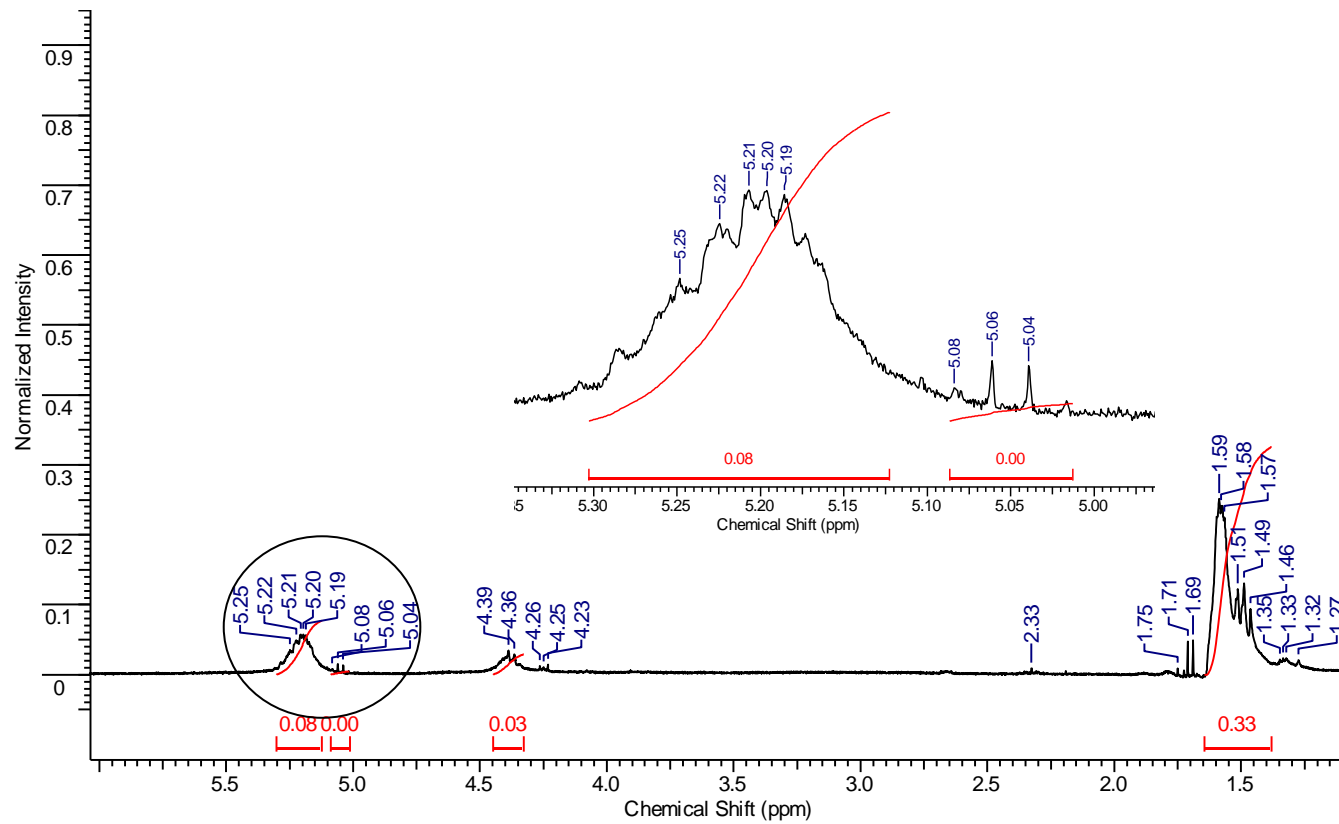
**Figure 4.3:** *¹H-NMR spectra of S-PLA_s oligomer. The insert shows the polymer (left) and monomer (right) peaks.*
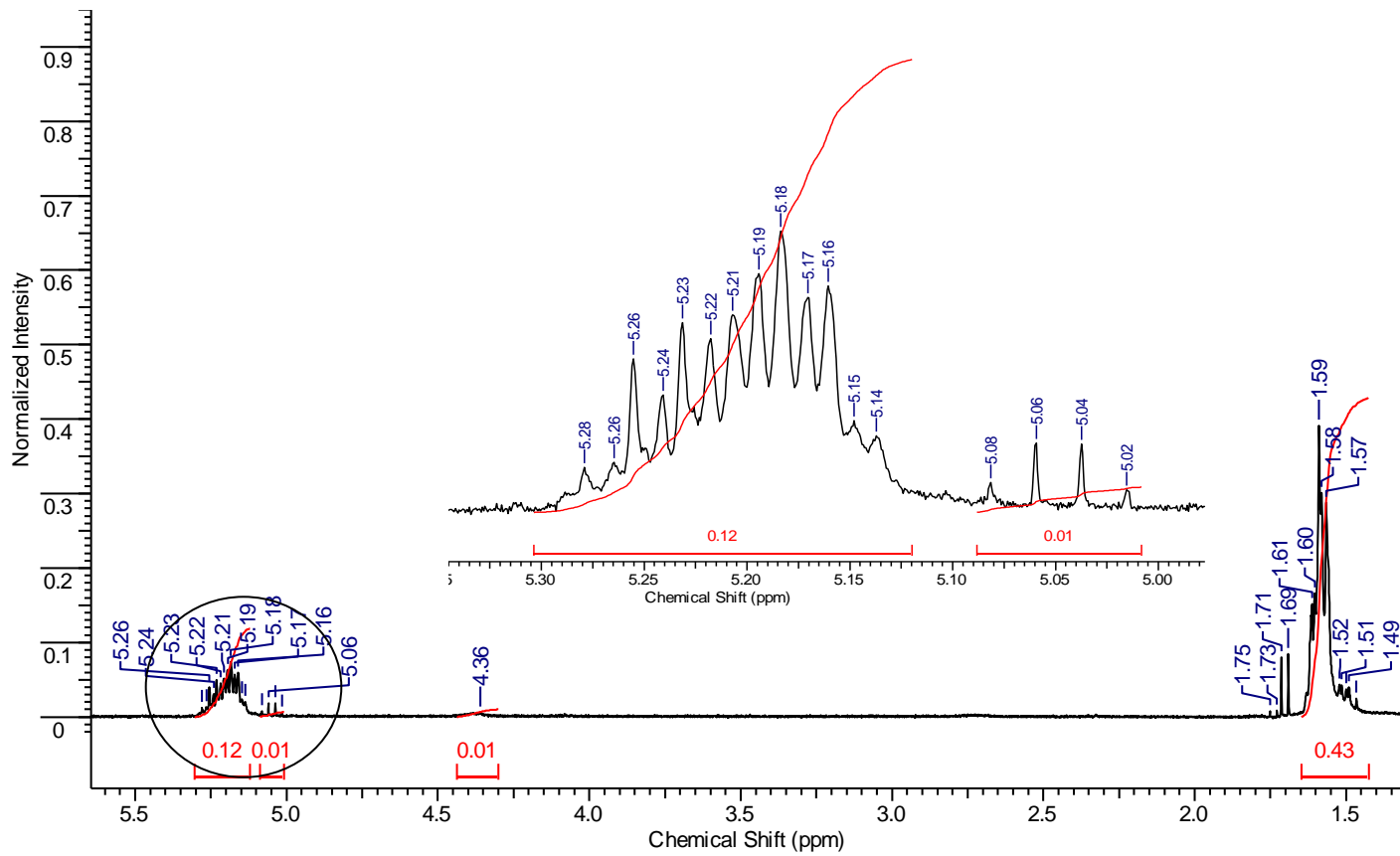
**Figure 4.4:** *¹H-NMR spectra of S-PLA_m oligomer. The insert shows the polymer (left) and monomer (right) peaks.*
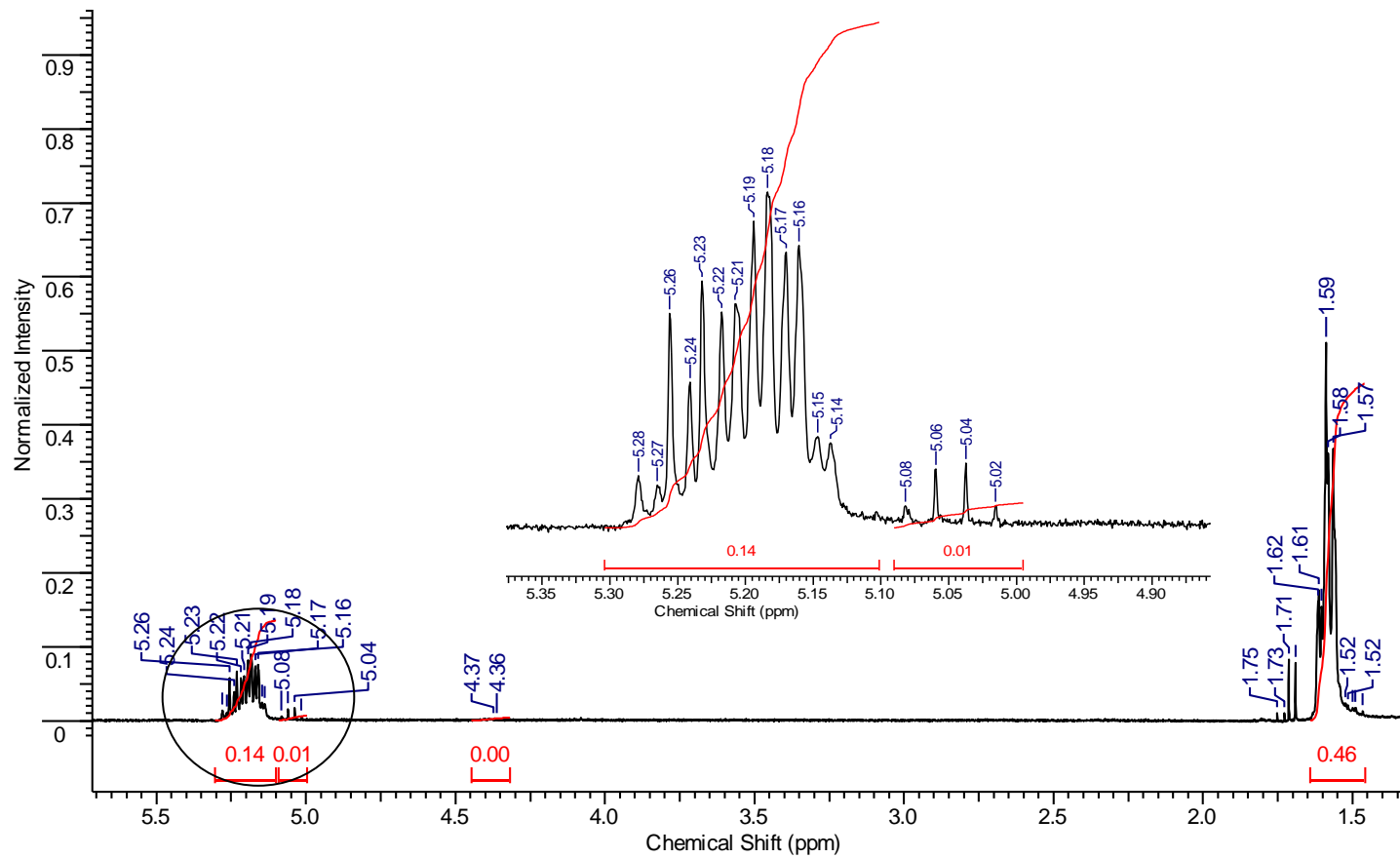
**Figure 4.5:** *¹H-NMR spectra of S-PLA_l oligomer. The insert shows the polymer (left) and monomer (right) peak*

All three spectra show three polymer peaks at δ 5.19, 4.36 and 1.59. Comparing the integrals of the polymer peaks at δ 5.19 to the monomer peak at approximately δ 5.08-5.02 provides an approximate conversion rate (inserts in Figure 4.3-4.5). For example the integral for the polymer peak in Figure 4.4 is 0.12 and the integral for the monomer peak is 0.01 which equates to ~8.33 ± 5 %. This suggests that approximately ~90 ± 5 % of S-PLA_m has been converted to polymer. Table 4.1 shows the approximate conversions for all three oligomers. There are also four additional peaks at δ 1.75-1.69 that appear on all three spectra. These can be attributed to the OH groups in sorbitol as confirmed by Haque [37].

The polymer peaks at δ 5.19 (CH) and δ 1.59 (CH$_3$) of the NMR spectra shown in Figure 4.3-4.5 are indicative of the repeat units in a PLA chain [37, 39]. The calculation for conversion was taken using the δ 5.19 peak because the δ 1.59 peak has the propensity to interfere with any residual lactic acid monomer in the system [39]. The peak at δ 4.36 is representative of the PLA chain end CH(CH$_3$)OH [37, 39]. It should be noted that interpretation of these spectra was conducted with the aid of a fellow research student from the Polymer Chemistry Department at the University of Nottingham. These spectra were used for the sole purpose of confirming the conversion.

**Table 4.1:** *Polymer-Monomer conversions as calculated from the peak integrals for all six coupling agents $^1$H-NMR spectra*

| Coupling agent | Polymer-Monomer conversion (%) |
|---|---|
| S-PLA_s | > 95 ± 5 |
| S-PLA_m | ~ 90 ± 5 |
| S-PLA_l | ~ 90 ± 5 |

### 4.3.3 Gel Permeation Chromatography (GPC) Analysis

GPC analysis was conducted using both the Polystyrene (PS) Standards and the Poly (methyl methacrylate) (PMMA) standards as discussed in Chapter 3 Section 3.3.2. Since the aim was to create three coupling agents with three distinct molecular weights, both sets of standards were initially used to assess the number average molecular weight ($M_n$), the peak molecular weight ($M_p$) and the polydispersity index (PDI). Note that PLA standards do not exist and both PS and PMMA standards have been used to assess the molecular weight of PLA-based polymers [40-41]. Also note that, like NMR analysis, the author was aided by the Polymer Chemistry Department at the University of Nottingham in interpretation of GPC results.

Initially, the synthesis of the S-PLA oligomers were stopped at 8 h in order to reach ~70% conversion and to keep the PDI closer to unity to prevent transesterification [35, 42]. Table 4.2 shows the corresponding GPC values for these initial oligomers. The results show very high PDI values which were not expected and subsequent NMR analysis (not shown in this thesis) yielded conversions < 70% and > 95%. The coupling agents were synthesised for 24 h to reach a conversion > 90% due to the lack of consistency in these results. It should be noted that these were analysed using PS standards only.

Table 4.3 shows the values for $M_n$, $M_p$ and PDI using both PS and PMMA standards for the coupling agents S-PLA_s, S-PLA_m and S-PLA_l synthesised for 24 h. As the $M_n$ values for S-PLA_s do not show a significant difference, transesterification is not considered a problem at shorter chain lengths. In order to keep consistency, S-PLA_m and S-PLA_l were also synthesised for the full 24 h (Chapter 3 Section 3.3.2).

**Table 4.2:** *Summary of the actual number average molecular weight ($M_n$), the peak average molecular weight ($M_p$) and the Polydispersity index (PDI) using PS standards for all three coupling agents stopped at 8 h*

| Coupling agent | $M_n$ | $M_p$ | PDI |
|---|---|---|---|
| S-PLA_s | 643 | 1176 | 2.01 |
| S-PLA_m | 337 | 676 | 2.17 |
| S-PLA_l | 9408 | 46618 | 4.04 |

**Table 4.3:** *Summary of the actual number average molecular weight ($M_n$), the peak average molecular weight ($M_p$) and the Polydispersity index (PDI) using both PS and PMMA standards for all three coupling agents with a synthesis time of 24 h*

| Coupling agent | $M_n$ | | $M_p$ | | PDI | |
|---|---|---|---|---|---|---|
| | PS | PMMA | PS | PMMA | PS | PMMA |
| S-PLA_s | 639 | 1221 | 829 | 1517 | 1.50 | 1.39 |
| S-PLA_m | 3412 | 4972 | 5113 | 8128 | 1.54 | 1.66 |
| S-PLA_l | 17719 | 25974 | 40999 | 53509 | 2.14 | 1.89 |

It is evident that the standards used during analysis affect the $M_n$ value. PMMA standards yield a $M_n$ value that is approximately twice that of the $M_n$ from PS standards. Even so, these results confirmed that three coupling agents of different chain lengths were synthesized. However, PMMA standards were solely used for the GPC analysis for this study as the chemical structure of PMMA is similar to that of PLA, i.e. similar repeat unit (*see* Figure 4.6). Therefore the analysis given by PMMA standards gave a closer estimation of $M_n$ values than PS standards.
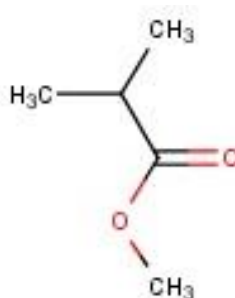


**Figure 4.6:** *Chemical structure of methyl methacrylate, monomer of Poly (methyl methacrylate)*

The results also confirmed > 90% conversion of the coupling with PDI values over 1.5. This high PDI value indicated more than 70% monomer-polymer conversion and consequently a broad variation in molecular weight distribution. At this point in the oligomer synthesis most of the monomer had converted to polymer [42]. The broad variation could be indicative of the proposed chemical structure of S-PLA (Figure 4.2 (d)) or, more likely, a combination of PLA chains formed from one or both primary hydroxyl groups. Nguyen *et al.* states that after 90% conversion transesterification processes contribute to polymer hyperbranching processes [43]. Therefore it can be assumed that PLA chains are forming off of one or more of the secondary hydroxyls. Studies are being conducted to confirm this.

The oligomers were not purified after synthesis, only dried at 50°C for 48h. It is likely that there were some impurities or residual monomer remaining. The GPC values given in Table 4.2 were taken after drying. There did not appear to be a significant difference in the values taken prior to drying. Figure 4.7 shows the molecular weight distribution for S-PLA_m using both PS and PMMA standards. The lack of a secondary peak to the left of the main peak is indicative of very little or no monomer present in the oligomers. This further confirms the conversion of the oligomers shown in Table 4.1.

GPC is not as sensitive for low molecular weight samples, making it difficult to obtain an accurate $M_n$ value [44]. As the coupling agents synthesized in this study were completely polymerised resulting in broad variations in chain lengths, the $M_n$ values obtained were accepted to be representative of the samples used to coat the fibres.
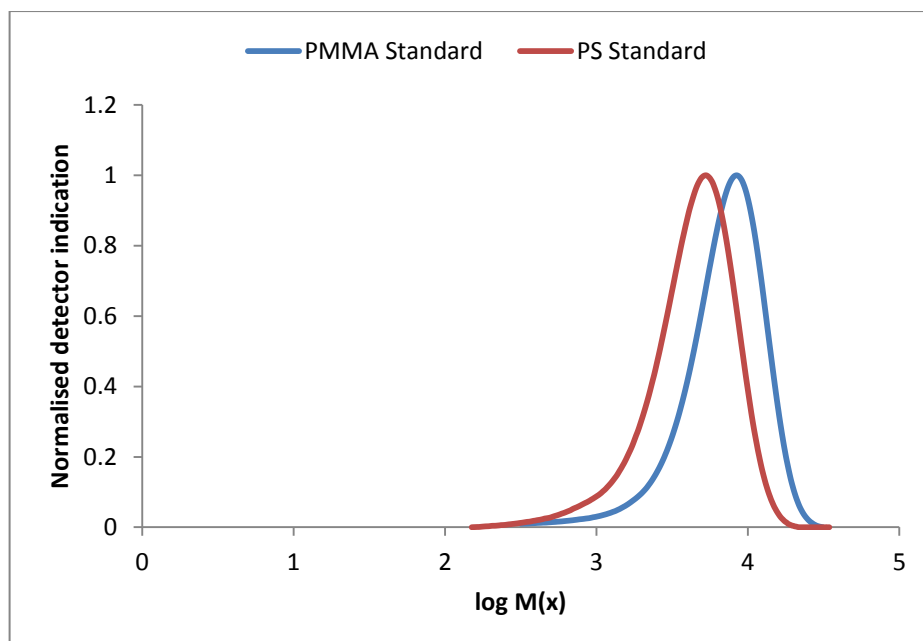
***Figure 4.7:*** *Graph showing the normalised detector indication of the molecular weight distributions for S-PLA_m using both Polystyrene (PS) and Poly (methyl methacrylate) (PMMA) standards.*

### 4.3.4 Differential Scanning Calorimetry (DSC) Analysis

The DSC analysis, conducted using the method described in Chapter 3 section 3.3.3, was used to observe the changes in the glass transition temperature ($T_g$) of S-PLA due the difference in chain length. The DSC traces for a single sample of S-PLA_s, S-PLA_m and S-PLA_l are shown in Figure 4.8. As stated in Chapter 3, the average $T_g$ was measured over three samples for each coupling agent.
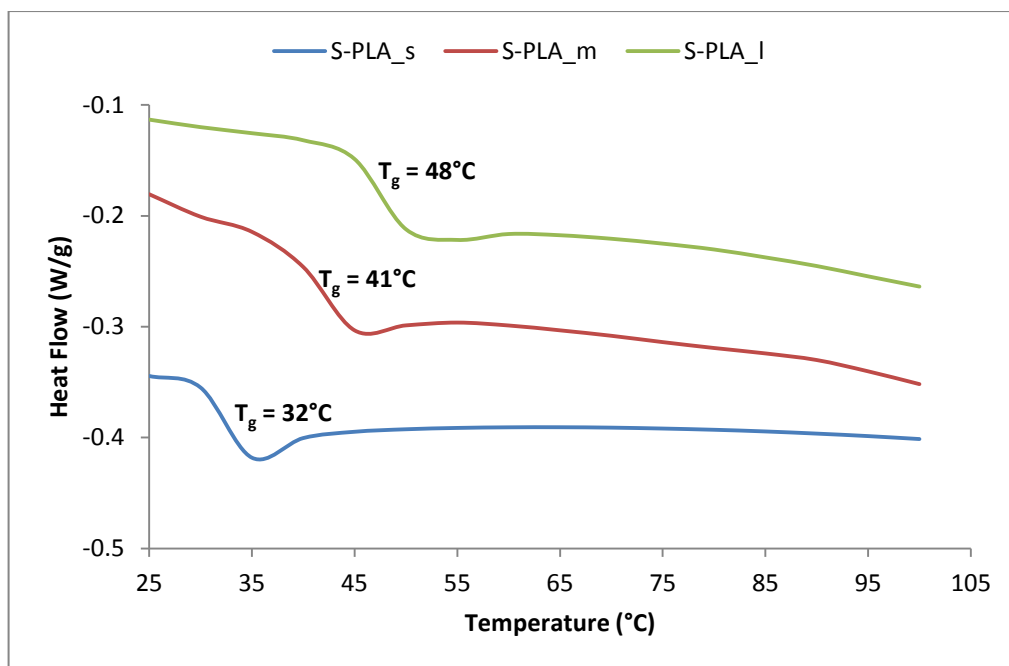
***Figure 4.8:*** *The DSC curves for sample S-PLA_s, S-PLA_m and S-PLA_l showing the shift in glass transition temperature, $T_g$ for a single sample of different oligomer chain lengths. The trace is shown for temperatures from 25°C to 100°C.*

Figure 4.9 shows the average $T_g$ values obtained for S-PLA_s (35.9°C), S-PLA_m (41.4°C) and S-PLA_l (48.0°C) plotted against the $M_n$ values. This data is extremely useful for compiling an initial Flory-Fox graph for S-PLA (Figure 4.9) which can be used to estimate the expected $T_g$ before synthesising the oligomer coupling agent [45]. The glass transition temperature, $T_g$, of the coupling agents S-PLA_s, S-PLA_m and S-PLA_l had a relationship with increasing chain length (Figure 4.9). At low molecular weights, the $T_g$ is affected by the polymer chain end, which in this case is sorbitol [46-47] confirming the theory set out by Flory-Fox equation, that the $M_n$ of a polymer is related to its $T_g$ [48-49]. It can also be suggested that increasing the chain length further will result in the $T_g$ tending towards that of PLA (55°C-60°C [50]) and that the longer the chain length the smaller the effect the functional chain end has on the $T_g$ [51]. This relationship also allows for the $T_g$ to be predicted should the synthesis of another chain length be investigated. The $T_g$ for PLA is also shown in Figure 4.9.
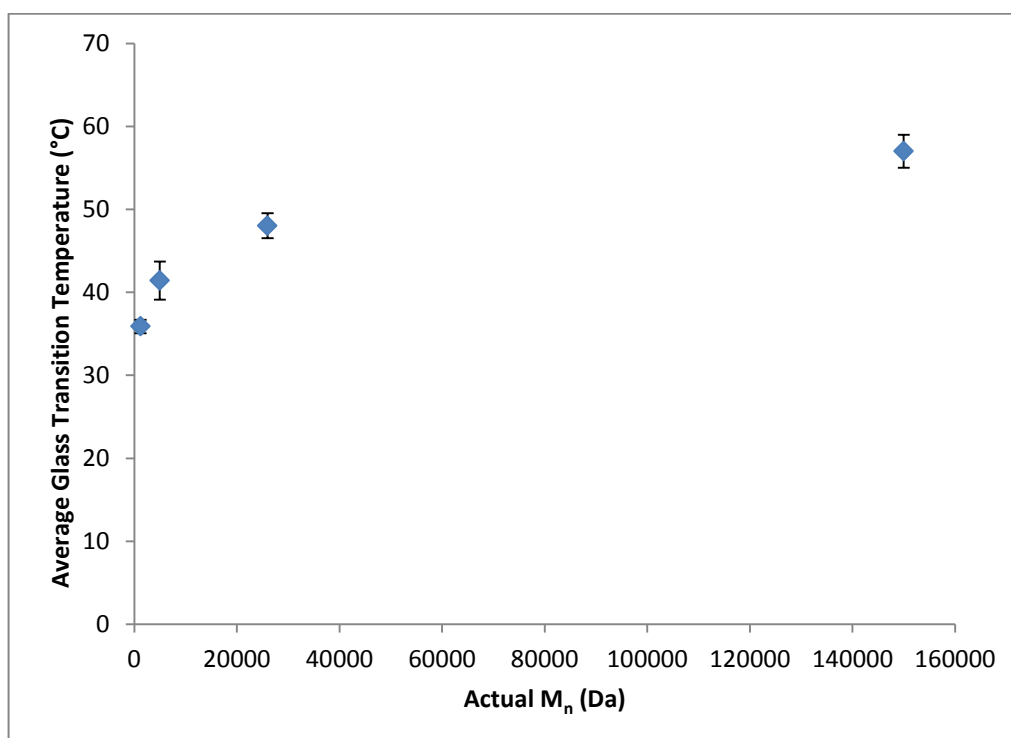
**Figure 4.9:** *Flory-Fox graph for S-PLA and PLA showing the change in average glass transition temperature, $T_g$, with increasing chain length. The $T_g$ for PLA was taken from the data sheet for NatureWorks 6201D [50].*

### 4.3.5 Fourier Transform Infrared (FTIR)

FTIR analysis was conducted using the method described in Chapter 3 section 3.3.4. The FTIR spectra between 4000 cm$^{-1}$ and 3100 cm $^{-1}$ for S-PLA_s and S-PLA_m are shown in Figure 4.10. The broad peak seen at 3600-3200 cm$^{-1}$ for both S-PLA_s and S-PLA_m suggested the presence of hydroxyl (OH) groups. These peaks are related to the stretching of the OH group [52-54]. The FTIR analysis conducted by Haque on S-PLA and sorbitol were similar to the results obtained in Figure 4.10. Haque attributed this peak to the free hydroxyl groups in sorbitol on the PLA chain confirming the presence of sorbitol in the oligomers synthesised in this study [37]. A sufficient signal for S-PLA_l could not be obtained due to the size of the oligomer chain. FTIR measures the head groups

present in the sample used for analysis. The head group in long chain polymers is difficult to detect as it is comparatively smaller than overall chain length.
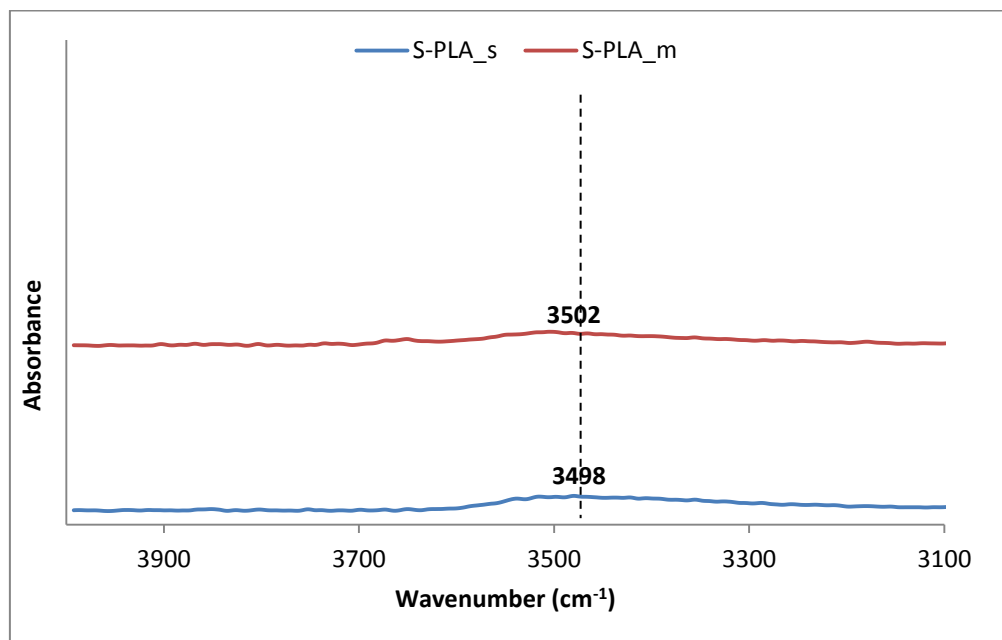


**Figure 4.10:** *FTIR spectra of S-PLA_s and S-PLA_m oligomers between 4000 and 3100 cm$^{-1}$*

### 4.3.6 Determining Fibre Coating Concentrations

The fibres were coated as described in Chapter 3 Section 3.4.3. The coating concentrations used were: S-PLA_s – 0.0064 moles: 100 ml; S-PLA_m – 0.0022 moles: 100 ml; S-PLA_l – 0.00013 moles: 100 ml. The S-PLA_m concentration was chosen to match the coating concentration used by Haque *et al.* [34]. It should be noted that Haque *et al.* used Polystyrene Standards to assess the molecular weight of coupling agents. Therefore the concentration of 0.0043 moles could not be used here. Using the molecular weight of Haque *et al.*'s S-PLA based on Poly (methyl methacrylate) Standards, the coating concentration was found to be 0.0022 moles. The coating concentration for S-PLA_l was chosen based on the ease at which the single fibres could be separated. This was not optimised as increasing the concentration of high molecular weight oligomeric samples (Table

4.3) meant that increasing amounts of the material would be required for coating. It was found that increasing the mass of S-PLA_l for dissolution in DCM (Chapter 3 Section 3.4.3) lead to an increase in the viscosity of the coating solution. This made it difficult to separate fibres from the bundle due to the occurrence polymer-polymer interactions. S-PLA_s was therefore selected to be optimised as it was easier to handle and manufacture.

### 4.3.7 Fibre Mechanical Properties

Control uncoated fibres and S-PLA_s, S-PLA_m and S-PLA_l coated P40 fibres were tensile tested as described in Chapter 3 Section 3.4.1. Figure 4.11 shows the initial fibre properties of control fibres and S-PLA_s, S-PLA_m and S-PLA_l coated P40 fibres. The tensile strengths obtained were 461 ± 73 MPa, 768 ± 175 MPa, 549 ± 190 MPa and 613 ± 183 MPa, respectively. The respective tensile moduli for the same fibres were 63 ± 3 GPa, 69 ± 7 GPa, 66 ± 5 GPa and 70 ± 8 GPa. The coated fibres all have a higher initial tensile strength than that of control. The statistical analysis showed that there was no significant difference in the tensile strengths and moduli of the S-PLA_m and S-PLA_l coated fibres when compared to those of the control fibres for a value of $p$ for $p > 0.05$. However it must be noted that the fibre tensile strength of the S-PLA_s coated fibres was significantly greater than that of control fibres and was statistically different to the tensile strengths of the other coated fibres for a value of $p$ for $p < 0.05$.
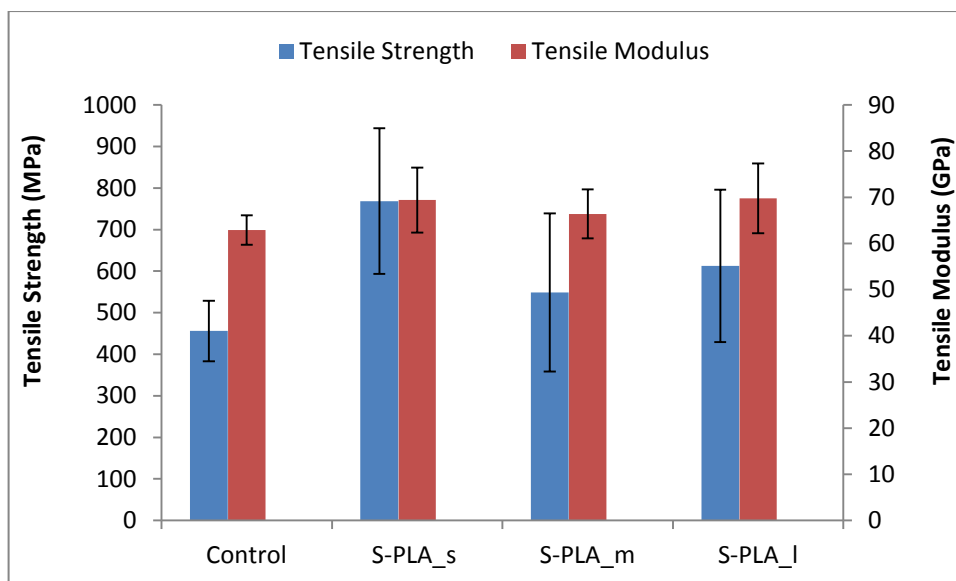
**Figure 4.11:** *Fibre strength and modulus of control fibres and S-PLA_s, S-PLA_m and S-PLA_l coated fibres prior to degradation, n ≥ 20*

Haque *et al.* obtained fibre strength of 321 ± 21 MPa for control P40 fibres which were significantly lower than the strength obtained for control P40 fibres in this study for a *p* value of *p* < 0.05 [34]. This was expected because the fibres in Haque *et al.*'s study were annealed for 1.5 hours at 474 °C [34, 37]. Annealing fibres decreases the fibre mechanical properties however it also lowers the degradation rate and changes the mode of PGF dissolution [12, 32, 37, 55-36]. The tensile strength of S-PLA_m coated fibres is statistically larger (*p* < 0.05) to that of the S-PLA coated fibres (340 ± 24 MPa) in Haque *et al.*'s study even though these fibres were coated with the same coating concentration [34]. The fibres in Haque *et al.*'s study were annealed prior to coating. This can be attributed to the lower tensile strength of the S-PLA coated fibres in Haque *et al.*'s study compared to the S-PLA coated fibres in this study.

Fibres in this study were not annealed due to the fact that the unidirectional (UD) fibre mats were aligned via an in house facility (Chapter 3 Section 3.5.1) and not manually [37, 57]. There is no method in place to anneal

the fibres without removing from the drum (*see* Figure 3.1). Removing the UD fibres without applying a binding agent would result in loss of UD orientation.

Figure 4.12 shows the tensile strengths of the control and coated fibres after degradation at 1, 3 and 7 days. The strengths of the control fibres shows a steady decrease from 461 ± 73 MPa prior to degradation to 310 ± 69 MPa after 7 days degradation in PBS at 37°C. The statistical analysis of control fibres between day 0 and day 7 showed that there is a significant difference in the tensile strength values. The tensile strengths of S-PLA_s, S-PLA_m and S-PLA_l coated fibres also decreased significantly over the 7 day period from 768 ± 175 MPa, 549 ± 190 MPa and 613 ± 183 MPa prior to degradation to 212 ± 4 MPa, 239 ± 4 MPa and 297 ± 5 MPa, respectively.

It can also be seen that the strengths of the coated fibres decreased by 68%, 43% and 33%, respectively after 1 day immersion in PBS at 37°C. Control fibres, on the other hand, experienced a 14% decrease in strength after 1 day immersion. This suggests that while coating P40 fibres with S-PLA initially increases the tensile strength of the fibre, the coating does not protect the fibre from degradation and apparently compromises the mechanical integrity of the fibre. This can be attributed to the hygroscopic nature of the sorbitol head group [37, 57]. Immersion of S-PLA coated fibres in an aqueous environment caused the coating to immediately absorb water that seeped through the coating to the fibre surface. This then triggered the hydration reaction that started fibre dissolution [58-59].
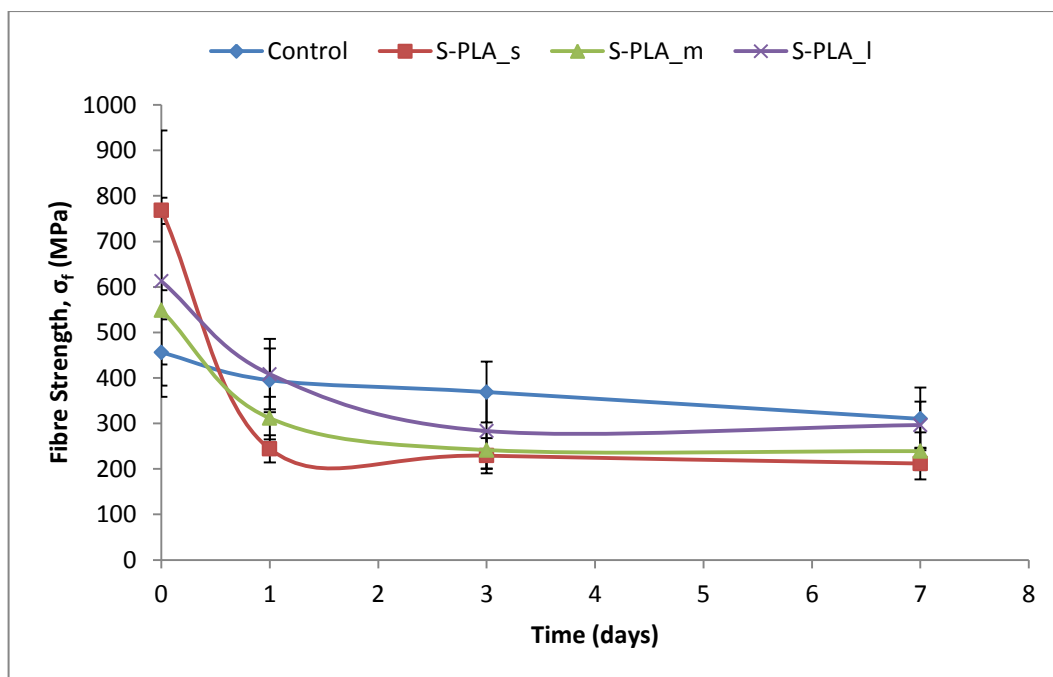
***Figure 4.12:*** *The fibre tensile strengths of control and S-PLA_s, S-PLA_m and S-PLA_l coated fibres before and after degrading in PBS at 37°C after 1, 3 and 7 days, n ≥ 20*

*4.3.7.1 Physical Analysis with Degradation*

Scanning Electron Microscopy (SEM) (Chapter 3 Section 3.3.6) was used to observe the uncoated and coated fibres prior to and post 1, 3 and 7 days immersion in PBS at 37°C. Figures 4.13 – 4.16 show the uncoated and coated fibres after 0, 1, 3 and 7 days of degradation. As-drawn control fibres had a smooth surface (Figure 4.13 (a)) as was expected [12, 21, 23, 41-42]. SEM micrographs of the control fibre showed evidence of some precipitation on the fibre surface after one day of degradation (Figure 4.13 (b)). After 3 days of immersion in PBS at 37°C, there appeared to be an increased amount of precipitates on the fibre surface (Figure 4.13 (c)). At day 7, it is clear that the outer layers of the fibre have begun to crack and peel away (Figure 4.13 (d)).
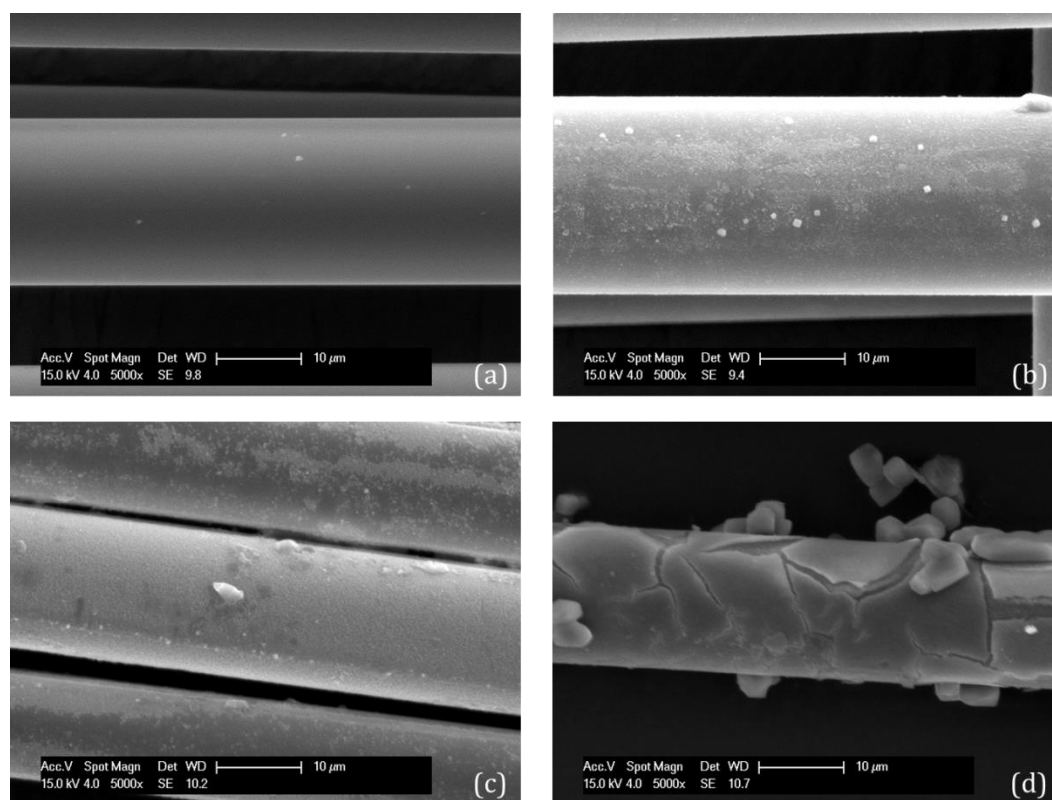
***Figure 4.13:*** *SEM micrographs of control P40 fibres after (a) day 0, (b) day 1, (c) day 3 and (d) day 7of immersion in PBS at 37°C*

Prior to immersion the coated fibres show that some of the coupling agent is evident on the surface (Figure 4.14 (a) and Figure 4.15 (a)). It is also clear that the coating didn't cover the fibre surface uniformly. It should be noted that increasing the magnification greater than 5000x at all time points resulted in the beam melting the oligomer on the fibre surface. This was a further indication that the S-PLA coating was present on the fibre surfaces. These micrographs are consistent with those obtained by Haque for P40 fibres coated with S-PLA [34, 37]. After 1 day of degradation, the S-PLA_s and S-PLA_m coated fibres appears to have begun cracking and peeling off of the fibre surface leaving it more uneven (Figures 4.14 and 4.15 (b)). This is reflected in the significant decrease of coated fibre strength after 1 day of degradation in PBS at 37°C (*See* Figure 4.12).
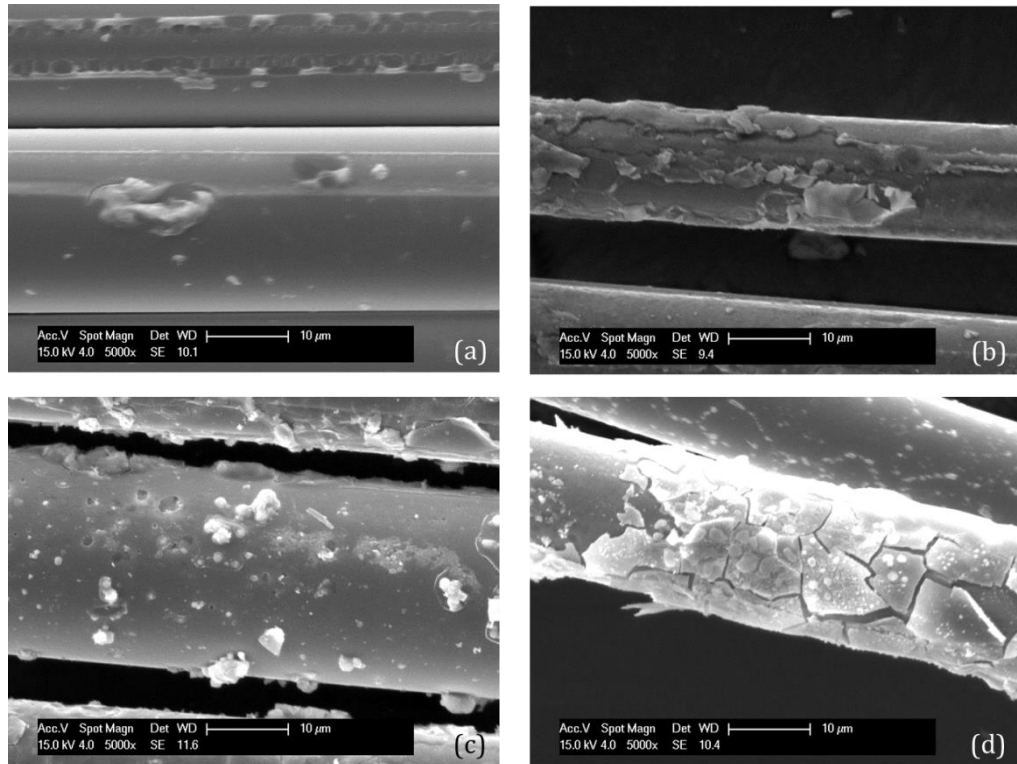
**Figure 4.14:** *SEM micrographs of S-PLA_s coated P40 fibres after (a) day 0, (b) day 1, (c) day 3 and (d) day 7of immersion in PBS at 37°C*
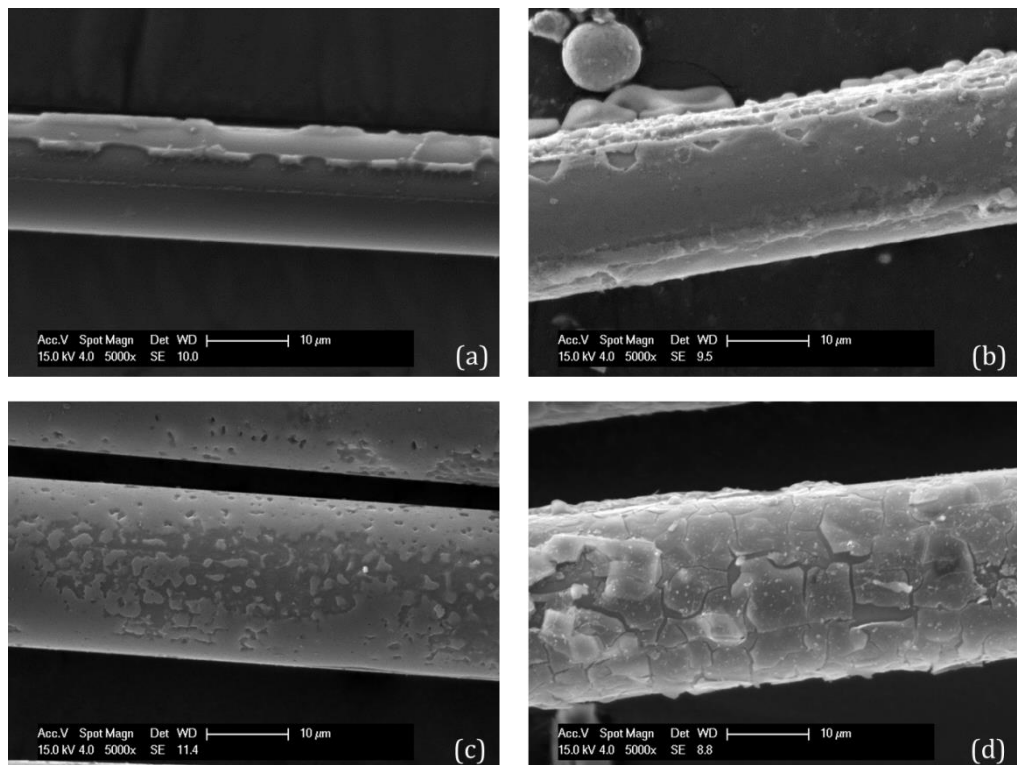


**Figure 4.15:** *SEM micrographs of S-PLA_m coated P40 fibres after (a) day 0, (b) day 1, (c) day 3 and (d) day 7of immersion in PBS at 37°C*

The micrographs of S-PLA_s and S-PLA_m after 3 days of immersion in PBS at 37°C showed pitting in the coating covering the fibres (Figures 4.14 and 4.15 (c)). At day 7, the micrographs show the outer layers of the fibres cracking and peeling off (Figures 4.14 and 4.15 (d)). Even though the coating appears to be degrading off the fibre, this is not reflected in the degraded fibre strengths for S-PLA_s and S-PLA_m coated fibres at day 3 and day 7 as seen in Figure 4.12.

Figure 4.16 shows the surfaces of the fibres coated with S-PLA_l after 0, 1, 3 and 7 days of degradation. Prior to degradation the SEM micrograph for S-PLA_l coated fibres showed that there is some coupling agent deposited on the fibre surface though apparently not as much as that for S-PLA_s and S-PLA_m. After 1 and 3 days of degradation, however, the images showed evidence of an abundance of the coupling agent on the surface of the fibres. This lends to the conclusion that the coating prior to degradation was more uniform than that of S-PLA_s and S-PLA_m. Figure 4.15 (b) shows that degradation appears to have taken effect after 1 day of degradation leading to the cracking and peeling of the coupling agent. This is shown in Figure 4.12 with the decrease in fibre strength for S-PLA_l coated fibres after 1 day of degradation in PBS at 37°C.

After 3 days of degradation, more of the coupling agent appears to have degraded off the fibre leaving more of the surface exposed. However, after 7 days, the fibre surface hasn't started peeling away like that of S-PLA_s and S-PLA_m coated fibres. This too can be seen in Figure 4.12 as the strength of S-PLA_l coated fibres after 7 days of degradation (297 ± 5 MPa) is greater than that of S-PLA_s and S-PLA_m coated fibres (212 ± 4MPa and 239 ± 4 MPa). Though all the coated fibres show evidence that coating is degrading off the fibres after 7 days of immersion in PBS at 37°C, the S-PLA_l coated fibres appeared to be degrading at a slower rate than the S-PLA_s and the S-PLA_m coated fibres.
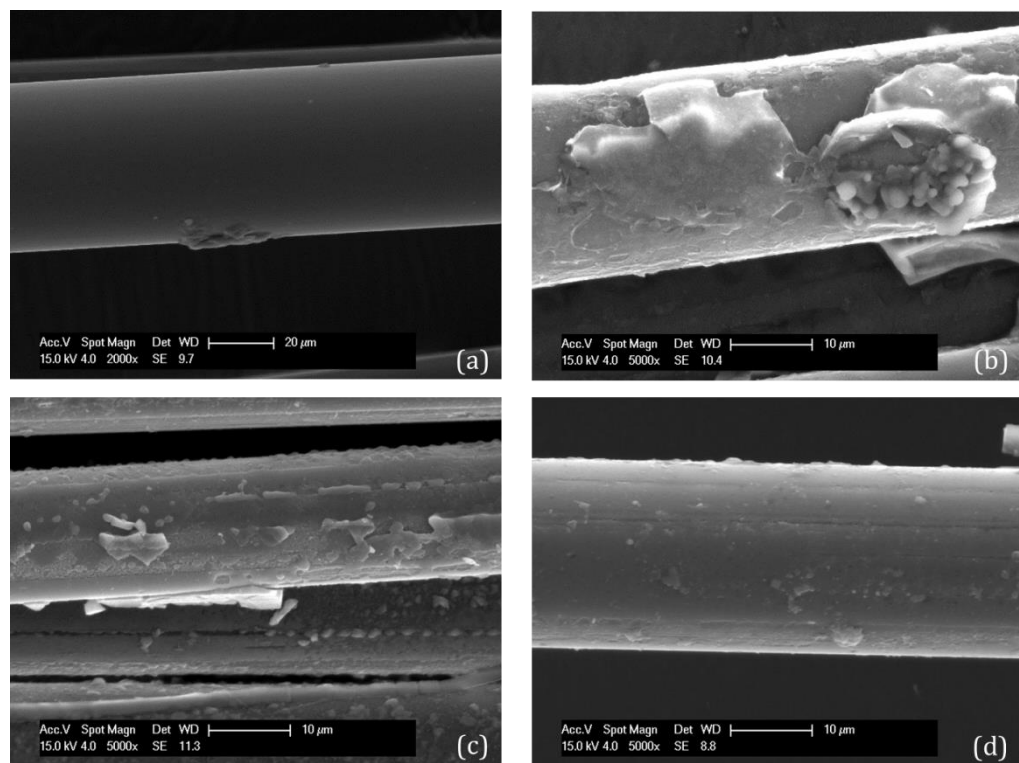
**Figure 4.16:** *SEM micrographs of S-PLA_l coated P40 fibres after (a) day 0, (b) day 1, (c) day 3 and (d) day 7of immersion in PBS at 37°C*

### 4.3.7.2 Weibull Analysis

A Weibull analysis (Chapter 3 Section 3.7.1) of the tensile strengths of the control and coated fibres was conducted to obtain Weibull shape (m) and scale ($\sigma_0$) parameters required to calculate the IFSS (Section 5.3.3). Table 4.4 shows a summary of m (also known as the Weibull modulus) and $\sigma_0$ (also known as the normalising strength) values for each batch of fibres prior to degradation and after degradation in PBS at 37°C at 1, 3 and 7 days. Initial $\sigma_0$ values of the coated fibres (613 – 678 MPa) appeared to be higher than that for control fibres (535 MPa). The $\sigma_0$ values for the control and the coated fibres decreased over the course of the 7 days. After 7 days it can be seen that the coated fibres had lower normalising strengths than the control fibres (338 MPa). The decrease in normalising strengths was similar to the decrease in tensile strength values

observed in Figure 4.12 [56]. With the exception of the $\sigma_0$ for S-PLA_s prior to degradation, the $\sigma_0$ values were found to be higher than the fibre tensile strengths both prior to and during degradation. Shaharuddin (who investigated several binary, ternary, quaternary and quinternary PGF formulations varying $P_2O_5$, CaO, $Na_2O$, $Fe_2O_3$ and $TiO_2$ content) observed a similar phenomenon for certain PGF formulations however did not attribute the increase to the difference in formulation as the practical strength of glass is controlled by surface damage [56, 60].

**Table 4.4:** *Summary of Weibull Shape and Scale parameters for control and S-PLA coated fibres prior to degradation and after 1, 3 and 7 days in PBS at 37°C*

|  | Time (days) | Shape Parameter, m | Scale parameter, $\sigma_0$ |
|---|---|---|---|
| **Control** | 0 | 5.76 | 535 |
|  | 1 | 5.60 | 424 |
|  | 3 | 6.12 | 397 |
|  | 7 | 5.19 | 338 |
| **S-PLA_s** | 0 | 3.43 | 628 |
|  | 1 | 8.39 | 327 |
|  | 3 | 6.83 | 288 |
|  | 7 | 5.60 | 241 |
| **S-PLA_m** | 0 | 3.11 | 614 |
|  | 1 | 8.19 | 331 |
|  | 3 | 7.36 | 258 |
|  | 7 | 7.04 | 255 |
| **S-PLA_l** | 0 | 3.98 | 678 |
|  | 1 | 6.03 | 440 |
|  | 3 | 4.10 | 313 |
|  | 7 | 6.62 | 318 |

Shaharuddin noted that it was difficult to prepare PGF with good mechanical properties [56]. This is due to the difficulty in maintaining the strength of the fibre during fibre drawing as the strength of the fibre is purported to be strongly dependent on the presence of flaws on the fibre surface and particulate contaminants on the fibre surface as a result of handling [19, 60-62]. Like the study conducted by Shaharuddin, the effects of flaws and surface

contamination are reflected by the large standard deviations obtained for the fibre strengths of control and S-PLA coated fibres (*See* Figure 4.11) [56].

The m values for the control fibres didn't differ much, staying in the range 5 – 6.1. The S-PLA_s and S-PLA_m coated fibres yielded m values that increased after 1 day of immersion in PBS (8.39 and 8.19) and then decreased such that by day 7 the m values were 5.60 and 7.04, respectively. The Weibull analysis of the S-PLA_l coated fibres yielded m values that displayed no trend over the 7 day degradation period. Haque *et al* and Felfel *et al.* both studied the mechanical properties of annealed P40 fibres and the m values obtained were 5.20 and 5.28, respectively [13, 63]. This is less than was obtained for un-annealed P40 fibres. Annealing PGFs decreases their mechanical properties and, as a result, the corresponding Weibull parameters will also decrease [12, 32, 56]. The Weibull shape parameter, m, gives information about the physics of fibre failure, i.e. a high m value is indicative of a smaller variation in stress to failure [19, 64]. The range of m values obtained from the Weibull analysis of fibres prior to and during degradation is in an accepted range (2-15) for brittle materials such as PGF [64].

### 4.3.8 Interfacial Shear Stress Study

The single fibre fragmentation test (SFFT) and the interfacial shear stress (IFSS) were conducted as stated in Chapter 3 Sections 3.4.4-3.4.6. The IFSS was calculated using the following equation (*also shown in* Chapter 3):

$$\tau_i = \frac{\sigma_f d}{2L_c}$$

*Equation 4.1*

$\tau_i$ is the IFSS; $\sigma_f$ is the fibre fragment strength (*See* Equation 3.4); $L_c$ is the critical fragment length (*See* Equations 3.2-3.3); d is the diameter of the fibre.

Figure 4.17 (a) shows a micrograph of a single fibre composite specimen immediately after the tensile test. The failure of the specimen can be identified as primarily due matrix cracking; however it was difficult to ensure that fibre breakage had occurred at each matrix crack across the fibre. In order to confirm the number of fibre fragments, the samples were heated to approximately 80°C for a few minutes to soften the PLA (Figure 4.17 (b)).

There are three modes of fracture that can occur during the single fibre fragmentation test (SFFT) (*see* Chapter 2 Section 2.7.1.1): 1. the initial fibre break followed by a disk-shaped matrix crack (a strong interface), 2. Initial fibre break followed by interfacial crack growth matrix crack (a strong interface with a matrix of lower shear than tensile strength capability) and 3. Initial fibre break followed by interfacial debonding (a weak interface) [18, 65-67]. Figure 4.17 (a) shows disk shaped matrix cracks across the fibre which suggests that the interface between P40 glass fibres and the PLA matrix is strong. Disk-shaped matrix cracks were the failure mechanism observed for all fibres – control and coated – after the SFFT prior to degradation.
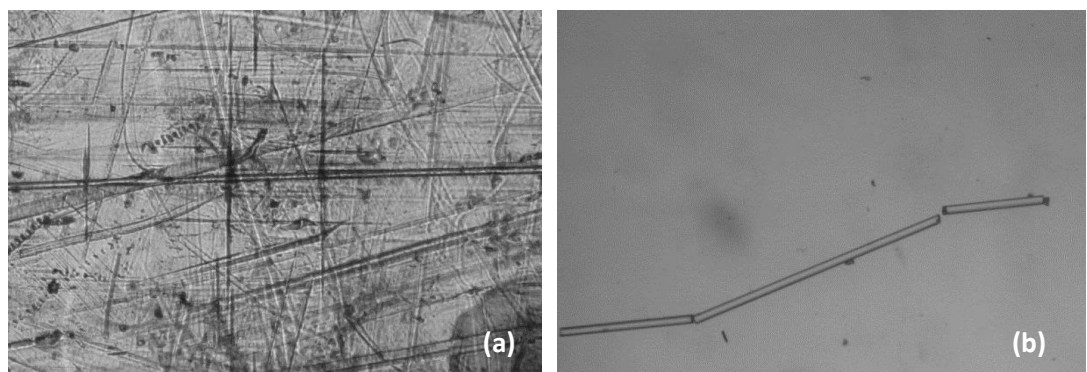


***Figure 4.17:*** *(a) Micrograph of fibre breaks after tensile test prior to softening the matrix (b) Clear fibre fragments after softening of matrix*

*4.3.8.1 IFSS Optimisation Test*

A coating optimisation test was carried out for S-PLA_s to find the coating concentration that would yield the greatest increase in IFSS. The tensile strengths and moduli of the fibres coated with varying concentrations of S-PLA_s can be seen in Figure 4.18. There are two different control values because the fibres are from two different P40 batches. There is no statistical difference in fibre properties between control-1 and control-2. Note that the strength for control-2 shown here is the same as that shown in Figure 4.11.

The IFSS values for these fibres are summarised in Figure 4.19. 0.005 moles was initially found to be the optimum coating yielding the largest IFSS. It was decided to investigate a concentration in between 0.005 moles and 0.0075 moles (i.e. 0.0064 moles) to find out if the IFSS for S-PLA_s could be improved. An IFSS test for S-PLA_s at 0.0064 moles concentration yielded a value of 24 ± 5 MPa, that while larger in value was not significantly different to that of S-PLA_s coated fibres at 0.005 moles. Even so fibre degradation and single fibre composite degradation studies were carried out using the 0.0064 moles coating concentration (*See* Section 4.3.7). The IFSS of the 0.005 moles and 0.0064 moles coated fibres (19 ± 5 MPa and 24 ± 5 MPa) were shown to be statistically significant to the control-2 at a *p*-value of $p < 0.05$. The IFSS values of control-1 and control-2 (14 ± 3 MPa and 12 ± 2 MPa) were not found to be statistically different to each other, as expected.

The IFSS decreased noticeably with a coating concentration greater than 0.0064 moles. This is likely due to large amounts of coupling agents present on the fibre surface leading to the formation of an interphase region. The IFSS measured at 0.0075 moles and 0.01 moles is the interface between the coupling agent and the fibre surface.
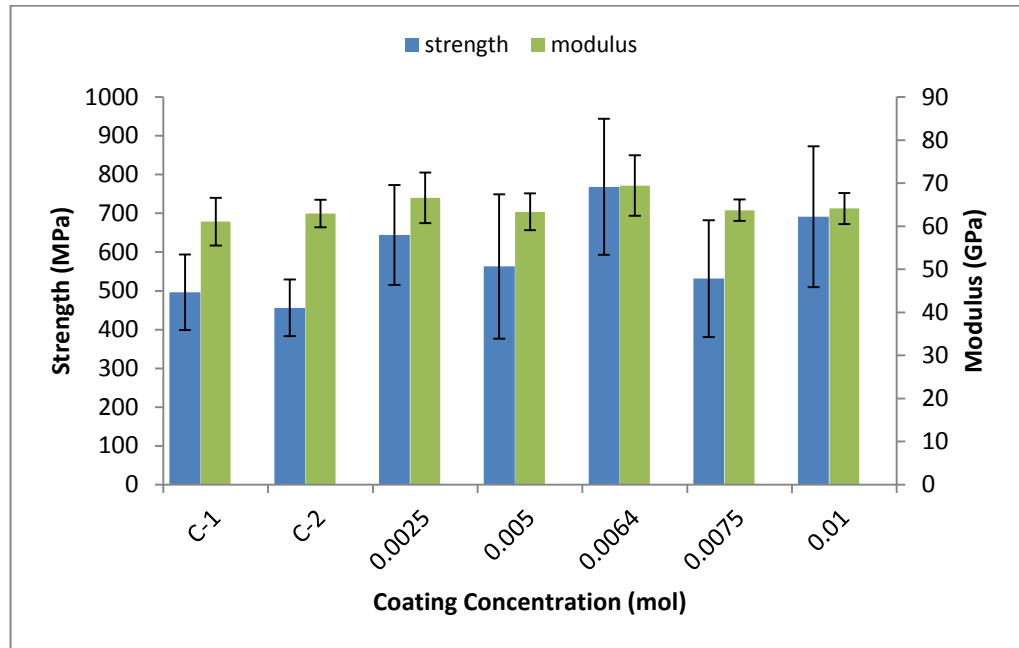
***Figure 4.18:*** *Tensile strength and modulus of S-PLA_s fibres at different concentrations. C-1 and C-2 represent two different batches of uncoated P40 fibre (n ≤ 20)*
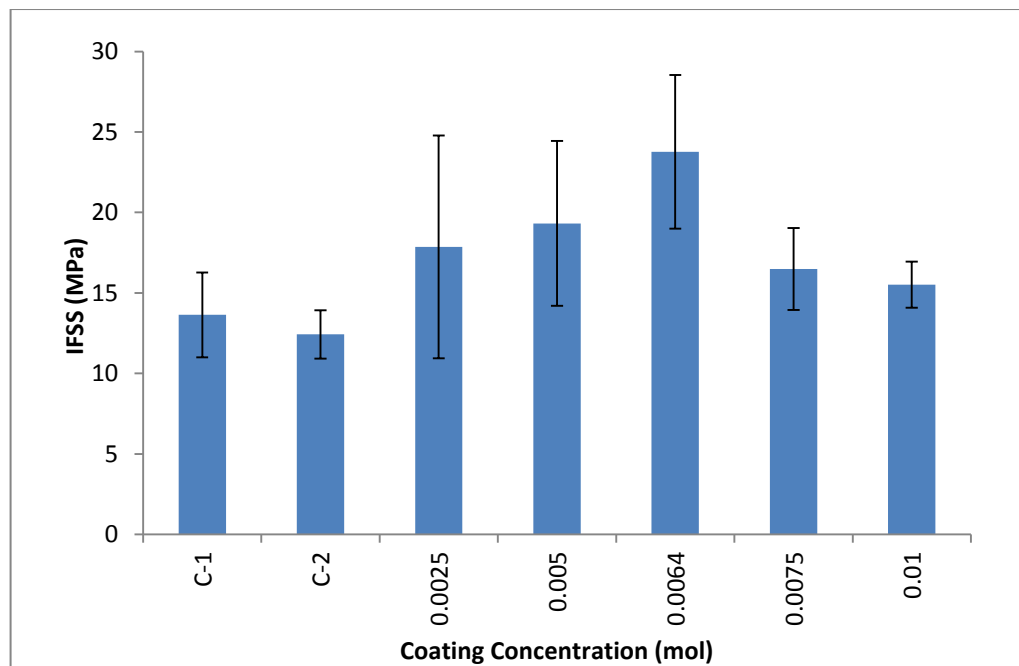


***Figure 4.19:*** *IFSS for single fibre composites with fibres coated with S-PLA_s with varying coating concentrations (n = 5-10)*

Figure 4.20 shows that IFSS values for control P40 fibres, S-PLA_s, S-PLA_m and S-PLA_l coated fibres were 11 ± 5 MPa, 24 ± 5 MPa, 24 ± 7 MPa and 23 ± 7 MPa, respectively. The IFSS was calculated as shown in Chapter 3 Section

3.4.6. The one-way ANOVA test found that the IFSS values of the coated fibres are all statistically significant compared to the IFSS of control for a *p*-value of $p < 0.05$. At a coating concentration of 0.0022 moles and a $M_n$ value of 4972 Da, S-PLA_m fibres have an IFSS value 24 ± 7 MPa when embedded in PLA. This is comparable to the IFSS value obtained by Haque *et al.* for S-PLA at a $M_n$ value of ~2881 Da – 23 ± 10 MPa [34].
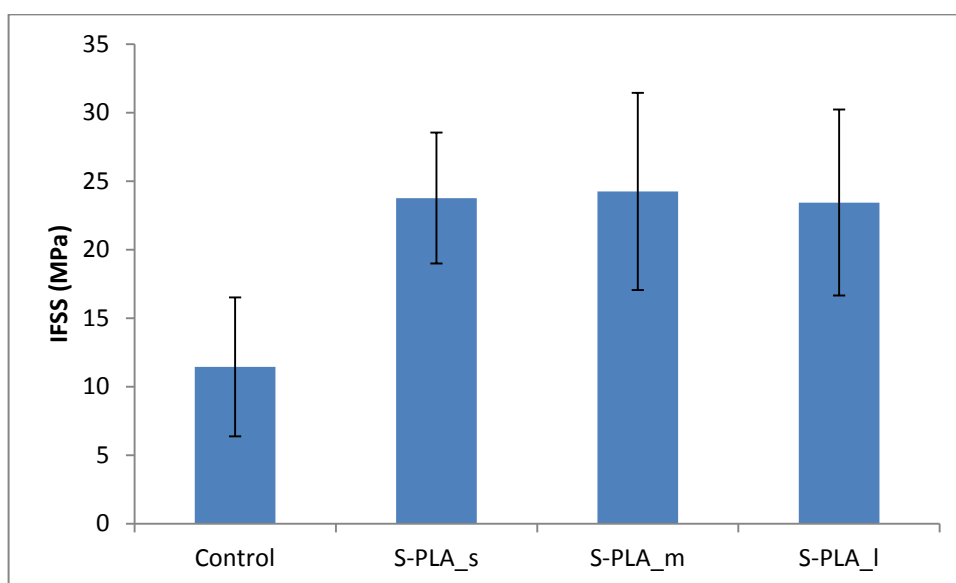


***Figure 4.20:*** *Summary of IFSS values for control and S-PLA_s, S-PLA_m and S-PLA_l coated fibres prior to degradation using the respective optimum concentrations (n = 10-15)*

S-PLA_l, at a lower concentration – 0.00013 moles – has a similar IFSS value (23 ± 7 MPa) to that of S-PLA_m when embedded in a PLA matrix. A low coating concentration means that there were fewer but longer chains to bond with hydroxyl (OH$^-$) groups on the fibre surface. The hypothesis was that the chain length of the oligomer would have an effect in the IFSS between P40 fibres and a PLA matrix. However, at a coating concentration of 0.0064 moles, S-PLA_s yielded an IFSS value of 24 ± 5 MPa that was not significantly different to IFSS values from S-PLA_m and S-PLA_l coated fibres. Initially the chain length of the oligomer did not appear to have a significant impact on the IFSS. At the right

coating concentration, a statistically similar IFSS value can be obtained irrespective of the molecular weight of the coupling agent.

Studies have been carried out to determine the effect matrix properties have on the IFSS [68-72]. Piggott states that the value composite shear stress is limited by the shear stress of the matrix [73]. According to the Tresca Criterion, the maximum shear stress, $\tau$, of a material can be approximated to half the tensile stress [6]. The tensile stress of PLA in literature is ~50 MPa [74] hence the shear stress of PLA is ~25 MPa. Felfel *et al*. measured the shear strength of a PLA (NatureWorks 3251D) rod to be 47 MPa [5] whereas the tensile strength of NatureWorks 6201D PLA used in this study was ~62 MPa giving a shear strength value of ~31 MPa. The IFSS values for S-PLA_s, S-PLA_m and S-PLA_l at the coating concentrations of 0.0064 moles, 0.0022 moles and 0.00013 moles are similar to the assumed shear stress (25 MPa) of PLA prior to degradation. The IFSS appears to be matrix limited (i.e. the brittle nature of PLA [75]) and a maximum of 25 MPa can be achieved with any of the oligomers used in this study.

*4.3.8.2 Degradation Study*

The degradation studies were carried out on single fibre composites embedded with control and S-PLA_s, S-PLA_m and S-PLA_l coated fibres as described in Chapter 3 Section 3.6.1. The coating concentrations of the coated fibres were 0.0064, 0.0022 and 0.00013 moles, respectively. Figure 4.21 shows the IFSS values using uncorrected (Figure 4.21 (a)) and corrected (Figure 4.21 (b)) Weibull parameters for degraded single fibre composites with embedded control and S-PLA_s, S-PLA_m and S-PLA_l coated fibres at day 0, 1, 3 and 7.
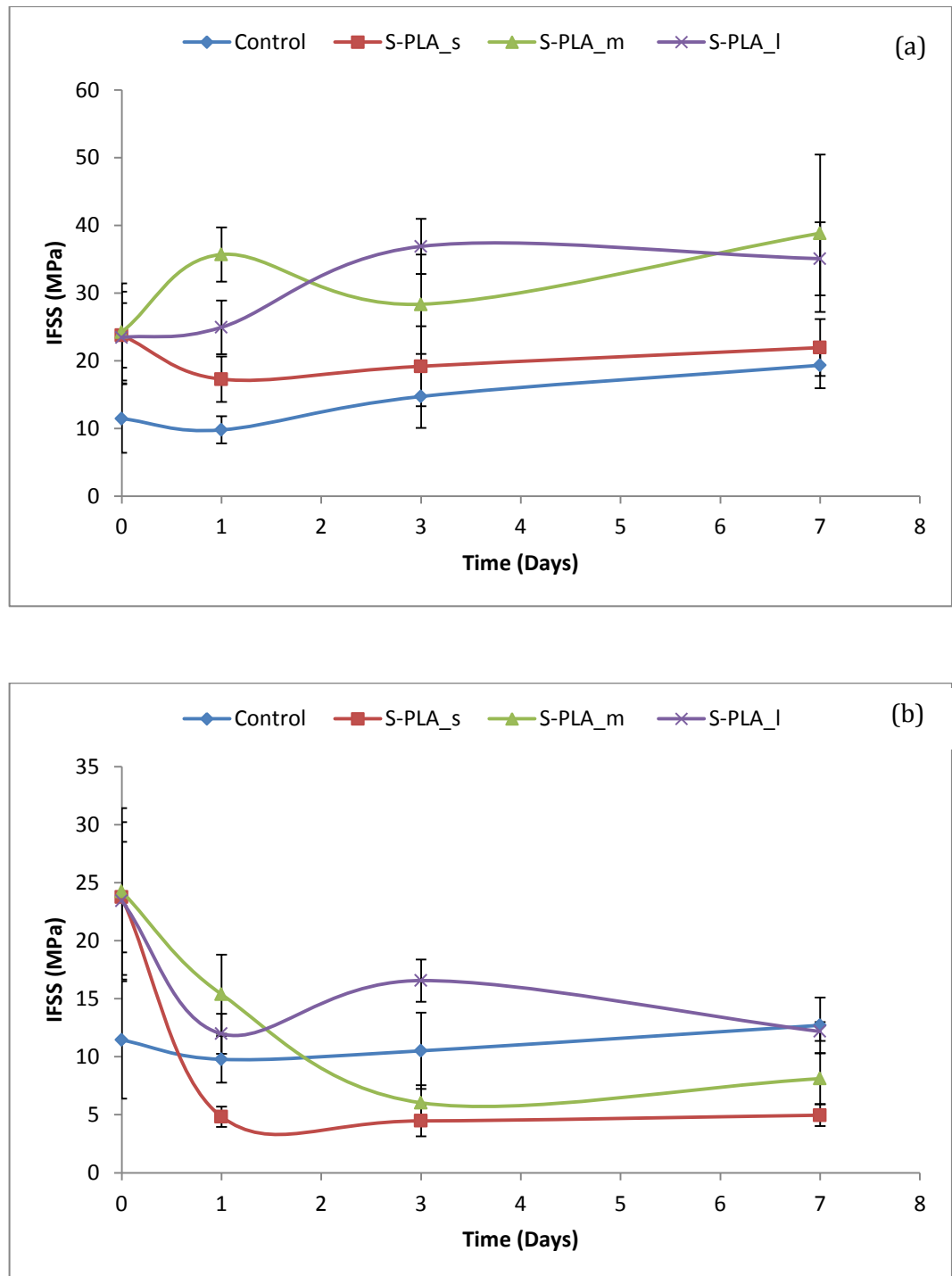
***Figure 4.21:*** *Summary of (a) uncorrected IFSS values and (b) corrected IFSS values for degraded single fibre composites with embedded control and S-PLA_s, S-PLA_m and S-PLA_l coated fibres after 0, 1, 3 and 7 days immersion in PBS at 37°C.*

The IFSS results shown in Figure 4.21 (a) were obtained based on the assumption that the fibre strengths in the degraded single fibre composites were similar to those at day 0 (Table 4.4). Using the uncorrected Weibull parameters, the IFSS appeared to be increasing over time. Figure 4.21 (a) shows that after 7

days of degradation there is almost a 50% increase in IFSS of the control uncoated fibres from 11 ± 5 MPa to 19 ± 3 MPa. A statistical analysis of this data showed that this increase is statistically significant for $p < 0.05$. Figure 4.21 (a) also shows that the S-PLA_s coated fibres at 0.0064 moles concentration don't show any significant difference in IFSS over 7 days.

After 7 days of immersion in PBS at 37°C, the IFSS of S-PLA_m (39 ± 12 MPa) and S-PLA_l (35 ± 5 MPa) was found to be statistically significant compared to that of control fibres (19 ± 3 MPa) ($p < 0.05$). The IFSS values of S-PLA_m and S-PLA_l increase over time after immersion in PBS over 7 days. The degraded IFSS values for S-PLA_m and S-PLA_l coated fibres shown in Figure 4.21 (a) significantly ($p < 0.05$) increase from 24 ± 7 MPa and 23 ± 7 MPa to 39 ± 12 MPa and 35 ± 5 MPa. There appears to be an overall increase in IFSS values for the coated fibres over time compared to the control data and compared to the day 0 data when using uncorrected Weibull parameters to determine the IFSS in degraded single fibre composites. The IFSS of single fibre composites with embedded S-PLA_m and S-PLA_l coated fibres increased to values that were greater than 25 MPa, suggesting that using the Weibull parameters of the fibres at day 0 overestimates the shear stress at the fibre-matrix interface.

Weibull parameters were obtained for the degraded fibres (Table 4.4) which allowed for the corrected IFSS to be calculated, shown in Figure 4.21 (b). These results show, with the exception of control, the IFSS decreasing over time. No significant difference was found between the IFSS of control fibres over time (Figure 4.21 (b)). However, the embedded coated fibres showed a decrease in the IFSS values over time compared to the respective day 0 IFSS values prior to degradation.

A statistical analysis of the IFSS of degraded single fibre composites embedded with S-PLA_s coated fibres after day 1, 3 and 7 (5 ± 1 MPa, 4 ± 1 MPa and 5 ± 1 MPa) were all found to be statistically insignificant when compared to each other. These values were however a significant ($p < 0.05$) decrease in IFSS when compared to that of day 0 (24 ± 5 MPa). Single fibre composites embedded with S-PLA_m and S-PLA_l coated fibres also had a significant ($p < 0.05$) difference in IFSS values for days 1, 3 and 7 (15 ± 3 MPa, 6 ± 2 MPa and 8 ± 2 MPa; 12 ± 2 MPa, 16 ± 2 MPa and 12 ± 1 MPa) compared to day 0 (24 ± 7 MPa and 23 ± 7 MPa). The IFSS values of single fibre composites embedded with S-PLA_m coated fibres for day 1 (15 ± 1 MPa) was also shown to be significantly ($p < 0.05$) different to the IFSS values for days 3 and 7 (6 ± 2 MPa and 8 ± 2 MPa). The IFSS values of single fibre composites embedded with S-PLA_l coated fibres for day 1, 3 and 7 were found to be statistically insignificant.

An overall decrease in IFSS for the coated fibres was seen compared to the control. This suggests a loss of interface between the fibre and the matrix due to insufficient bonding [5, 15, 32, 76] which is particularly true for S-PLA_s coated fibres. There was a greater decrease in IFSS from day 0 to day 1 for S-PLA_s coated fibres (~78%) suggesting that coupling agents with shorter chain lengths will result in a rapid decrease in IFSS. Sorbitol is also hygroscopic in nature therefore the presence of water at the interface could have led to the hydrolysis of the chemical bond between the fibre and matrix [22]. There also was a significant ($p < 0.05$) difference between the IFSS for control and S-PLA_m coated fibres at day 1 and for control and S-PLA_l coated fibres at day 3. It should also be noted that the IFSS for S-PLA_l coated fibres (Figure 4.21 (b)) was greater than that of control until day 7. This suggests that though sorbitol is attracting water, the longer chain oligomer provide some hindrance to hydrolysis.

The fibre strength in a SFFT is estimated by using a Weibull distribution [77-79]. However it is difficult to estimate this value during degradation. Using Weibull parameters for fibre strength at day 0 seems to overestimate the IFSS whereas using the corrected Weibull parameters underestimates the IFSS. This is because the fibre embedded in a PLA matrix does not degrade in the same way as a fibre bundle in an aqueous environment. Haque *et al.* dissolved the PLA around the embedded fibre using chloroform and tested the fibre for mechanical properties [33]; however it is unclear if this is an accepted method for measuring the properties of the single fibre.

The Kelly-Tyson model used here to calculate the IFSS assumes that there is a constant shear stress (i.e. that the matrix is perfectly plastic) at the interface even when the fibre has fragmented to a length equivalent to $L_c$ and that the fibre strength is constant [23, 30, 78-80]. Aveston *et al.* also assumes that the fibre fragment lengths are uniformly distributed with the fibre fragment length $L_f$ being ¾ of $L_c$ (Equation 3.3) [81]. Kimber and Keer argue that the fibre fragment length is not uniformly distributed and for the case of negligible variability in fibre strength the correct factor by which $L_c$ must be multiplied is 0.668 [82]. Applying this to the initial IFSS data (Figure 4.20), gives IFSS values for control, S-PLA_s, S-PLA_m and S-PLA_l of 10 ± 4 MPa, 21 ± 4 MPa, 21 ± 6MPa and 20 ±6 MPa. There is a 1% reduction in IFSS for the control and a 12-16% reduction in IFSS values for S-PLA_s, S-PLA_m and S-PLA_l with this 'corrected' factor. However, there is no significant difference between these values and the IFSS values shown in Figure 4.20.

While the SFFT can be used to assess the effect of coating the fibres on IFSS prior to degradation, this interfacial test method limits the ability to analyze the effect degradation has on the samples due to uncertainty in fibre strength. A

degradation study needs to be carried out on full body composites in order to deduce the effect of the coupling agents on the macroscopic mechanical properties after immersion in an aqueous environment. This will help to see if the mechanical properties of the composite can be retained due to the coupling agents.

### 4.3.9 Changing Glass Formulation to Improve Composite Production

In the manufacture of unidirectional full body composites it is important that the fibre mats prepared are aligned uniformly. Earlier studies involving the production of UD PGF reinforced PLA composites, created UD mats manually [37, 57]. During composite production, these UD mats shifted causing fibre misalignment that affected the distribution of fibres in the composite. To improve this process an in-house facility was constructed that would produce UD mats while the fibre was being drawn (*see* Figure 3.1). For this to be possible, it is vital that the fibre be drawn continuously as required.

In Chapter 2 Section 2.6, it was mentioned that the ease of drawing fibres continuously was dependent on the content of $P_2O_5$ present in the PBG formulation [83]. P40 fibres were difficult to draw continuously for a UD mat to be formed ($\sim$ 1 drum per day, enough for 1 composite with fibre volume fraction ($V_f$) of 20%). The fibre would stop in the middle of the production of a UD mat requiring the need to restart the process. This was due to small processing window and thermal stability for P40 glasses [56]. The inability to draw continuous fibre mats with P40 glass was not time or cost effective as more glass would have to be made and unsuccessful fibre mats would have to be scrapped.

$45P_2O_5\text{-}24MgO\text{-}16CaO\text{-}11Na_2O\text{-}4Fe_2O_3$ (P45) UD fibre mats were drawn successfully and with more ease than P40 fibres ($\sim$ 2-3 drums per day, where

each drum can be used for 1 composite for $V_f$ of 20%). This glass formulation was more cost effective and less material waste was observed. The ability to produce enough UD mats for 2-3 composites per day also improved the production time. In order for P45 fibres to be used for subsequent composite production in this study, it was necessary to conduct a study that investigated the difference between the IFSS of P40 and P45 uncoated and coated fibres.

The S-PLA_s coupling agent was used to coat the fibres and the sizing solution was reused. The aim of this was to investigate if the sizing solution could be used again in order to reduce the amount of coupling agent that needed to be manufactured and thereby reduce raw material cost. When the sizing solution was used the second time, a different bundle of fibres was dipped in. The first bundle of coated fibres was denoted S-PLA_s-A and the second bundle of coated fibres was denoted S-PLA_s-B. Figure 4.22 shows the results from this study including the IFSS results of single fibre composites P40 control and P40 S-PLA_s.

These results are shown in Figure 4.22 for two reasons: 1. to show that the SFFT is repeatable with statistically insignificant results and 2. the fibre rig that was used to draw UD mats was different to the rig that was initially used to pull P40 fibre for the IFSS study. The drum of the rig (Figure 3.1) used to pull UD mats was spun at a lower speed than the older rig and therefore produced fibre at a different diameter range. The fibres used in the study above had an average fibre diameter of 20 μm and the fibres pulled from the new rig shown in Figure 3.1 had an average diameter of 30 μm. The P40 and P45 fibre pulled from the new rig had the same average diameter. Increasing the diameter of P40 fibres did decrease the fibre tensile strength (Figure 4.23) from an average of 461 ± 73 MPa to 348 ± 64 MPa. The decrease in fibre diameter did not produce a significant decrease in the IFSS (Figure 4.22). P45 fibres had a higher tensile

strength than P40 at the same diameter range but again did not affect the IFSS values (Figure 4.22). The variation in fibre tensile strength with fibre diameter for P40 old, P40 and P45 is shown in Figure 4.24.
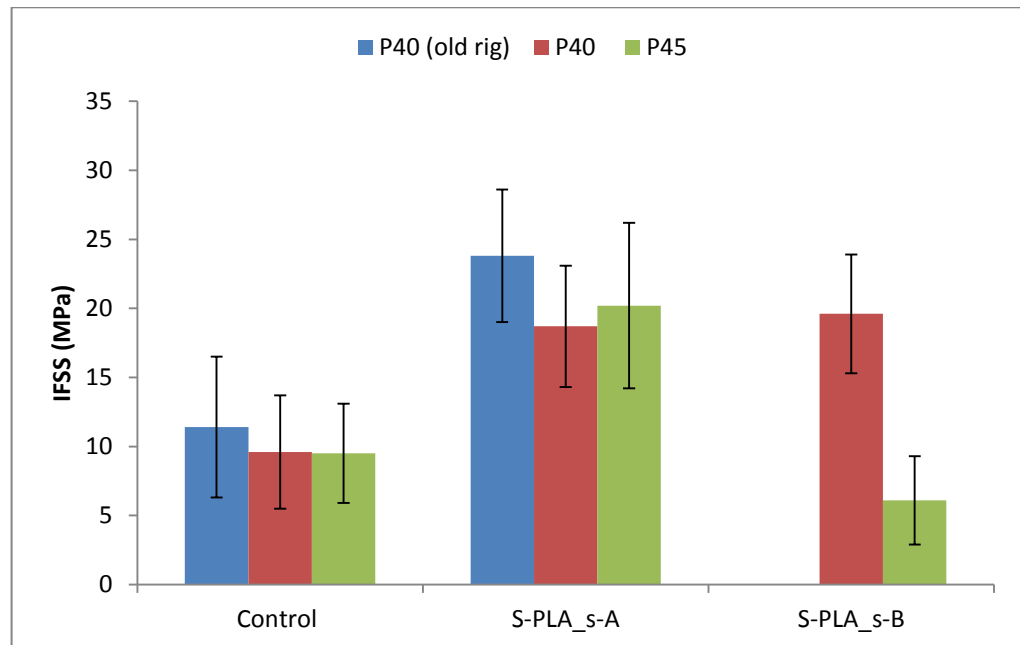


***Figure 4.22:*** *Comparison of IFSS between embedded control and S-PLA_s coated P40 and P45 fibres, n = 5-15*
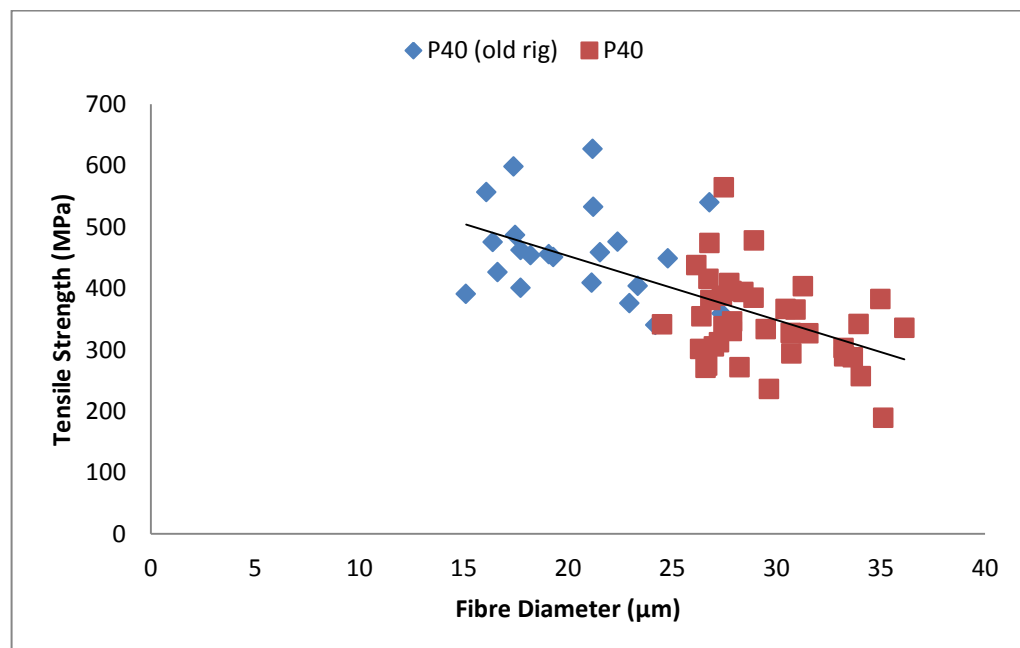


***Figure 4.23:*** *Decrease in tensile strength with increase in diameter for P40 glass fibres*
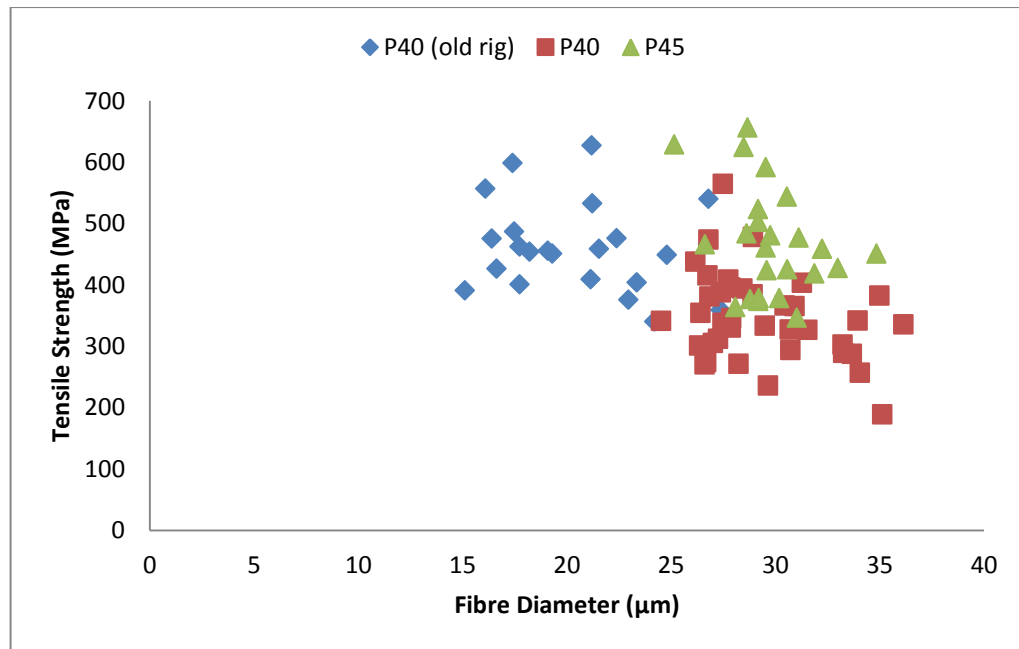
***Figure 4.24:*** *Variation in fibre tensile strength with fibre diameter for P40 old, P40 and P45, n ≥ 20*

Figure 4.22 shows that there is no statistical difference between the IFSS of single fibre composites of embedded control P40 and P45 fibres even when compared to the IFSS of the single fibre composite embedded with P40 fibre pulled from the older rig. The IFSS of the control P40 and P45 fibre were 11 ± 5 MPa, 10 ± 4 MPa and 10 ± 4 MPa. The IFSS of S-PLA_s-A for embedded P40 and P45 fibres were 24 ± 5 MPa, 19 ± 5 MPa and 20 ± 6 MPa and were also found to be statistically insignificant when compared to each other. These IFSS values were found to be statistically significant ($p < 0.05$) when compared to the respective control IFSS values, leading to the conclusion that P45 fibres could be used in place of P40 fibres for the full body composite study.

Using the sizing solution twice however yielded different results between single fibre composites with embedded P40 coated fibre and those with P45 coated fibre. The IFSS of P40 coated with S-PLA_s-B was 20 ± 4 MPa, while that of P45 fibre significantly decreased to 6 ± 3 MPa. This was also a significant difference from the P45 IFSS values obtained for S-PLA_s-A. The test was

repeated twice more for the S-PLA_s-B coated P45 fibre and it yielded results that were ~6 ± 3 MPa each time. It is unclear why this occurred as the only difference between the fibres is the phosphate and sodium concentration. It is however evident that the sizing solution cannot be used twice when coating the fibres.

## 4.4 CONCLUSIONS

Sorbitol-initiated PLA has been successfully manufactured and characterised at three different chain lengths: S-PLA_s, S-PLA_m and S-PLA_l. NMR analysis showed that all three oligomers converted over 90% of the monomer to polymer. GPC analysis showed that the standards used affected $M_n$, $M_p$ and PDI values. The $M_n$ values obtained for S-PLA_s, S-PLA_m and S-PLA_l using PMMA standards were 1221, 4972 and 25974 g mol$^{-1}$, respectively. PMMA standards were used for GPC analysis for the rest of the study as the structure of PMMA is similar to that of PLA and therefore gives a closer estimation of $M_n$ than PS standards. An increase in $T_g$ was observed as the chain length of S-PLA increased confirming that it follows the Flory-Fox equation. FTIR analysis confirmed sorbitol was present on the S-PLA chain. A spectrum was not obtained for the largest oligomer, S-PLA_l, due to the size of the oligomer chains in this sample.

S-PLA_s, S-PLA_m and S-PLA_l were coated onto P40 fibres for IFSS testing. The tensile strengths of coated fibres increased compared to the strength of control, however the increase was only significant for S-PLA_s coated fibres (768 ± 175 MPa). The fibre strength of coated fibres decreased significantly after 7 days immersion in PBS at 37°C. The coating concentration was dependent on the molecular weight of the coupling agent taking into consideration the ease of separating single fibres after coating. Working with S-PLA_l was difficult due to polymer-polymer interactions that made it difficult to separate the fibres and a

low coating concentration had to be used. Optimising the coating concentration for S-PLA_s showed the optimum concentration to be 0.0064 moles with an IFSS value of 24 ± 5 MPa compared to the control IFSS value of 12 ± 2 MPa. The IFSS values for S-PLA_s, S-PLA_m and S-PLA_l were found to be significantly different to that of the control prior to degradation. Though the chain length of the coupling agent appears to have no significant effect on the IFSS at the right concentration, it is also likely that the matrix properties limited the value of the IFSS.

Degradation studies on single fibre composites embedded with S-PLA_s, S-PLA_m and S-PLA_l coated fibres over 1, 3 and 7 days showed a 50-60% increase in IFSS over time compared to the control with uncorrected Weibull parameters. With the corrected Weibull parameters, obtained from degrading the fibres over 1, 3 and 7 days, the IFSS of S-PLA_s, S-PLA_m and S-PLA_l coated fibres was shown to decrease by 63%, 67% and 48% after 7 days respectively compared to the control. This can be attributed to the loss of the interface that occurred due to insufficient bonding and/or due to hydrolysis of the chemical bond between the fibre and the matrix. The long chain oligomers show a greater resistance to degradation. The estimation of the fibre strength is very important in the calculation of the IFSS using the SFFT method. It is difficult to estimate the strength of the fibre embedded in a matrix during degradation and therefore difficult to find the exact effect of the coupling agents on the mechanical properties of degraded single fibre composites.

P45 fibres can be used in place of P40 fibres for full body composite manufacture in the interest of decreasing production time, cost and material waste. A degradation study of full body composites would be better suited to

observe any retention of mechanical properties and any improvement in interfacial properties provided by the use of coupling agents.

## 4.5 REFERENCES

1. S. Ramakrishna, J. Mayer, E. Wintermantel and K.W. Leong, "Biomedical applications of polymer-composite materials: a review", *Composites Science and Technology*, vol. 61, no. 9, pp. 1189-1224, 2001.

2. A.U. Daniels, M.K.O. Chang, K.P. Andriano and J. Hellar, "Mechanical properties of biodegradable polymers and composites proposed for internal fixation of bone", *Journal of Applied Biomaterials*, vol. 1, no. 1, pp. 57-78, 1990.

3. B.L. Eppley, L. Morales, R. Wood, J. Pensler, J. Goldstein, R.J. Havlik, M. Habal, A. Losken, J.K. Williams, F. Burstein, A. a Rozzelle, and A. M. Sadove, "Resorbable PLLA-PGA Plate and Screw Fixation in Pediatric Craniofacial Surgery: Clinical Experience in 1883 Patients", *Plastic and Reconstructive Surgery*, vol. 114, no. 4, pp. 850-857, 2004.

4. V.K. Ganesh, K. Ramakrishna, and D.N. Ghista, "Biomechanics of bone-fracture fixation by stiffness-graded plates in comparison with stainless-steel plates", *Biomedical Engineering Online*, vol. 4, pp. 46-61, 2005.

5. R. Felfel, I. Ahmed, A.J. Parsons, L.T. Harper and C.D. Rudd, "Initial mechanical properties of phosphate-glass fibre- reinforce rods for use as resorbable intramedullary nails", *Journal of Materials Science*, vol. 47, no. 12, pp. 4884-4894, 2012.

6. M.L. Busam, R.J. Esther and W.T. Obremskey, "Hardware removal: indications and expectations", *Journal of the American Academy of Orthopaedic Surgeons*, vol. 14, no. 2, pp. 113-120, 2006.

7. P.H. Long, "Medical Devices Orthopaedic Applications", *Toxicologic Pathology*, vol. 36, no.1 , pp. 85-91, 2008.

8. X.E. Guo, "Mechanical properties of cortical bone and cancellous bone tissue", In: S.C. Cowin, ed., *Bone Mechanics Handbook*, CRC Press: Boca Raton, FL, 2001, pp. 10.1-10.23.

9. F.G. Evans, "Mechanical properties and histology of cortical bone from younger and older men", *The Anatomical Record*, vol. 185, no. 1, pp. 1-11, 1976.

10. B.D. Ratner, A.S. Hoffman, F.J. Schoen and J.E. Lemons, *Biomaterials Science: An Introduction to Materials in Medicine*, New York: Academic Press, 2012.

11. J. Black and G.W. Hastings, *Handbook of Biomaterials Properties*, London, U.K.: Chapman and Hall, 1998.

12. I. Ahmed, P.S. Cronin, E. a Abou Neel, a J. Parsons, J.C. Knowles, and C.D. Rudd, "Retention of mechanical properties and cytocompatibility of a phosphate-based glass fibre/polylactic acid composite", *Journal of Biomedical Materials Research Part B: Applied Biomaterials*, vol. 89, no. 1, pp. 18-27, 2009.

13. R.M. Felfel, I. Ahmed, A.J. Parsons, P. Haque, G.S. Walker, and C.D. Rudd, "Investigation of Crystallinity, Molecular Weight Change, and Mechanical Properties of PLA/PBG Bioresorbable Composites as Bone Fracture Fixation Plates", *Journal of Biomaterials Applications*, vol. 25, no. 7, pp. 765-789, 2012.

14. N. Han, I. Ahmed, A.J. Parsons, L. Harper, C.A. Scotchford, B.E. Scammell and C.D. Rudd, "Influence of screw holes and gamma sterilization on properties of phosphate glass fibre-reinforced composite bone plates", *Journal of Biomaterials Applications*, vol. 27, no. 8, pp. 990-1002, 2011.

15. F.A. Ramirez and L.A. Carlsson, "Modified single fibre fragmentation test procedure to study water degradation of the fibre/matrix interface

toughness of glass/vinylester", *Journal of Material Science*, vol. 44, no. 12, pp. 3035-3042, 2009.

16. V.M. Karbhari, "E-glass/vinylester composites in aqueous environments: effects on short-beam shear strength", *Journal of Composites for Construction*, vol. 8, no. 2, pp. 148-157, 2004.

17. A. Kootsookos and A.P. Mouritz, "Seawater durability of glass- and carbon-polymer composites", *Composites and Science Technology*, vol. 64, no. 10-11, pp. 1503-1511, 2004.

18. X.F. Zhou, J.A. Nairn and H.D. Wagner, "Fibre-Matrix adhesion from the single fibre composite test: nucleation of interfacial debonding", *Composites Part A: Applied Science and Manufacturing*, vol. 30, no. 12, pp. 1387-1400, 1999.

19. D. Hull and T.W. Clyne, *An Introduction to Composite Materials*, Cambridge, UK: Cambridge University Press, 1996.

20. H.F. Wu, D.W. Dwight and N.T. Huff, "Effects of silane coupling agents on the interphase and performance of glass-fibre-reinforced polymer composites", *Composites Science and Technology*, vol. 57, no. 8, pp. 975-983, 1997.

21. A.T. DiBenedetto, "Tailoring of interfaces in glass fibre reinforced polymer composites: a review", *Materials Science and Engineering*, vol. 302, no. 1, pp. 74-82, 2001.

22. E. Plueddemann, *Silane Coupling Agents*, New York City, New York: Plenum Press, 1991.

23. M. J. Lodeiro, S. Maudgal, L. N. Mccartney, and R. Morrell, "Critical Review of Interface Testing Methods for Composites," Teddington, Middlesex, United Kingdom, 1998.

24. L.T. Drzal, P.J. Herrera-Franco and H. Ho, "Fibre-matrix interface tests", *Comprehensive Composite Materials: Test Methods, Nondestructive Evaluation and Smart Material*, vol. 5, pp.71-111, 2000.

25. E.V. Pisanova and S.F. Zhandarov, "On the mechanism of failure in microcomposites consisting of single glass fibres in a thermoplastic matrix", *Composites Science and Technology*, vol. 57, no. 8, pp. 937-943, 1997.

26. M.R. Piggott, "Why interface testing by single fibre methods can be misleading?", *Composites Science and Technology*, vol. 57, no. 8, pp. 965-974, 1997.

27. X.-F. Zhou, H.D. Wagner and S.R. Nutt, "Interfacial properties of polymer composites measured by push-out and fragmentation tests", *Composites Part A: Applied Science and Manufacturing*, vol. 32, no. 11, pp. 1543-1551, 2001.

28. M.J. Pitkethly, J.P. Favre, U. Gaur, J. Jakubowski, S.F. Mudrich, D.L. Caldwell, L.T. Drzal, M. Nardin, H.D. Wagner, L. Di Landro, A. Hampe, J.P. Armistead, M. Desaeger and I. Verpoest, "A round-robin programme on interfacial test methods", *Composites Science and Technology*, vol. 48, no. 1-4, pp. 205-214, 1993.

29. A. N. Netravali, R. B. Henstenburg, S. L. Phoenix, and P. Schwartz, "I: Experiments on Graphite Fibers in Epoxy", *Polymer Composites*, vol. 10, no. 4, pp. 226-241, 1989.

30. M. A. Slivka, C. C. Chu, and I. A. Adisaputro, "Fiber-matrix interface studies on bioabsorbable composite materials for internal fixation of bone fractures. I. Raw material evaluation and measurement of fiber-matrix interfacial adhesion", *Journal of Biomedical Materials Research*, vol. 36, no. 4, pp. 469-77, Sep. 1997.

31. D. Tripathi and F.R. Jones, "Review: Single fibre fragmentation test for assessing adhesion in fibre reinforced composites", *Journal of Material Science*, vol. 33, no. 1, pp. 1-16, 1998.

32. S. Cozien-Cazuc, "Characterisation of Resorbable Phosphate Glass Fibres", University of Nottingham, 2006.

33. P. Haque, I.A. Barker, A.J. Parsons, K.J. Thurecht, I. Ahmed, G.S. Walker, C.D. Rudd and D.J. Irvine, "Influence of compatibilizing agent molecular structure on the mechanical properties of phosphate glass fiber-reinforced PLA composites," *Journal of Polymer Science Part A: Polymer Chemistry*, vol. 48, no. 14, pp. 3082-3094, 2010.

34. P. Haque, A.J. Parsons, I.A. Barker, I. Ahmed, D.J. Irvine, G.S. Walker, and C.D. Rudd, "Interfacial properties of phosphate glass fibres/PLA composites: Effect of the end functionalities of oligomeric PLA coupling agents," *Composites Science and Technology*, vol. 70, no. 13, pp. 1854-1860, 2010.

35. I. Barker, "Innovations in mass transfer by biodegradable composites and hyperbranched polymers", University of Nottingham, 2010.

36. K. A. Porter, "Ring Opening Polymerisation of Lactide for the synthesis of Poly (Lactic Acid)", Seminar Abstracts Fall 2005-Spring 2006, University of Illinois Organic Chemistry, 2006, pp. 25-32.

37. P. Haque, "Oligomeric PLA Coupling Agents for Phosphate Glass Fibres/PLA Composites", University of Nottingham, 2011.

38. G. Schwach, J. Coudane, R. Engel and M. Vert, "More about the polymerisation of lactide in the presence of stannous octoate", *Journal of Polymer Science Part A: Polymer Chemistry*, vol. 35, no. 16, pp. 3431-3440, 1997.

39. P. Lan and W. Wang, "H-NMR spectroscopy analysis of homo and copolymers of L-Lactic Acid", *Journal of Fibre Bioengineering and Informatics*, vol. 2, no. 2, pp. 137-140, 2009.

40. J. A. P. P. Van Dijk and J. A. M. Smit, "Characterisation of poly(D,L-Lactic Acid) by gel permeation chromatography", *Journal of Polymer Science Polymer Chemistry Edition*, vol. 21, no. 1, pp.197-208, 1983.

41. M. Hirata, K. Kobayashi and Y. Kimura, "Synthesis and properties of high-molecular-weight stereo di-block polylactides with nonequivalent D/L ratios", *Journal of Polymer Science Part A: Polymer Chemistry*, vol. 48, no. 4, pp. 794-801, 2010.

42. N.T. Nguyen, E. Greenhalgh, M.J. Kamaruddin, J. El Harfi, K. Carmichael, G. Dimitrakis, S.W. Kingman, J.P. Robinson and D.J. Irvine, "Understanding the acceleration in the ring-opening of lactones delivered by microwave heating", *Tetrahedron*, vol. 70, no. 4, pp. 996-1003, 2014

43. N.T. Nguyen, K.J. Thurecht, S.M. Howdle and D.J. Irvine, "Facile one-spot synthesis of highly branched polycaprolactne", *Polymer Chemistry*, vol. 5, no. 8, pp. 2997-3008, 2014.

44. A. B. Robertson, J. A. Cook, and J. T. Gregory, "Use of gel permeation chromatography to study the synthesis of bisphenol-A carbonate oligomers," In: *Polymerization Kinetics and Technology*, American Chemical Society, 2009, pp. 258-273.

45. T.G. Fox and P.J. Flory, "Second-order transition temperatures and related properties of polystyrene: I. Influence of molecular weight", *Journal of Applied Physics*, vol. 21, pp. 581-591, 1950.

46. M. W. Muggli, T. C. Ward, Q. J. Tchatchoua, and J. E. Mcgrath, "End-group effect on physical aging and polymer properties for poly(ether sulfones)", *Journal of Polymer Science Part B: Polymer Physics*, vol. 41, no. 22, 2003.

47. X. Jiang, C. Z. Yang, K. Tanaka, A. Takahra, and T. Kajiyama, "Effect of chain end group on surface glass transition temperature of thin polymer film", *Physics Letters A*, vol. 281, no. 5-6, pp. 363-367, 2001.

48. P. C. Hiemenz and T. P. Lodge, *Polymer Chemistry*, Second Edi. Boca Raton, FL: CRC Press, 2007.

49. K. O'Driscoll and R. A. Sanayei, "Chain-Length Dependence of the glass transition temperature," *Macromolecules*, vol. 24, no. 15, pp. 4479-4480, 1991.

50. Matweb, "NatureWorks® Ingeo™ 6201D Injection Grade PLA Data Sheet." [Online]. Available: http://www.matweb.com/search/datasheet.aspx?matguid=a1b0e140fecf4c91b2562534b87d8ca5&ckck=1 [Accessed: 15-Dec-2011].

51. Y. H. Kim and R. Beckerbauer, "Role of end groups on the glass transition of hyperbranched polyphenylene and triphenylbenzene derivatives", *Macromolecules*, vol. 27, no. 7, pp. 1968-1971, 1994.

52. J. Coates, "Interpretation of infrared, a practical approach", *Encyclopaedia of Analytical Chemistry*, R.A. Meyers, Ed., pp. 10815-10837, 2000.

53. M. S. Lopes, A. L. Jardini and R. M. Filho, "Synthesis and characterisation of poly(lactic acid) by ring-opening polymerization for biomedical applications", *Chemical Engineering Transactions*, vol. 38, pp. 331-336, 2014.

54. C. D'A. C. Erbetta, R. J. Alves, J. M. Resende, R.F. de S. Freitas and R. G. de Sousa, "Synthesis and characterization of poly(D,L-lactide-co-glycolide) copolymer", *Journal of Biomaterials and Nanobiotechnology*, vol. 3, no. 2, pp. 208-225, 2012.

55. J. Choueka, J.L. Charvet, H. Alexander, Y.H. Oh, G. Joseph, N.C. Blumenthal and W. LaCourse, "Effect of annealing temperature on the degradation of reinforcing fibres for absorbable implants", *Journal of Biomedical Materials Research,* vol. 29, no. 11, pp. 1309-1315, 1995.

56. S. Shaharuddin, "Manufacture and Characterisation of Novel Resorbable Phosphate Based Glass Fibres for Biomedical Applications", University of Nottingham, 2012.

57. M.S. Hasan, I. Ahmed, A.J. Parsons, G.S. Walker and C.A. Scotchford, "The influence of coupling agents on mechanical property retention and long-term cytocompatibility of phosphate glass fibre reinforced PLA composites", *Journal of the Mechanical Behaviour of Biomedical Materials*, vol. 28, pp. 1-14, 2013.

58. B.C. Bunker, G.W. Arnold, and J.A. Wilder, "Phosphate glass dissolution in aqueous solutions"*, Journal of Non-Crystalline Solids*, vol. 64, no. 3, pp. 291-316, 1984.

59. I. Ahmed, C.A. Collins, M.P. Lewis, I. Olsen and J.C. Knowles, "Processing, characterisation and biocompatibility of iron-phosphate glass fibres for tissue engineering", *Biomaterials*, vol. 25, no. 16, pp. 3223-3232, 2004.

60. C.R. Kurkjian, "Mechanical properties of phosphate glasses", *Journal of Non-Crystalline Solids*, vol. 263 & 264, pp.207-212, 2000.

61. V. Pukh, L. Baikova, M. Kireenko and L. Tikhonova, "On the kinetics of crack growth on glass", *Glass Physics and Chemistry*, vol. 36, no. 6, pp. 560-566, 2009.

62. A.A. Griffith, "The phenomenon of rupture and flaw in solids", *Philosophical Transactions of the Royal Society of London Series A*, vol. 221, pp. 163-198 1921.

63. P. Haque, I. Ahmed, A. Parsons, R. Felfel, G. Walker and C. Rudd, "Degradation properties and microstructural analysis of $40P_2O_5$-$24MgO$-$16CaO$-$16Na_2O$-$4Fe_2O_3$ phosphate glass fibres", *Journal of Non-Crystalline Solids*, vol. 375, pp. 99-109, 2013.

64. A.J. Parsons, I. Ahmed, J. Yang, S. Cozien-Cazuc and C.D. Rudd, "Heat-treatment of phosphate glass fibres and its effect on composite property retention", *16th international Conference on Composite Materials*, 2007, Kyoto.

65. J.V. Mullin and V.F. Mazzio, "Basic failure mechanisms in advanced composites", NAS-w-2093, NASA, 1971.

66. A.C. Johnson, S.A. Hayes and F.R. Jones, "The role of matrix cracks and fibre/matrix debonding on the stress transfer between fibre and matrix in a single fibre fragmentation test", *Composites Part A: Applied Science and Manufacturing*, vol. 43, no. 1, pp. 65-72, 2012.

67. L.T. Drzal and M. Madhukar, "Fibre-matrix adhesion and its relationship to composite mechanical properties", *Journal of Materials Science*, vol. 28, no. 3, pp. 569-610, 1993.

68. L.T. Drzal, "The effect of polymeric matrix mechanical properties on the fibre-matrix interfacial shear strength", *Materials Science and Engineering*, vol. 126, no. 1-2. pp. 289-293, 1990.

69. D. Tripathi, F. Chen and F.R. Jones, "The Effect of Matrix Plasticity on the Stress Fields in a Single Filament Composite and the Value of Interfacial Shear Strength Obtained from the Fragmentation Test", *The Royal Society of London Proceedings Series A: - Mathematical and Physical Sciences*, vol. 452, no. 1946, pp. 621-653, 1996.

70. C. Galiotis, R.J. Young, P.H.J. Yeung and D.N. Batchelder, "The study of model diacetylene-epoxy composites", *Journal of Material Science*, vol. 19, pp. 3640-3648, 1984.

71. Y. Termonia, "Theoretical study of the stress transfer in single fibre composite", *Journal of Material Science*, vol. 22, pp. 504-508, 1987.

72. Y. Termonia, "Dependence of the critical fibre length on the modulus in the single fibre composites", *Journal of Material Science Letters*, vol. 12, no. 10, pp. 732-733, 1993.

73. M.R. Piggott, *Load Bearing Fibre Composites*, Pergamon, Oxford, 1980, p. 116.

74. J.C. Jaeger, *Elasticity, Plasticity and Flow*, 3rd Edition, Methuen, London, 1969, pp.89-95.

75. X. Liu, D.M. Grant, A.J. Parsons, L.T. Harper, C.D. Rudd and I. Ahmed, "Magnesium coated bioresorbable phosphate glass fibres: investigation of the interface between fibre and polyester matrices", *BioMed Research International*, vol. 2013, pp. 1-10, 2013.

76. A. Mohanty, M. Misra and L. Drzal, *Natural Fibres, biopolymers and biocomposites*, Ch.16, Boca Raton, FL, 2005.

77. I. Ahmed, I.A. Jones, A.J. Parsons, J. Bernard, J. Farmer, C.A. Scotchford, G.S. Walker, and C.D. Rudd, "Composites for bone repair: phosphate glass fibre reinforced PLA with varying fibre architecture", *Journal of Materials Science. Materials in Medicine*, vol. 22, no. 8, pp. 1825-1834, 2011.

78. S. Lee, T. Nguyen, J. Chin and T.J. Chuang, "Analysis of the single-fibre fragmentation test", *Journal of Materials Science*, vol. 33, no. 21, pp. 5221-5228, 1998.

79. C.Y. Hui, S.L. Phoenix and D. Shia, "The single filament composite test: a new statistical theory for estimating the interfacial shear strength and Weibull parameters for fibre strength", *Composites Science and Technology*, vol. 57, no. 12, pp. 1707-1725, 1997.

80. M. Nardin and J. Schultz, "Relationship between fibre-matrix adhesion and the interfacial shear strength in polymer-based composites", *Composite Interfaces*, vol. 1, no. 2, pp. 177-192, 1993.

81. J. Aveston, G.A. Cooper, and A. Kelly, "Single and multiple fracture: the properties of fibre composites", Conference Proceeding, National Physics Laboratory, Teddington: *The Properties of Fibre Composites*, IPC Science and Technology Press, Guildford, 1971, pp. 15-26.

82. A.C. Kimber and J.G. Kreer, "On the theoretical average crack spacing in brittle matrix composites containing continuous aligned fibres", *Journal of Material Science Letters*, vol. 1, no. 8, pp. 353-354, 1982.

83. I. Ahmed, M. Lewis, I. Olsen and J.C. Knowles, "Phosphate glasses for tissue engineering: Part 2. Processing and characterisation of a ternary based $P_2O_5$-CaO-$Na_2O$ glass fibre system", *Biomaterials*, vol. 25, no. 3, pp. 501-507, 2004.

# CHAPTER 5

# MECHANICAL AND DEGRADATION PROPERTIES OF S-PLA

# SIZED PGF/ PLA UNIDIRECTIONAL COMPOSITES

## 5.1 SUMMARY

*In this chapter, control (C) and S-PLA_s coated bioresorbable phosphate glass fibres (PGF) were used to reinforce PLA. The S-PLA coated unidirectional (UD) mats were dip coated (DC) and spray coated (SP) to investigate the effect of the coating method on the composite properties. PGF/PLA unidirectional (UD) composites were prepared via laminate stacking and compression moulding with fibre volume fractions of ~20%. Samples were prepared with fibres oriented longitudinally and others with fibres oriented transversely. The composites were degraded in phosphate buffered saline (PBS) at 37 °C for 28 days.*

*Initial flexural strength for C-long, DC-long and SP-long composites was $158 \pm 23$ MPa, $248 \pm 16$ MPa and $212 \pm 9$ MPa and the modulus was $9 \pm 1.3$ GPa, $14 \pm 1.3$ GPa and $16 \pm 0.4$ GPa, respectively. Initial transverse flexural strength for C-trans, DC-trans and SP-trans was $43 \pm 4$ MPa, $47 \pm 1$ MPa and $54 \pm 8$ MPa and the modulus was $4 \pm 0.1$ GPa, $5 \pm 0.2$ GPa and $4 \pm 0.5$ GPa, respectively. After 14 days, the strength of C-long and DC-long samples were statistically similar for a p-value of $p > 0.05$ while the strength of the SP-long samples had decreased to a value similar to that of PLA. The modulus of C-long was less than that for DC-long and SP-long samples. The respective transverse strength and moduli also decreased significantly for a p-value of $p < 0.05$.*

*The water uptake and mass loss of the composite samples had an initial increase after 1 day of immersion. No significant increase was observed over the following 9-13 days, after which a rapid increase was observed. PLA showed no*

*significant change in flexural properties, water uptake and mass loss over 28 days and had no evidence of crystallisation. A crystallisation peak at ~16.5° was detected for all composite samples at all of the time points however the peak did not change in intensity over 28 days.*

## 5.2 INTRODUCTION

It is well known that fibre volume fraction ($V_f$) and fibre orientation can affect the mechanical properties of bioresorbable phosphate glass fibre (PGF) reinforced polylactic acid (PLA) composites [1-3]. While both randomly (RM) oriented fibre reinforced composites and unidirectional (UD) composites had a significant increase in the flexural strength and modulus when compared to unreinforced PLA, UD composites revealed a greater increase in flexural strength and modulus [1-2]. UD oriented fibres increase the reinforcing effect in composites due to the stress loads being axially distributed along the fibre lengths. When the fibres in a composite are aligned in the direction of maximum stress the composite has better properties than composites with randomly oriented fibres [1, 4].

Even though the initial properties of these composites are good, subsequent degradation studies have shown a rapid decline in mechanical properties after immersion in deionised water or phosphate buffered saline (PBS) at 37°C [1-3, 5]. This lack of retention of mechanical properties has been attributed to the loss of interface between the fibre and the matrix [1-3, 5-7] after submersion in aqueous media. The RM composites showed a better retention of mechanical properties than UD composites. This was attributed to the moisture absorption of the RM and UD composites. UD fibres are believed to wick fluid into the composite samples which enhanced the breakdown of the

interface between the fibres and the matrix. Comparatively the discontinuous arrangement of the RM mats made them less susceptible to wicking, thus slowing down the interface breakdown [1, 8].

Coupling agents such as 3-Aminopropyl triethoxy silane (APS) and novel coupling agents such as glycerol-ended PLA (G-PLA) and sorbitol-ended PLA (S-PLA) have been investigated to improve the interface between PGF and PLA [6-7, 9]. Parsons *et al.* coated $40P_2O_5$-24MgO-16CaO-16Na$_2$O-4Fe$_2$O$_3$ (P40) fibres with two different sizing agents: APS and HEMA (2-hydroxyethyl methacrylate). RM fibre mats were produced and used to reinforce PLA. Initial properties showed that the composites with coated fibres had lower flexural strength values (APS: ~85 MPa; HEMA: 80 MPa) than composite samples with uncoated (control) fibres (90 MPa). After 28 days of immersion in deionised water at 37°C, control, APS and HEMA composites had flexural strengths of ~78 MPa, ~60 MPa and 70 MPa, respectively. Initial flexural moduli of the APS and HEMA composites (APS: ~5.7 GPa; HEMA: ~6.4 GPa) increased compared to the control composite (~5 GPa). The modulus of the APS composite decreased to ~4.5 GPa after 28 days immersion in deionised water at 37°C similar to that of the control composite. The modulus of the HEMA composite decreased to approximately 5.7 GPa over 28 days immersion at 37°C. [9]

Hasan *et al.* investigated the effects of coated and uncoated (control) $45P_2O_5$-24MgO-16CaO-11Na$_2$O-4Fe$_2$O$_3$ (P45) UD fibre mats when reinforced with PLA. Three different coupling agents were used: APS, S-PLA and hexamethylene diisocyanate (HDI). It was found that APS and S-PLA composites both yielded initial flexural strength and modulus values (300 MPa and 22 GPa, and 260 MPa and 25 GPa, respectively) which were significantly greater than the flexural strengths and moduli for control (215 MPa and 20 GPa) and HDI (190

MPa and 20 GPa) composites. Degradation in PBS at 37°C showed that the flexural strength and modulus of all the coated UD composites decreased significantly after the first 7 days of immersion. The greatest reduction in mechanical properties and largest water uptake was seen in S-PLA composites. It was suggested that the hydrophilicity of S-PLA had not reacted with the fibre surface. It should be noted that all the composites in this study had a $V_f$ ~35%. [7, 10]

Most of the UD PGF composites that have been investigated in the literature were tested with the fibres oriented in the longitudinal direction (0°), i.e. the direction of maximum stress or, fibre dominated properties. According to Drzal *et al.* the longitudinal tensile, compressive and flexural strengths are dominated by fibre properties. Off-axis strength properties such as transverse tensile, transverse flexural, in-plane shear and interlaminar shear strength, are dominated by matrix and interfacial properties [4, 11-13]. Testing the composite with fibres aligned transversely (90°), meant that the applied load was concentrated on the fibre, matrix and the interface equally, i.e. the fibre-matrix adhesion is expected to have a dominant effect on the composite properties [11].

A study by Drzal and Madhukar demonstrated the relationship between fibre-matrix adhesion and composite mechanical properties in three high fibre $V_f$ carbon fibre reinforced epoxy composites: 1. "AU4" – fibres as received, 2. "AS4" – fibres were surface treated with electrochemical oxidation for adhesion to epoxy matrices and 3. "AS4C" – fibres coated with 100-200 nm layer of epoxy applied from an organic solvent on to the surface-treated AS-4 fibres. The single fibre fragmentation tests (SFFT) showed that AU4, AS4 and AS4C single fibre composites had interfacial shear strengths of 37, 68 and 82 MPa, i.e. low, intermediate and high levels of adhesion, respectively. It was found that there

was little difference between the longitudinal flexural and tensile moduli and the longitudinal flexural and tensile strengths for all three full body composites. The transverse flexural strengths for all three composites (21.4 ± 5.8 MPa GPa, 50.2 ± 3.4 MPa and 75.6 ± 14 MPa, respectively) had a significant improvement when compared to the transverse tensile strengths. They also showed that the transverse strengths increased with increasing levels of adhesion demonstrating an increase in interfacial properties. The transverse moduli (10.2 ± 1.5, 9.9 ± 0.5 GPa and 10.7 ± 0.6 GPa), on the other hand, did not show any significant differences. The transverse properties were also much less than the longitudinal, fibre dominated properties. [12]

Haque compared uncoated and sorbitol-initiated coated UD P40 fibre reinforced PLA composites. Initial mechanical properties were tested (0° tension, 0° three point flexural bending and in-plane shear) and a degradation study in PBS at 37°C for 7 days was conducted. Initial tensile strength and modulus of S-PLA sized UD composites showed a 34% and 33% increase when compared to control composites (61 ± 5 MPa and 12 ± 2 GPa to 82 ± 9 MPa and 16 ± 2 GPa). After 7 days immersion, it was found that the tensile strength of S-PLA coated UD composites was still higher than that of the of the control composite, however the values of both had decreased significantly. The modulus of the control composite remained unchanged while that of the S-PLA coated composite had increased to 30 ± 5 GPa. [14]

Similarly the flexural strength and modulus values of S-PLA composites from the same study were 38% and 39%, respectively, greater than that of the control prior to degradation. After 7 days, the strength and moduli of both control and S-PLA composites decreased and were statistically similar: 101 ± 3 MPa and 11 ± 2 GPa, 105 ± 2 MPa and 13 ± 0.4 GPa. The in-plane shear strength

of S-PLA coated composites was 32% greater than that of control and as in the flexural and tensile tests, the values of both decreased after 7 days immersion in PBS at 37°C. It should be noted that the in-plane shear of S-PLA decreased ~25% while the control decreased by 50% after degradation [14].

The study of single fibre composites (SFC) in Chapter 4 had the advantage of observing and investigating a more detailed interaction of the fibre-matrix interface. It also allowed the observation of the effect the coupling agent had on the interface on a smaller scale. In this chapter, the macroscopic properties, namely the longitudinal and transverse flexural properties, of a full body composite were investigated. Three different types of composites were manufactured: 1. Control (uncoated) composites, 2. Dip coated UD composites and 3. Spray coated UD composites. S-PLA_s was used to coat the UD fibre mats as it was observed that the chain length did not affect the interfacial shear stress (IFSS) (*discussed in* Chapter 4). S-PLA_s was easier to manufacture and handle than longer chain length coupling agents. A degradation study was carried out to observe the retention of the mechanical properties and to assess the mass loss and water uptake of these composites.

## 5.3 RESULTS AND DISCUSSION

Unidirectional (UD) mats were manufactured and coated as stated in Chapter 3 Sections 3.5.1-3.5.2 with $45P_2O_5$-$24MgO$-$16CaO$-$11Na_2O$-$4Fe_2O_3$ (P45) fibres. The control and coated UD composites were manufactured using the laminate stacking and compression moulded method described in Section 3.5.3. It should be noted that the fibre alignment was not disturbed during the dip coating process (*see* Figure 3.4 (c)). Consequently the fibre alignment in control, DC and SP composites were found to be greatly improved over manually aligned UD

fibre prepregs [1, 7, 14]. Table 5.1 summarises the GPC data used to characterise the S-PLA_s coupling agent made for UD mat coating. The same coating concentration used in Chapter 4 for S-PLA_s fibres was used here (0.0064 moles). S-PLA_s was chosen because it was easier to handle and produce for full body composite manufacture.

*Table 5.1: Summary of GPC data for S-PLA coupling agent manufactured for UD mat coating*

| $M_n$ | $M_p$ | PDI |
|:---:|:---:|:---:|
| 657 | 705 | 2.72 |

### 5.3.1 Flexural Properties

The flexural properties of control, dip coated and spray coated composites was conducted using the method described in Chapter 3 Section 3.5.4.

#### 5.3.1.1 Using Rule of Mixtures

The rule of mixtures can be used to calculate the elastic modulus ($E_1$) for a fibre reinforced composite [15]. This is given by

$$E_1 = V_f E_f + (1 - V_f) E_m \qquad\qquad \textbf{\textit{Equation 5.1}}$$

Where $E_f$ is the elastic modulus of the fibres; $E_m$ is the elastic modulus of the matrix; $E_1$ is the composite elastic modulus in the longitudinal direction and $V_f$ is the fibre volume fraction. An equation to calculate the transverse modulus ($E_2$) can be derived using the same equal stress model that was used to derive Equation 5.1.

$$E_2 = \left[ \frac{V_f}{E_f} + \frac{\left(1 - V_f\right)}{E_m} \right]^{-1}$$

***Equation 5.2***

The rule of mixtures is typically used to estimate the tensile stress and stiffness of fibre reinforced composites [15]. Using a span-to-thickness ratio of 16:1, Haque compared the tensile and flexural moduli of control and S-PLA coated PGF/ PLA composites (12 ± 2 GPa and 9 ± 2 GPa and, 16 ± 2 GPa and 11.9 ± 3 GPa respectively). It was found that the results were statistically insignificant according to a *t* test [14]. The rule of mixtures can therefore be used to predict the flexural moduli of control and S-PLA coated PGF/ PLA composites [16]. Table 5.2 shows the summary of the comparison between theoretical and experimental flexural modulus for longitudinal control, S-PLA dip-coated and S-PLA spray coated PGF/ PLA composites. The modulus of the coated fibres was the same as that for the uncoated fibres (55 GPa) which is why the predicted longitudinal modulus is the same for all the composite samples.

Equation 5.2, known as the Reuss Model, is considered to be simple and convenient, but it is a poor approximation for the transverse modulus [15]. It is typically used to predict the transverse tensile modulus. According Drzal and Madhukar, there is no significant difference between the tensile modulus and flexural modulus and fibre coatings do not affect the composite modulus [11]. In addition, Haque shows no statistical difference between the tensile and flexural moduli of control and S-PLA coated composites, as mentioned above, and between the moduli of control and S-PLA coated composites [14]. Therefore, Equation 5.2 was used to calculate the predicted transverse modulus. These values are shown in Table 5.3 along with the corresponding experimental results. It should be noted that the theoretical transverse modulus (3 GPa) is, as

expected, an underestimation. Hull and Clyne attributed this to plastic deformation and creep that occurs during transverse testing of composites with thermoplastic polymers [15].

*Table 5.2:* Comparison between the longitudinal experimental and theoretical flexural modulus for control and S-PLA coated PGF/PLA composites

| Sample Codes | Theoretical Flexural Modulus (GPa) | Experimental Flexural Modulus (GPa) |
|---|---|---|
| C-long | | 9 ± 1 |
| DC-long | 13 | 14 ± 1 |
| SP-long | | 16 ± 0.4 |

*Table 5.3:* Comparison between the transverse experimental and theoretical flexural modulus for control and S-PLA coated PGF/PLA composites.

| Sample Codes | Theoretical Flexural Modulus (GPa) | Experimental Flexural Modulus (GPa) |
|---|---|---|
| C-trans | | 4 ± 0.1 |
| DC-trans | 3 | 5 ± 0.2 |
| SP-trans | | 4 ± 0.5 |

*5.3.1.2 Longitudinal Properties*

Figure 5.1 shows the initial flexural strengths and moduli for PLA, and for longitudinal control (C-long), dip coated (DC-long) and spray coated (SP-long) composites. The flexural strength and modulus of C-long (158 ± 23 MPa; 9 ± 1 GPa) is 63% and 200% greater than that of PLA (97 ± 8 MPa; 3 ± 0.4 GPa). This significant increase was expected due to studies conducted by Ahmed *et al.*, Felfel *et al.*, Hasan *et al.* and Haque that showed the improvement in flexural properties of PLA composites due to PGF reinforcement [1-3, 5, 10, 13]. Aligning the fibres all in one direction in a full body composite increases the reinforcing effect as the loads are axially distributed along the fibre lengths [1].

The flexural modulus for C-long composites was statistically similar to that obtained for PGF reinforced PLA in the literature [1-2, 14, 16]. The flexural

strengths obtained in these studies were found to be significantly ($p < 0.05$) different. Hasan *et al.* had a greater flexural strength and modulus for control composites 215 MPa and 20 GPa that was due to an increase in $V_f$ of ~35% [7]. Han *et al.* also reported a similar increase in flexural strength and modulus for $50P_2O_5\text{-}40CaO\text{-}5Na_2O\text{-}5Fe_2O_3$ fibre reinforced composites with increasing volume fraction [17]. It was also found that using a larger number of thinner UD fibre prepregs (UD fibre mats with PLA to bind the fibres together) yielded a significant increase in mechanical properties. Han *et al.* attributed this to improved fibre dispersion and wet-out of the fibres in the composites produced. A flexural modulus of 208 MPa was obtained for composites with $V_f$ ~25% and 8 thin fibre mats [17].
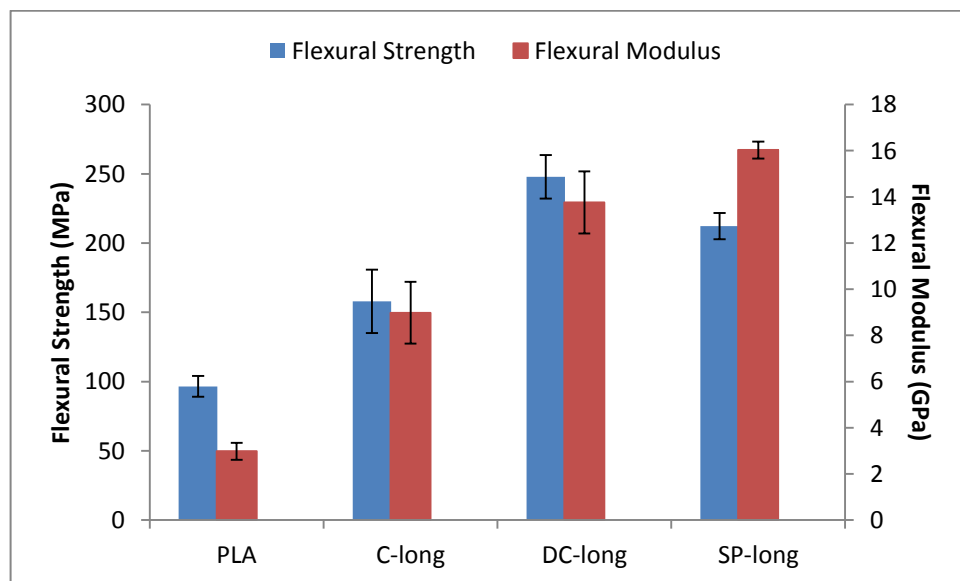


***Figure 5.1:*** *The initial flexural strengths and flexural moduli of PLA and, C_long, DC_long and SP_long composites*

In this study 6-7 thin fibre mats were used to prepare UD P45 reinforced composites with a lower $V_f$ of ~20% and achieved a flexural strength of 158 ± 23 MPa. This was larger than that observed by Haque and Felfel *et al.* (118 MPa and 115 MPa, respectively) for $40P_2O_5\text{-}24MgO\text{-}16CaO\text{-}16Na_2O\text{-}4Fe_2O_3$ (P40) fibre

reinforced composites with a $V_f$ of ~25-28% [2, 14]. However it appeared to be greater than the initial flexural strength value for UD $50P_2O_5$-40CaO-5Na$_2$O-5Fe$_2$O$_3$ reinforced PLA (129 MPa; $V_f$ = 23.51%) obtained by Ahmed *et al.* [1]. The initial values seen in Ahmed *et al.*'s study were comparable to the values obtained by Sharmin for $45P_2O_5$-24MgO-16CaO-15Na$_2$O (P45B0) reinforced PLA composites. The addition of 5 mol% boron oxide to the glass fibre formulation ($45P_2O_5$-24MgO-16CaO-10Na$_2$O-5B$_2$O$_3$ (P45B5)) increased the initial flexural strength to 156 MPa and the flexural modulus to 12.25 GPa. The increase mechanical properties were attributed to the increase in the fibre strength found with the addition of boron oxide [16, 18].

The initial flexural strength for Sharmin's P45B5 fibres reinforced with PLA (156 MPa) was comparable to the initial flexural strength for C-long composites but not to the flexural strength obtained for Sharmin's $45P_2O_5$-24MgO-16CaO-12Na$_2$O-3Fe$_2$O$_3$ (P45Fe3) reinforced composites (138 MPa) [16]. This variation in UD longitudinal flexural properties was attributed to the glass fibre formulation and the subsequent mechanical properties of the fibres (*see* Chapter 2 Section 2.6), i.e. higher fibre properties yields higher composite mechanical properties [1, 5, 16, 19-22]. Sharmin reported the tensile strength of P45Fe3 fibres as 511 ± 121 MPa [16]. However the tensile strength of S-PLA_s coated P45 fibres, in the current study, was 680 ± 121 MPa (*as described in* Chapter 3 Section 3.4.1). Sharmin also investigated the addition of iron oxide to the P45B5 fibres. It was found that with 3 mol% of Fe$_2$O$_3$ in P45B5 fibres the (resulting) P45B5Fe3 fibre tensile strength increased to 1007 ± 184 MPa and when used as reinforcement in PLA, the composites had a significant increase in flexural strength and modulus (184 MPa and 12.28 GPa). The increase in fibre properties with addition of both boron oxide and iron oxide also increased the properties of the composites reinforced with these fibres [16].

The flexural strength and modulus for both the DC-long (248 ± 16 MPa; 14 ± 1 GPa) and SP-long (212 ± 9 MPa; 16 ± 0.4 GPa) composites were shown to have significantly ($p$ < 0.05) increased when compared to that of the uncoated C-long composite. The DC_long composite revealed a 57% increase in the flexural strength and a 56% increase in flexural modulus whereas the SP-long composite had a 34% increase in flexural strength and a 78 % increase in flexural modulus. This indicated that the S-PLA coating had improved flexural properties prior to degradation similar to the interfacial shear stress (IFSS) discussed in Chapter 4 Section 4.3.8. However, the dip coating method had a significant ($p$ < 0.05) increase in the initial flexural strength when compared to the spray coating method, while the modulus of SP-long composites was noticeably larger.

Hasan *et al.* showed S-PLA coated fibres increased the flexural strength and modulus of P45 reinforced PLA composites by 21% and 20%, respectively ($V_f$ = ~35%) [7, 10]. Additionally, work by Haque showed increases in flexural strength and modulus by 34% and 33%, respectively for PLA composites reinforced with S-PLA coated P40 fibres ($V_f$ = 32%) [14]. However, in both of these studies the fibres were annealed and the UD mats were prepared manually. This meant that the distribution of the fibres was uneven and the fibres were not properly aligned [7, 10, 14]. Consequent misalignment of fibres meant that they were not in the direction of maximum stress. The UD mats in this study were produced via a dedicated in-house facility (*see* Figure 3.1), which meant that the fibre alignment in the composites was much better. The composites in the studies conducted by Hasan *et al.* and Haque has a 10-15% larger $V_f$ than the present study. While the larger $V_f$ yielded an increase in the initial flexural properties, the misalignment of the fibres and uneven distribution meant that the flexural properties did not have as large a percentage increase.

Figure 5.2 shows the effect of the flexural strengths of PLA, C-long, DC-long and SP-long composites over 28 days of immersion in PBS at 37°C. As expected, PLA showed very little variation in flexural strength over the course of 28 days of immersion [2, 16]. The flexural strength of the C-long composites decreased over the first 3 days of immersion in PBS. At day 10 of immersion, the flexural strength increased slightly before decreasing steadily for the rest of the study. The decrease was significant ($p < 0.05$) from day 14 however there was no significant difference between the flexural strengths at day 21 and day 28. After 28 days, the flexural strength of C-long composites (74 ± 14 MPa) had decreased significantly ($p < 0.05$) by 53% and was less than that of PLA at the same time point (98 ± 2 MPa), though not significantly different.
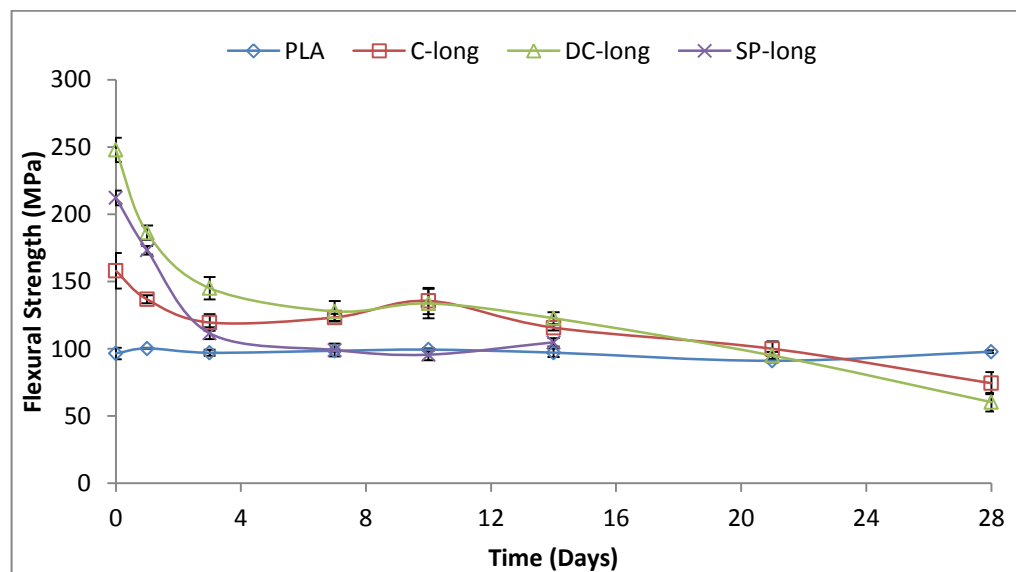


**Figure 5.2:** *The flexural strength of PLA, C-long, DC-long and SP-long composites over 28 days after immersion in PBS at 37°C*

The flexural strengths of the DC-long and SP-long composites decreased significantly ($p < 0.05$) after 1 day of immersion in PBS at 37°C. The DC-long composites had a significantly ($p < 0.05$) greater value in flexural strength until 1 week of immersion when it then followed the same profile as the C-long composites. After 28 days of immersion, the DC-long composites had a flexural

strength (60 MPa) that was less than that of PLA but also statistically similar to that of C-long ($p > 0.05$).

The SP-long composites were only degraded up to 14 days due to a limited number of samples manufactured (Chapter 3 Section 3.6.2). After 3 days of immersion, the flexural strength of SP-long composites (112 ± 8 MPa) was less (but not statistically different) than that of the C-long composites (120 ± 11 MPa). By the end of the first week of immersion, the flexural strengths for SP-long composites had stabilised and had a similar profile to that of PLA for the next week.

The flexural modulus of PLA, C-long, DC-long and SP-long composites over 28 days immersion in PBS of 37°C is shown in Figure 5.3. Again, the flexural moduli of PLA over the course of the 28 days did not show any significant difference. The moduli of C-long composites did not show any significant difference over the first three days of immersion. After day 3, the modulus decreased steadily until the end of the study and did not reveal a significant difference in values. The modulus of DC-long composites decreased immediately after 1 day of immersion, yet there did not appear to be a significant difference in the modulus values from day 1 to day 14 of immersion. After two weeks of immersion, the modulus decreased until the end of the study when the flexural modulus of DC-long samples was the same as that of PLA (3 ± 0.1 MPa). It should be noted that the modulus of DC-long at day 28 (3 ± 0.6 GPa) was statistically the same as PLA at day 28 (3 ± 0.1 GPa) ($p > 0.05$) and less than that of C-long (4 ± 0.4 GPa).

The flexural modulus of SP-long composites had the greatest significant decrease (50%) over the initial three days of the study (16 ± 0.4 MPa to 8 ± 0.5 MPa) compared to the moduli of both C-long and DC-long. However, like the

flexural strength values, the modulus showed very little statistical variation ($p <$ 0.05) after day 3 to the end of the 14 day study. At day 14, the flexural modulus of SP-long was also not significantly different than that of C-long and DC-long, however DC-long had a significantly ($p < 0.05$) different flexural modulus profile compared to C-long from day 7 to day 28.
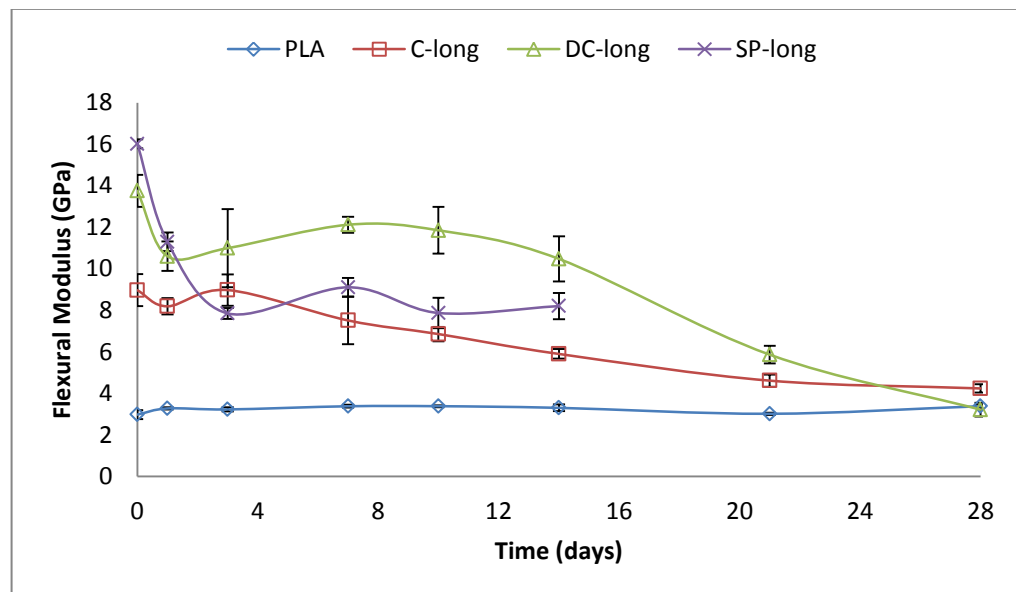


***Figure 5.3:*** *The flexural modulus of PLA, C-long, DC-long and SP-long composites over 28 days after immersion in PBS at 37°C*

The degradation of the flexural strengths show that the dip coated fibres had a greater retention of mechanical properties than the spray coated properties for the first week of the study. The loss of flexural strength and modulus in C-long composites can be attributed to a degradation of the fibre-matrix interface [1, 2, 16]. Haque's study showed that the flexural strength of S-PLA coated composites decreased to a value similar to that of control after 7 days of immersion in PBS at 37°C [14]. Figure 5.2 shows a similar occurrence with DC-long composites. The strengths and moduli of S-PLA coated composites appear to have experienced a greater reduction in value than the C-long samples during the first few days of the study. This may be due to the hygroscopic nature of sorbitol

[7]. The wicking of water along the exposed fibre ends is most likely the route for attack of the sorbitol head group at the interface [8]. That C-long and DC-long composites have a statistically similar strength profile after day 7 (Figure 5.2), suggested that DC-long composites experienced a loss of the fibre-matrix interface to a similar state as that of C-long composites. This can be due to a hydrolysis reaction as result of water absorbed by the sorbitol head group [7, 10]. It most likely this reaction that also caused a loss of the fibre-matrix interface of SP-long composites causing the flexural strength to decrease to that of PLA after 7 days of immersion.

The degradation of the flexural moduli showed that the dip coated fibres had a greater retention of mechanical properties than the spray coated properties after 1 day of immersion to day 14 (Figure 5.3). It can be concluded, however, that the S-PLA coating had a positive effect on the retention of the flexural modulus.

Ahmed $et$ $al.$ immersed UD $50P_2O_5$-$40CaO$-$5Na_2O$-$5Fe_2O_3$ reinforced PLA in deionised water at 37°C for up to 4.5 weeks and found that the flexural strength and modulus decreased to less than half the initial values (129 MPa and 11.5 GPa, respectively) during the first three days of immersion. The flexural strength continued to decrease to ~30 MPa by day 28. The flexural modulus saw a further decrease to 2 GPa by day 7 and remained at this value to the end of the study. [1]

While Sharmin's study showed an increase in flexural properties of composites with boron oxide, samples immersed in PBS at 37°C for 28 days showed that the flexural properties degraded to less than that of unreinforced PLA after 7-10 days. Composites with P45B5Fe3 fibres managed to retain their flexural properties for up to 14 weeks [16]. The composites in this study had

flexural properties greater than PLA for a longer duration (up to 21-28 days). Boron oxide increased the strength of the fibres and thus the flexural properties of the composites, however the increased 4 mol% iron oxide in the fibres in this study appear to have aided in retarding the degradation process for a few more days. This was confirmed by the degradation study conducted by Felfel *et al.* on UD P40 reinforced PLA composites in PBS at 37 °C for 95 days [2].

### *5.3.1.3 Transverse Properties*

Figure 5.4 shows the initial flexural strength and moduli for PLA, and for transverse control (C-trans), dip coated (DC-trans) and spray coated (SP-trans) composites. The transverse flexural strengths for C-trans, DC-trans and SP-trans composites decreased significantly when compared to the flexural strength of PLA for $p < 0.05$. This was expected due to the fact that composite properties are greater when tested in the same direction as the fibre orientation, i.e. longitudinally [11]. According to Drzal *et al.* the transverse flexural properties of composites are more useful when analysing the interfacial properties of a composite than the longitudinal flexural properties. This is because the bending stresses on the transverse composites are directly on the fibre-matrix interface [11-12, 23]. Drzal suggested that the specimen failure occurred due to tensile or compressive failure of the interface or matrix or a combination of the two [11-12].
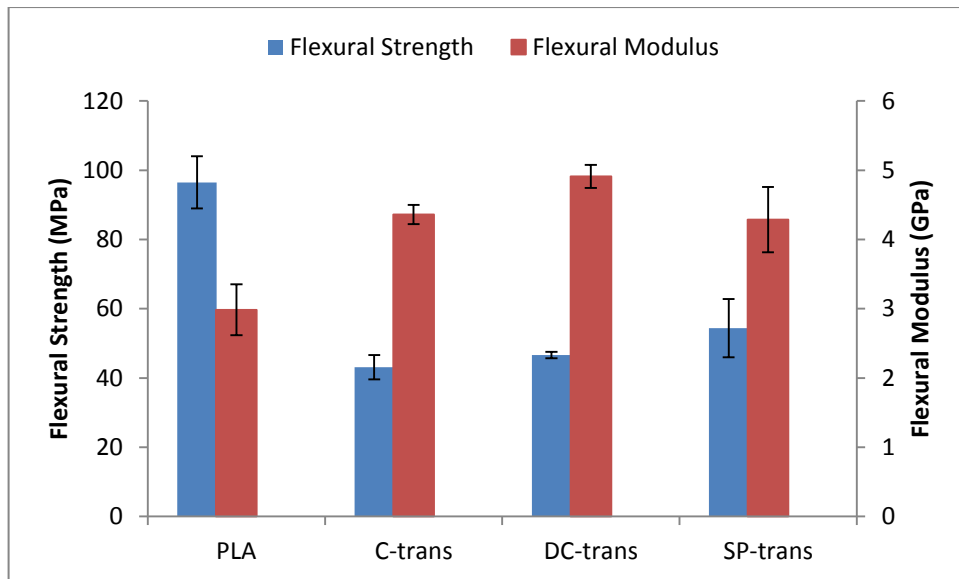
**Figure 5.4:** *The initial flexural strengths and flexural moduli of PLA and, C_trans, DC_trans and SP_trans composites*

The flexural strength of C-trans (43 ± 4 MPa) decreased by 56 % when compared to the flexural strength of PLA (97 ± 8 MPa). The flexural strengths of DC-trans and SP-trans increased by 9 % and 26 %, respectively when compared to that of C-trans, however appear to have no significant difference when compared to each other or when compared to C-trans. This suggested that the initial increase in interfacial strength in DC and SP composites was insignificant. It also suggested that the fibre coating method was insignificant in the improvement of PGF/PLA composite properties. De Kok and Peijs found that interface strength needed for perfect bonding was dependent on $V_f$ and that at increased $V_f$ a higher level of adhesion was required [24]. It would be prudent to see if this is the case for PGF/PLA composites. The fibre coating concentration used was the same as that used for S-PLA_s in Chapter 4 (i.e. the optimum concentration for single fibre composites). De Kok *et al.* stated that there is a maximum transverse strength as the failure mode changes from debonding to matrix dominated [11, 25] or fibre dominated [26] failure above a specific level

of fibre treatment [24]. Increasing the coating concentration may yield the optimum concentration for full body PGF/ PLA composites.

The flexural moduli of C-trans, DC-trans and SP-trans (4 ± 0.1 GPa, 5 ± 0.2 GPa and 4 ± 0.5 GPa, respectively), on the other hand, appear to have significantly increased compared to that of PLA (3 ± 0.4 GPa). There is no significant difference between the flexural moduli of C-trans and SP-trans composites, i.e. there is little effect of the interfacial shear stress on the transverse modulus [12]. There is, however, a statistical difference ($p < 0.05$) between the flexural moduli of C-trans and DC-trans composites and DC-trans and SP-trans composites.

Figure 5.5 shows the effect of the transverse flexural strengths of PLA, C-trans, DC-trans and SP-trans composites over 28 days of immersion in PBS at 37°C. The flexural strength of PLA plotted here is the same as that plotted in Figure 5.2. The transverse flexural strengths of the C-trans, DC-trans and SP-trans composites are all significantly ($p < 0.05$) less than the flexural strength of PLA and the flexural strength profiles of C-long, DC-long and SP-long.
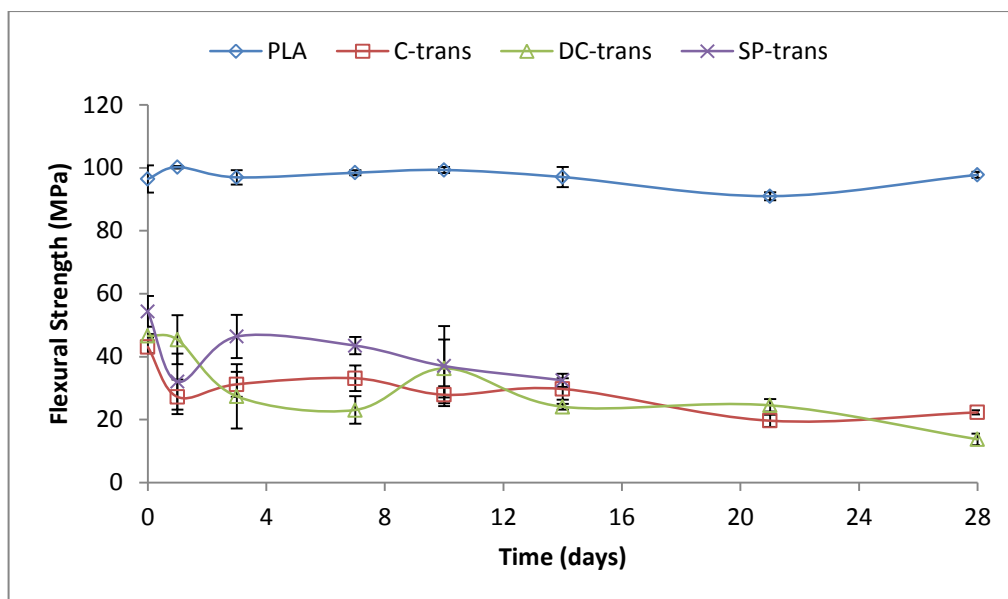
***Figure 5.5:*** *The flexural strength of PLA, C-trans, DC-trans and SP-trans composites over 28 days after immersion in PBS at 37°C*

The flexural strength of C-trans had an initial decrease after one day of immersion. There was no statistical difference ($p > 0.05$) in the transverse flexural strength from day 3 to day 28 of immersion. The flexural strength of C-trans composites decreased 49% from 43 ± 4 MPa to 22 ± 1 MPa by the end of the 28 day study. The transverse flexural strength of DC-trans composites decreased after the first day of immersion from 45 ± 14 MPa to 23 ± 8 MPa at day 7. At 10 days there was a slight (statistically insignificant for $p > 0.05$) increase in the DC-trans flexural strength (37 ± 16 MPa) before decreasing back to 24 ± 2 MPa after 14 days of immersion. The transverse flexural strength does not differ significantly over the next week. However, after 28 days the transverse flexural strength was statistically ($p < 0.05$) less than that of C-trans and had decreased to 70% of the initial DC-trans flexural strength value.

The transverse flexural strength of SP-trans composites initially decreased after one day of immersion before increasing at day 3 to 46 ± 12 MPa. The flexural strength then decreased steadily over the next 11 days when SP-trans has a statistically similar transverse flexural strength (33 ± 4 MPa) to that

158

of C-trans (30 ± 6 MPa) after 14 days of immersion. The transverse flexural strength of the SP-trans composites was greater than that of the C-trans during the course of the study suggested that the spray coat method yielded a stronger interface for the first two weeks of immersion in PBS at 37°C compared to that of the dip coat method. In spite of the initial decrease in transverse flexural strength, SP-trans composites appeared to have better retention of interfacial strength than C-trans and DC-trans, particularly between days 3 and 10.

Figure 5.6 shows the transverse flexural moduli of PLA, C-trans, DC-trans and SP-trans composites over 28 days of immersion in PBS at 37°C. Like Figure 5.5, the flexural modulus of PLA plotted here is the same as that in Figure 5.3. The transverse flexural modulus of the C-trans, DC-trans and SP-trans composites appeared to decrease over time. The transverse flexural modulus of C-trans composites decreased significantly from 4 ± 0.1 GPa to 3 ± 0.3 GPa after 1 day of immersion in PBS and then had a statistically significant increase at day 3 ($p < 0.05$). Over the next 18 days, the transverse flexural modulus decreased to 2 ± 0.2 GPa and did not change during the last week of the study.
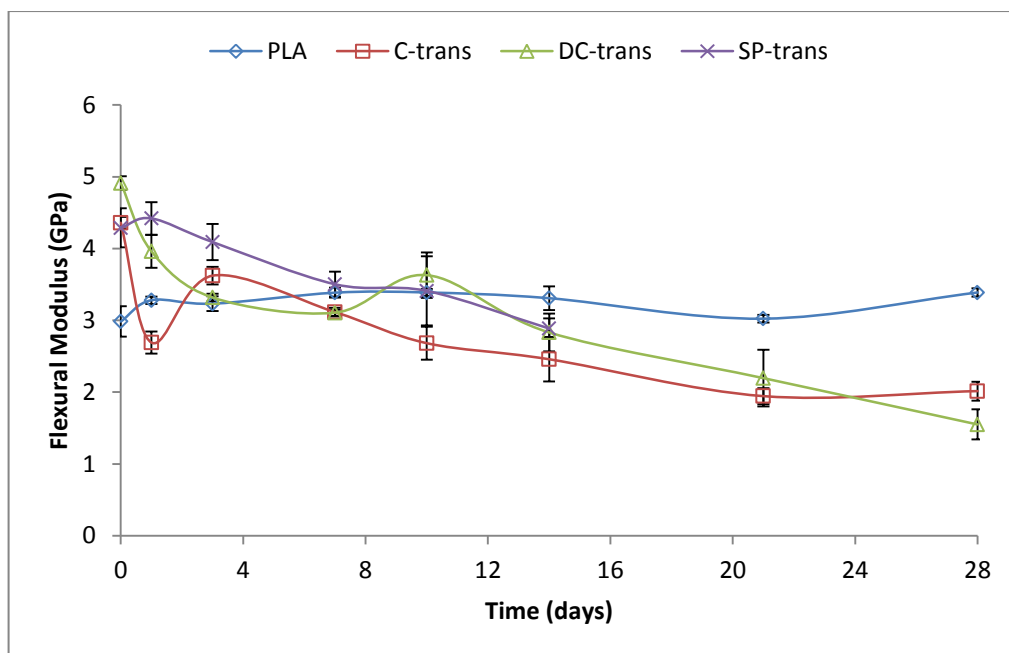
***Figure 5.6:*** *The flexural modulus of PLA, C-trans, DC-trans and SP-trans composites over 28 days after immersion in PBS at 37°C*

The transverse flexural modulus of the DC-trans composite decreased significantly ($p < 0.05$) over the course of the first week of immersion; however, there was a slight increase in the modulus at day 10 before continuing to decrease to a modulus of $2 \pm 0.4$ GPa after 28 days of immersion. This increase in modulus is comparable to the increase in transverse strength observed at day 10 for DC-trans composites. The transverse modulus for SP-trans composites began to decrease after day 1 of immersion reaching a modulus of $3 \pm 0.2$ GPa after 14 days of immersion. The decrease in flexural modulus for SP-trans was found to be statistically insignificant ($p > 0.05$). The degradation profile of the flexural modulus of SP-trans, like the profile of SP-trans flexural strength, remained greater than that of C-trans. SP trans flexural moduli were only statistically significant ($p < 0.05$) than C-trans and DC-trans between days 1 and 7 (not inclusive) of immersion.

As expected, the transverse flexural modulus of the coated and uncoated composites appeared to have little statistical difference ($p > 0.05$) indicating that

the interfacial strength had little to no effect [11-12]. However, the significant difference observed in the SP-trans flexural strength and modulus degradation profile at day 3 to day 7 (day 10 for strength) needs to be investigated further. The SP method shows promise in retaining interfacial shear strength compared to the DC method. This can be attributed to the difference in coating methodology discussed in more detail in Section 5.3.5.

### 5.3.2 Degradation Study

The degradation study conducted (as described in Chapter 3 Sections 3.6.2 – 3.6.4) measured the water uptake percentage, the mass loss, the wet mass change and change in pH for PLA samples, control and S-PLA_s coated unidirectional (UD) composites. The respective results for samples with fibres aligned longitudinally were plotted separately from those with fibres aligned transversely. The results for PLA samples were plotted alongside both.

#### 5.3.2.1 Water Uptake and Wet Mass Change

The water uptake percentage of PLA, C-long, DC-long and SP-long over 28 days of immersion in PBS at 37°C is shown in Figure 5.7. The water absorption increased for all the samples during the first day of immersion to 0.86%, 0.64%, 0.63%, and 0.73%, respectively. After the initial day of immersion, the water uptake for PLA did not change statistically ($p > 0.05$) for the rest of the study. The C-long samples, in comparison, had a slight increase in water absorption over the course of the first week. The percentage water uptake continued to increase until day 14 (2%) after which the water absorption rate takes on a linear profile and increased a further 10%. The C-long composite samples revealed a significant increase in water uptake of 12% after 28 days of degradation.
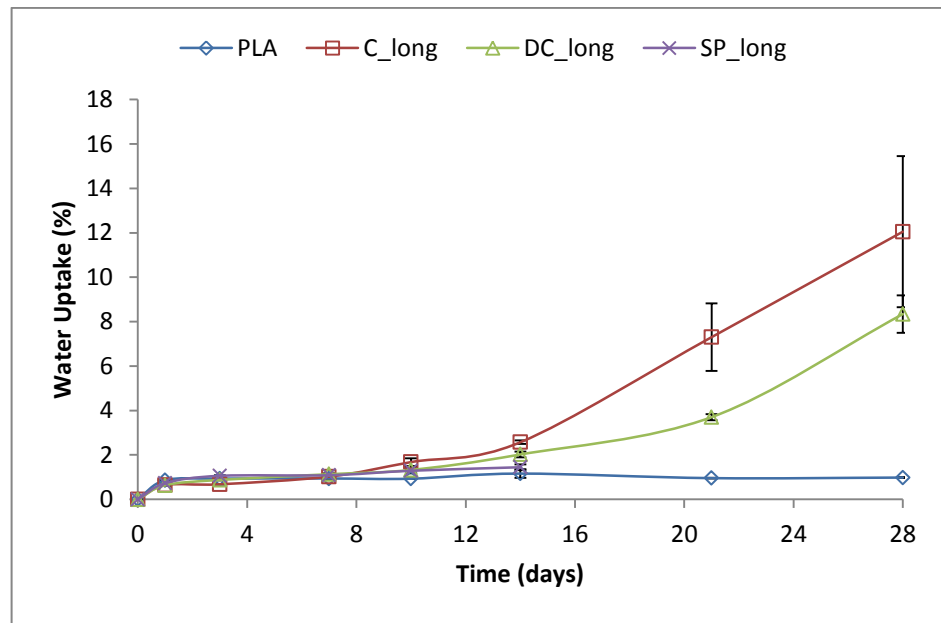
**Figure 5.7:** *The percentage water uptake for PLA, C-long, DC-long and SP-long composites over 28 days of immersion in PBS at 37°C*

The DC-long composites and the SP-long composites had a statistically ($p$ > 0.05) similar water absorption profile for the first 10 days of the degradation study. Figure 5.7 shows that the water absorption of the DC-long composites began to increase significantly after 10 days of immersion and continued to increase until the end of the study. DC-long composites had water absorption of ~8.3% after 28 days of degradation in PBS. The SP-long composites did not show an increase in water uptake over 14 days of immersion (~1.4%). However as it had a lower percentage water uptake than both C-long composites and DC-long composites (2% and 2.6%, respectively) the SP-long composites showed some resistance to water uptake.

The percentage water uptake for PLA, C-trans, DC-trans and SP-trans over 28 days immersion in PBS at 37°C are shown in Figure 5.8. As in Figure 5.7, there is an increase in water absorption after one day of immersion for all the composites aligned in the transverse direction at 0.75%, 1.3% and 0.87%,

respectively. These absorption percentages for the transverse composites at day 1 of immersion are slightly greater than those for the longitudinal composites. The C-trans, DC-trans and SP-trans samples all have statistically similar ($p >$ 0.05) water absorption profiles for the first 7 days of the degradation study. The water uptake percentage for the C-trans composite samples started to increase gradually after the first week of study and increased significantly after day 14 (~9.6%) before tapering off during the last week. By day 28, C-trans samples had water absorption of 15%. Like the C-long composites, the C-trans composites had a greater percentage of water uptake compared to the DC-trans and SP-trans composites particularly in the last two weeks of the study.
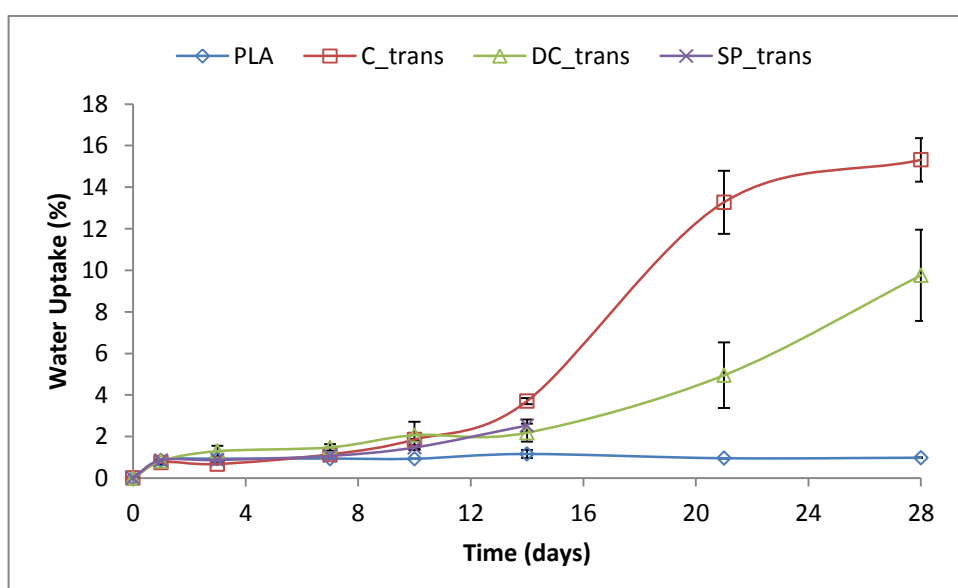


***Figure 5.8:*** *The percentage water uptake for PLA, C-trans, DC-trans and SP-trans composites over 28 days of immersion in PBS at 37°C*

The water uptake of the DC-trans composites was statistically similar ($p >$ 0.05) to that of SP-trans composites. Like the C-trans composite samples, the percentage water uptake of the DC-trans and the SP-trans composite samples started to gradually increase after the first week of immersion. The DC-trans samples showed no statistical difference, for $p >$ 0.05, in percentage water uptake

during the second week of immersion even though there was a slight increase when compared to the percentages in the first week. From Day 14 to Day 28 the DC-trans samples developed a parabolic water uptake profile and the final percentage water uptake for DC-trans samples was 9.8% at the end of the study.

It should be noted that at day 14 the SP-trans samples had a water uptake greater than that of DC-trans although it was not significant. As the SP-trans study only went until day 14, it is not possible to determine which method of coating had an overall least percentage water uptake for transversely aligned samples. However, it can be concluded that the coating did reduce the water uptake percentage when compared to the control composite samples.

Composites have been shown to absorb more water than the pure polymer samples [2, 13, 27]. This has been attributed to a capillary action called wicking. Exposed fibre ends absorb water and degrade the fibre-matrix interface, particularly in resorbable fibre reinforced composites [1-2, 8]. UD composites were shown to have a higher percentage water uptake than random mat (RM) composites [1-2]. Felfel *et al.* suggested that this was due to the poor impregnation of UD fibres in the matrix compared to that of RM fibres. Random fibre orientation is also less prone to wicking [1-2]. Better impregnation of fibres in the polymer matrix will decrease composite water uptake as this means that the matrix will encase more of the fibres in the prepregs, i.e. better wet-out [17, 28-30]. Han *et al.* reported that composites that had better fibre wet-out and dispersion in matrix lost very little material and had the slowest rate of mass change [17].

There are four known types of degradation for fibre reinforced composites: 1. Physical degradation (such as swelling); 2. Matrix degradation; 3. Degradation of the bonding interfaces between the fibre and matrix; and 4.

Weakening of the fibre strength [31]. No swelling was seen in the composite samples in this study until C-long at day 28. The statistical insignificance of the water uptake of PLA (Figures 5.7 and 5.8) means that PLA was not affected by immersion in PBS at 37°C for 4 weeks similar to studies by Felfel *et al.* and Sharmin [2, 18]. Therefore matrix degradation did not occur in this time frame.

As control composite samples had a higher water uptake than both dip coated and spray coated S-PLA_s composites, it is evident that the coupling agent protects the fibres from water absorption. Hasan *et al.* showed a significant continuous increase in water uptake for S-PLA coated UD composites when compared to uncoated control fibres from 0 to 28 days immersion in PBS at 37°C [7, 10]. This increase is likely due to a larger coating concentration of 0.025 moles of S-PLA on the fibres compared to the concentration used in the current study (0.0064 moles). Haque also showed an increase in water uptake for S-PLA coated UD composites after 7 days immersion in PBS 37 °C compared to control composite samples [14]. Both Hasan *et al.* and Haque attributed this to the hygroscopic nature of the sorbitol [7, 14].

The current study showed a completely different response to water uptake of S-PLA coated composites (Figures 6.7 and 6.8). Both longitudinal and transverse samples show that the coating appears to protect the flaws on the fibre surface, preserve the interface and reduce the dissolution rate of the composites. This is likely due to the difference in coating concentration, i.e. amount of coupling agent on the fibre surface. Too much coupling agent may improve fibre-matrix adhesion however will have an adverse effect on the composite macroscopic properties [24, 32]. In the case of water uptake and the change in wet mass, an increased amount of S-PLA on the fibres means there are an increased number of hygroscopic sorbitol head groups available to absorb

water from the degradation medium. As a result of this increased water uptake, hydrolysis may occur at a faster rate as seen in the study by Hasan *et al.* [7, 10].

The percentage change in wet mass for PLA, C-long, DC-long and SP-long composite samples over 28 days immersion in PBS at 37°C is shown in Figure 5.9. The wet mass change of all the samples increased gradually during the initial phase. The mass of PLA samples reached saturation after this and did not change significantly over the remainder of the study. After day 3, the C-long samples had a gradual increase in wet mass change over the next 18 days. During the last week of the study, the percentage wet mass change decreased insignificantly to 7.6 ± 3.6 %. This decrease is likely due to the dissolution of fibres and the loss of fibre-matrix interface caused by hydrolysis as a result of water absorption. Fibre dissolution would result in material leaching out of the composite, thereby reducing the mass of the sample [2, 16-17].

DC-long and SP-long samples maintained a mass change profile statistically similar to that of PLA samples until day 7 of the degradation study. The percentage mass change for both sets of samples increased slightly over the next three days. After day 10 the wet mass change of DC-long samples increased steadily for the remainder of the study reaching a final wet mass percentage of 8.8 ± 0.7 %. The wet mass change of the SP-long samples increased as well but at a lower rate than the DC-long samples. At day 14 the SP-long samples had a percentage wet mass change of 1.2 ± 0.4 % which is ~50% of the percentage mass change of the DC-long samples at day 14 (2.3 ± 0.5 %). This confirms the water uptake profile of SP-long composites (Figure 5.7). A lower water uptake means a lower mass gain for SP-long composites.
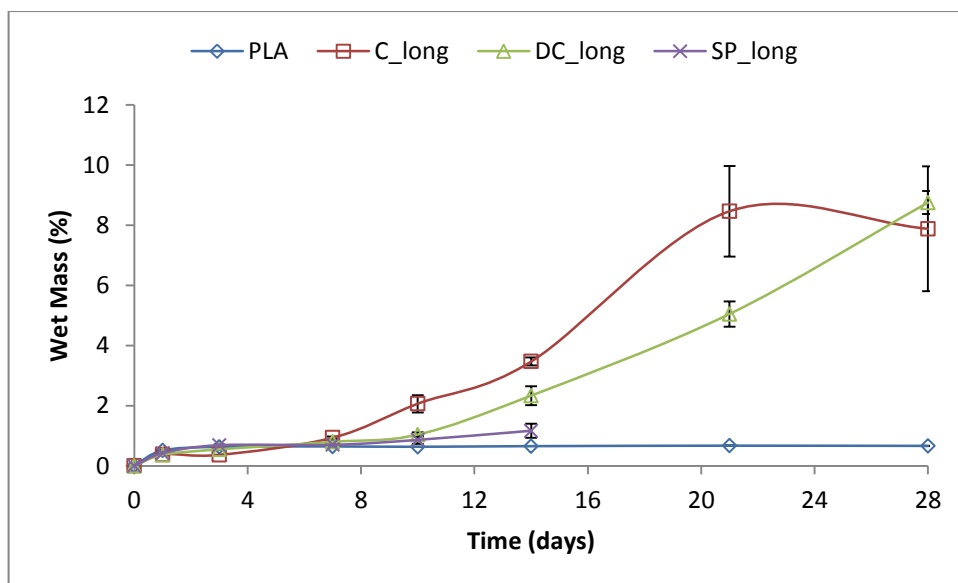
***Figure 5.9:*** *The percentage wet mass change for PLA, C-long, DC-long and SP-long composites over 28 days of immersion in PBS at 37°C*

Figure 5.10 shows the percentage wet mass change for PLA, C-trans, DC-trans and SP-trans composite samples over 28 days immersion in PBS at 37°C. The percentage wet mass change for C-trans samples do not differ significantly between days 1 and 3 after the initial increase in mass. After day 3 the wet mass change gradually increased, reaching a maximum percentage of 8.6 ± 0.7 % at Day 21. The change in wet mass then decreased over the course of the last week in the study to 4.7 ± 0.2 % by day 28. The wet mass change of the DC-trans samples increased gradually during the first week of the study (Day 7: 1.1 ± 0.3 %). The percentage wet mass of the DC-trans increased by a factor of two by the end of the second week (Day 14: 2.2 ± 1.5 %). After Day 14, the percentage wet mass change increased by a factor of four during the last two weeks of the study. The percentage wet mass change of DC-trans after 28 days was 8.0 ± 5.2 %. This was a statistically insignificant ($p > 0.05$) increase compared to the percentage wet mass of C-trans at day 28.

The SP-trans samples appeared to have the same wet mass change profile as the PLA samples during the first 10 days of immersion. The wet mass

change of SP-trans samples increased at a greater rate during the last four days of the study to 3.0 ± 0.8 % at Day 14. There was no significant difference between the wet mass change of SP-trans and DC-trans samples at Day 14, even though the SP-trans wet mass was greater than that of DC-trans.
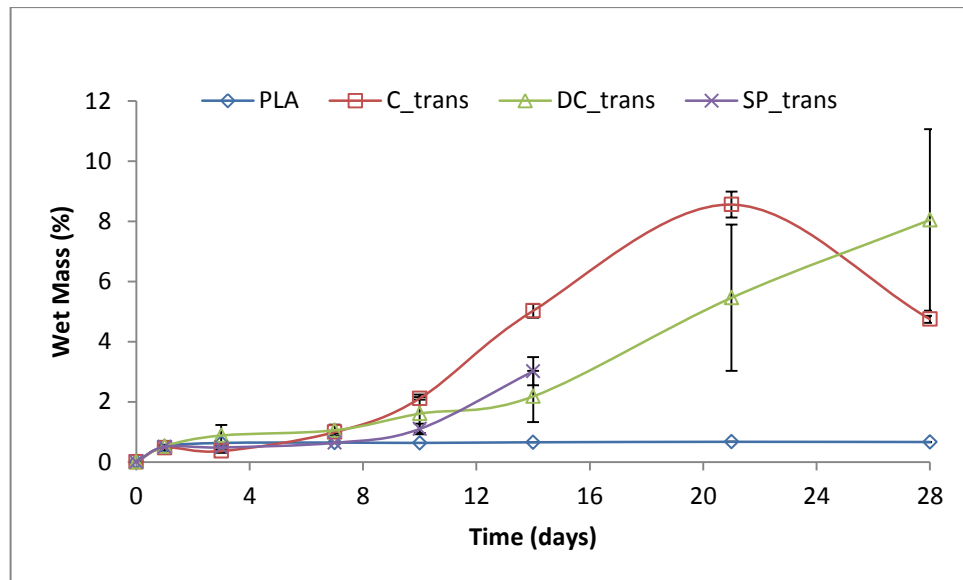


**Figure 5.10:** *The percentage wet mass change for PLA, C-trans, DC-trans and SP-trans composites over 28 days of immersion in PBS at 37°C*

Figures 5.9 and 5.10 both show that the percentage wet mass for all composites are more or less unchanged during the first week of immersion. The change in percentage wet mass increased earlier in transverse samples than in longitudinal samples due to the increased number of exposed fibre ends [8]. Slivka *et al.* found that calcium phosphate fibre reinforced PLLA composite samples that had fibres exposed to degradation media (open-ended) showed a greater loss in interface than composite samples with fibre ends embedded completely within the matrix (close-ended) [28].

The increase in wet mass change seen in composite samples during the final two weeks of immersion corresponds to the respective water uptake profiles. The initial phase is similar to that observed by Felfel *et al.* in the study of

P40 UD composites [2]. PLA reinforced with Sharmin's borophosphate glass fibres showed an immediate increase in wet mass change for 7-10 days before a decrease was seen [16]. It was suggested that the addition of $Fe_2O_3$ to P45B5 fibres strengthened the cross-linking in phosphate chains by creating P-O-Fe bonds which resulted in a reduced mass loss [16, 22, 33]. This is most likely the case during the first week of immersion in this study. The increase in water uptake seen by Sharmin and Felfel *et al.* after the initial phase was attributed to a continuous loss of the fibre-matrix interface [2, 16, 34]. It is likely that the fibre-matrix interface was lost due to the increase in water uptake and mass loss seen during the final two weeks of this study. This would have led to rapid fibre dissolution and loss of fibre strength which in turn led to the decrease in flexural properties (*see* Section 5.3.5 *for SEM micrographs*) [31].

### *5.3.2.2 pH*

The pH analysis of the degradation media (PBS) for PLA, C-long, DC-long and SP-long over 28 days is shown in Figure 5.11. The pH of the PBS for PLA varied slightly around 7.4 which were close to the starting value at Day 0 [2, 16]. The profile of the pH of C-long, DC-long and SP-long samples was statistically similar ($p > 0.05$) for the first week of the degradation study [14]. The pH of the PBS solution for C-long and DC-long samples began to decrease and become slightly acidic after 10 days. The pH of the C-long solution was 6.7 at day 21, significantly less ($p < 0.05$) than that of the DC-long solution (7.1). However by day 28 the pH of both solutions was statistically similar, 6.5 and 6.7 respectively.
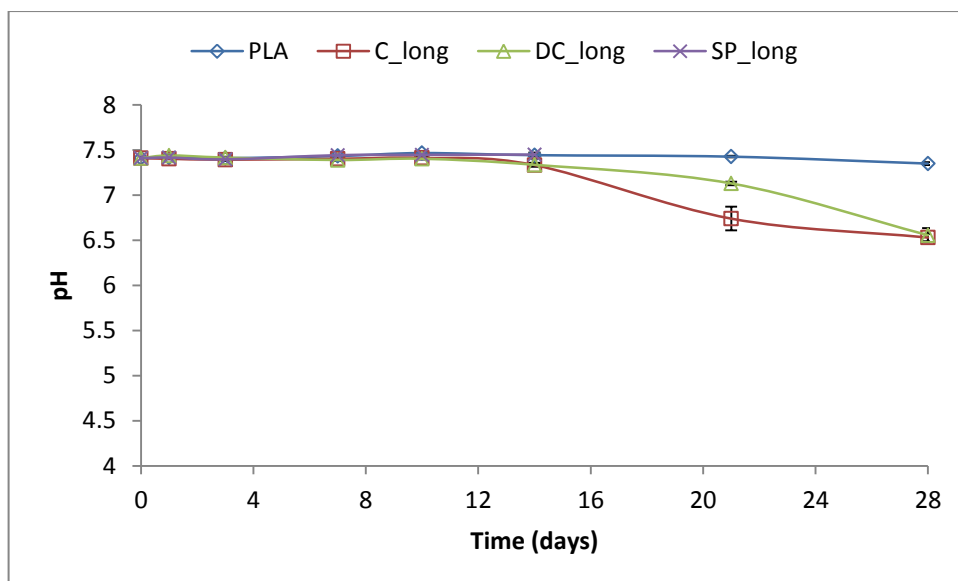
***Figure 5.11:*** *The change in pH of PBS for PLA, C-long, DC-long and SP-long composites over 28 days of immersion in PBS at 37°C*

The pH analysis of the degradation media (PBS) for PLA, C-trans, DC-trans and SP-trans over 28 days is shown in Figure 5.12. The pH profile for PLA shown in Figure 5.12 is the same as that shown in Figure 5.11. The pH of C-trans, DC-trans and SP-trans PBS solution had the same profile as the solution for PLA and does not vary statistically during the first week of the study [14]. The pH of the PBS solution of C-trans started to decrease gradually from day 7 until day 14. At day 21 the pH decreased significantly to 5.5 before increasing again to a pH of 6.8.

The pH of the PBS solution for SP-trans had the same profile as that for DC-trans and PLA from initial immersion to day 14 of the degradation study with no significant difference. All three sets of samples had a pH of 7.4 at day 14. After day 14 the pH of the PBS solution for DC-trans samples decreased through to the end of the study. At day 28 the pH for DC-trans samples was 6.7, less than that of C-trans but not a significant difference.
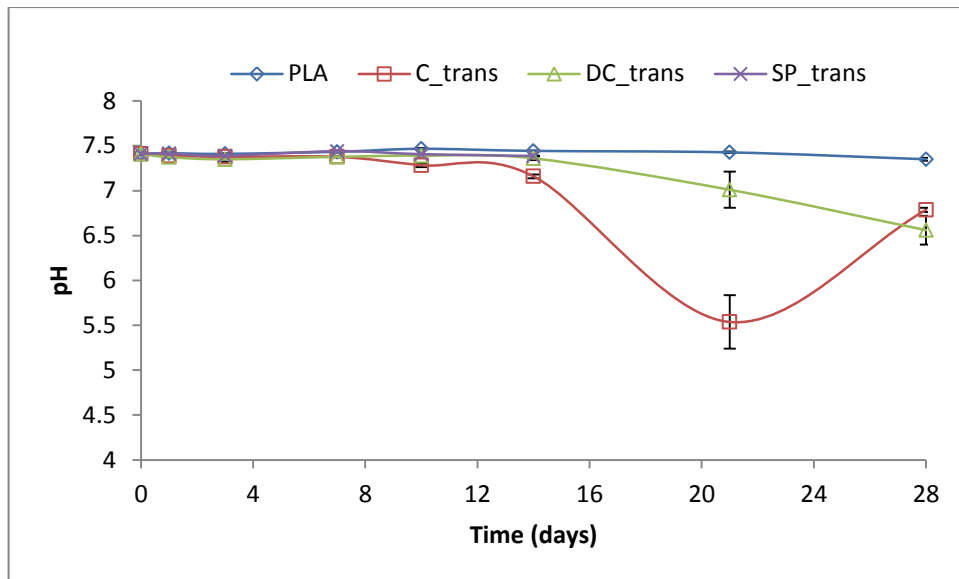
***Figure 5.12:*** *The change in pH of PBS for PLA, C-trans, DC-trans and SP-trans composites over 28 days of immersion in PBS at 37°C*

Felfel *et al.* saw no change and no significant difference in the pH of PBS for PLA and UD P40/PLA composites over 95 days [2]. Sharmin saw a drop in pH at day 10 that corresponded to the change in wet mass [16]. The decrease in pH seen at day 21 for both control and DC samples in this study also correlated well with the increase in water uptake and mass loss. This increase in acidity can be attributed to phosphoric acid formation as a result of phosphate ions being released into the degradation medium during fibre degradation [5, 16]. It can be suggested that as this increase in acidity is reduced for dip coated samples; the S-PLA coating is still protecting the fibre surface and therefore retarding the release of ions into the PBS solution to form phosphoric acid.

### 5.3.3 X-ray Diffraction (XRD) Analysis

XRD analysis was conducted using the method described in Chapter 3 Section 3.3.5. The XRD spectra for PLA prior to degradation and at 7, 14, 21 and 28 days immersion in PBS at 37°C is shown in Figure 5.13. It is evident from the XRD

spectrum of PLA (Polymer Grade: NatureWorks 6201D) that it is mostly amorphous for the duration of this study [2, 14].
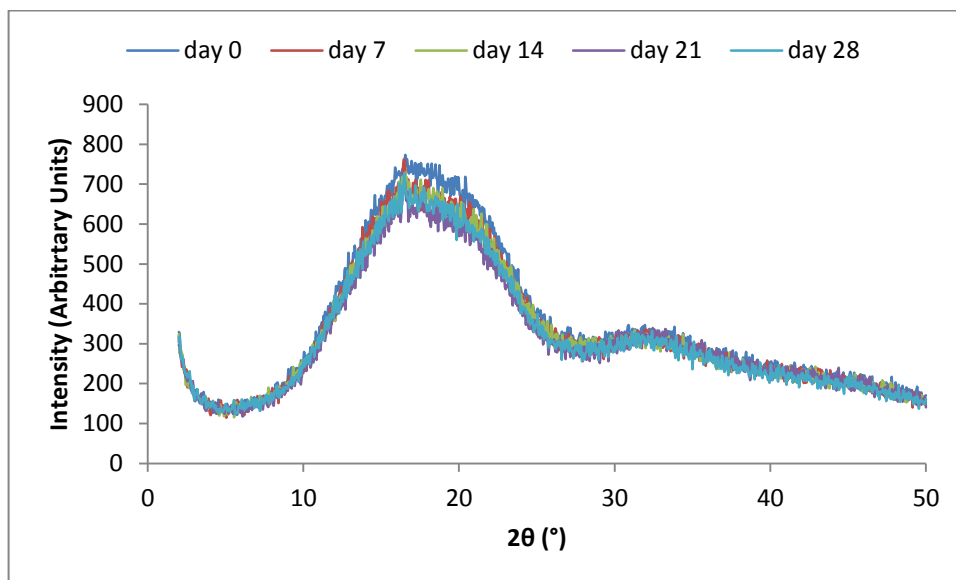


**Figure 5.13:** *XRD spectra of PLA before degradation, and at days 7, 14, 21 and 28 of immersion in PBS at 37°C*

The fibre reinforced composites produced in this study had XRD spectra before and after degradation similar to that shown in Figure 5.14 for C-long composites. The composites had a sharp peak at ~16.5° (Miller indices of (200) and (110)) and a smaller peak at 18.5-19° (Miller index of (203)) [35]. The presence of the crystallisation peak in composites from day 0 indicates that crystalline phase of NatureWorks PLA grade 6201D has increased after composite production. This additional crystallisation may have occurred due to the increase in polymer chains as a result of a reduction in molecular weight rather than the plasticisation effect of water [36]. This reduction is likely to have taken place during composite manufacture as a result of thermal degradation of the polymer. The intensity of the crystallisation peak at ~16.5° remains the same throughout the study and this coupled with the fact that degradation of PLA was not observed (Section 5.3.2) suggested that the crystallisation is not a result of

matrix degradation during immersion. Zhou *et al.* characterised this peak during an investigation of XRD of PLLA degraded in PBS [37]. This is different from the XRD spectra observed by Haque for composites with a NatureWorks PLA grade 3051D prior to and after degradation in PBS for 7 days at 37°C. The spectra remained amorphous for both control and S-PLA coated composites before and after degradation [14].
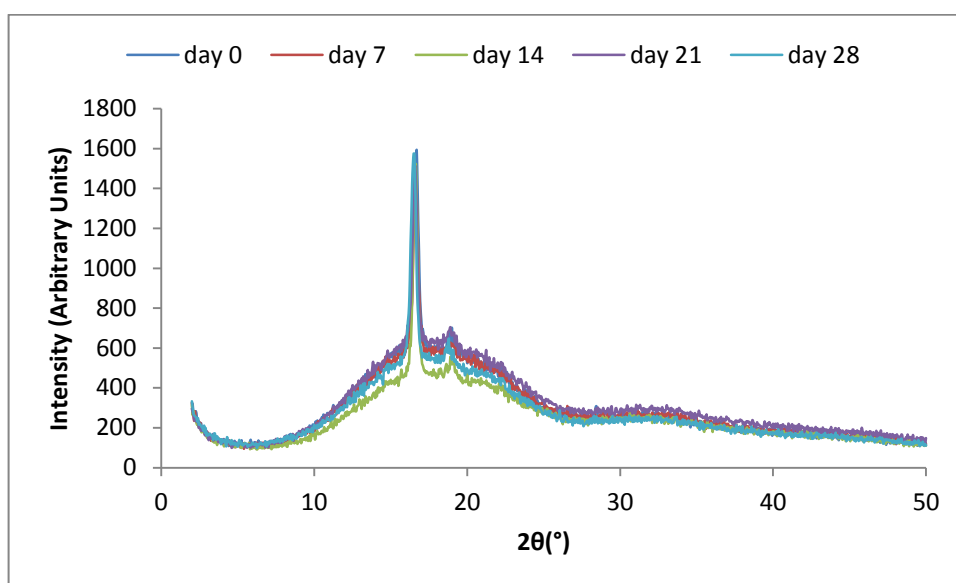


**Figure 5.14:** *XRD spectra of C-long before degradation, and at days 7, 14, 21 and 28 of immersion in PBS at 37°C*

### 5.3.4 Pycnometry Analysis

The density analysis was conducted as described in Chapter 3 Section 3.5.4. The density analysis for PLA, C-long, DC-long and SP-long against time (28 days) is shown in Figure 5.15. The density of PLA decreased from 1.34 g/cm$^3$ to 1.28 g/cm$^3$ over the course of 28 days of degradation. However it was not a significant decrease in density. C-long composites had a decrease in density over the first week of immersion in PBS at 37°C but, like PLA, the density did not show any significant change by the end of 28 days. SP-long composite samples did not have a change in density over the course of the 14 days of degradation in PBS at 37°C.

The density of DC-long composites decreased over the 28 day study from 1.61 g/cm$^3$ to 1.38 g/cm$^3$ but the change was not found to be statistically significant ($p > 0.05$).
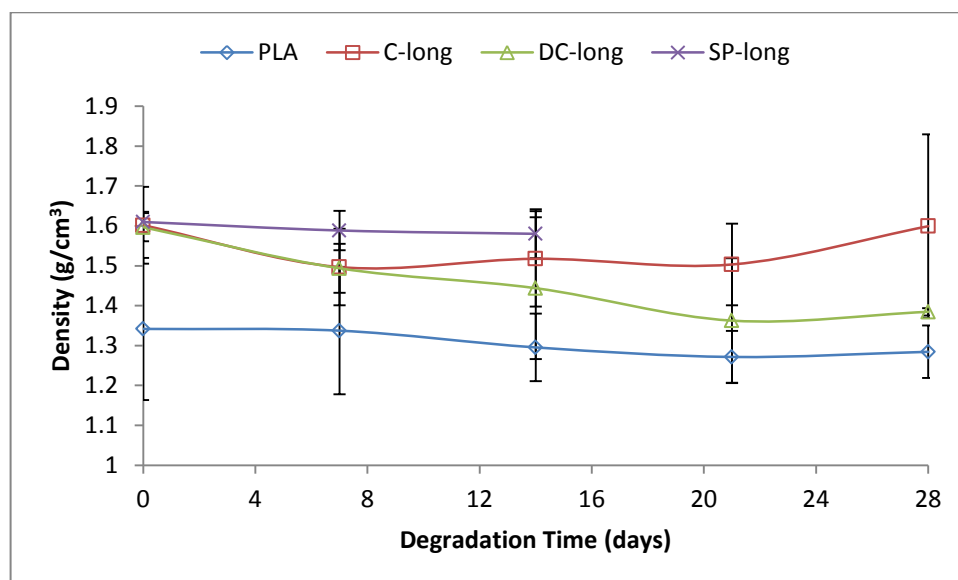


***Figure 5.15:*** *The density change of PLA, C-long, DC-long and SP-long composites with time during degradation in PBS at 37°C.*

Figure 5.16 shows the density analysis for PLA (same as plotted in Figure 5.15), C-trans, DC-trans and SP-trans against time (28 days). The density of C-trans decreased from 1.63 g/cm$^3$ to 1.47 g/cm$^3$ with no statistically significant difference ($p > 0.05$). DC-trans composites had a decrease in density over the course of the first 14 days of immersion. The density for DC-trans composites did not change significantly during the last 14 days. Similar to SP-long samples (Figure 5.15), SP-trans samples did not have a significant change in density within the two weeks of degradation in PBS at 37°C.

The density of PLA is sensitive to the level of crystallinity [2]. The lack of significant change in density for PLA suggests that no crystallinity was formed after 28 days degradation. Zhang *et al.* found that the density of the crystalline phase is higher than that of the amorphous phase [38]. The initial increase in

density for longitudinal and transverse composites is an indication that a crystalline phase has formed, confirmed by the XRD spectra in Figures 5.13 and 5.14. Again the lack of increase in density for all the composite samples corroborates the data from XRD analysis. The increase in density for composites compared to PLA was observed by Felfel *et al.* and it was suggested that this was due to the addition of glass fibre (2.7 g/cm$^3$) [2]. The decrease in density seen for DC-long, C-trans and DC-trans composites can be attributed to water wicking and subsequent fibre degradation (Section 5.3.2).
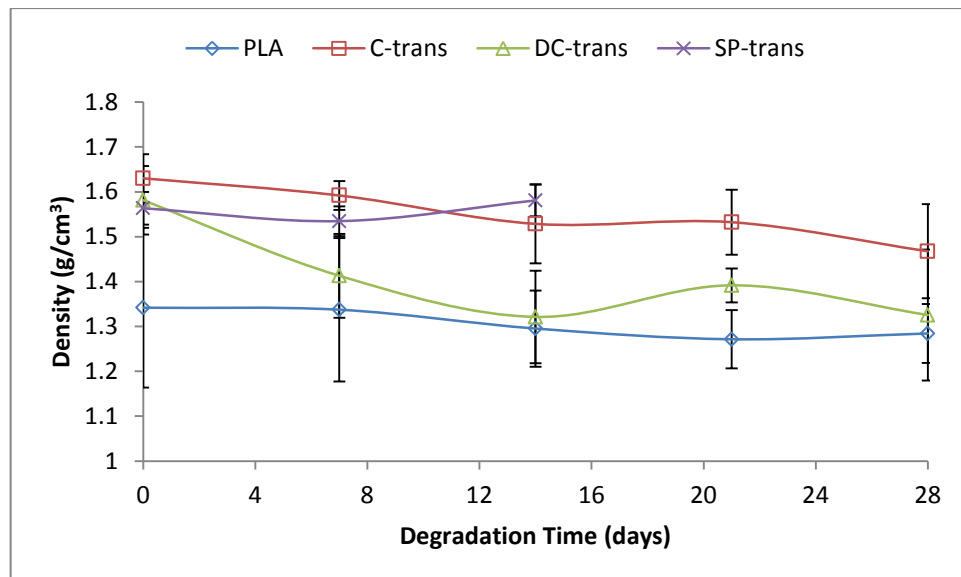


***Figure 5.16:*** *The density change of PLA, C-trans, DC-trans and SP-trans composites with time during degradation in PBS at 37°C*

### 5.3.5 Scanning Electron Microscopy (SEM)

SEM micrographs were taken using the method described in Chapter 3 Section 3.3.6. Figure 5.17 shows the fractured surface for PLA specimens at day 0, before degradation (Figure 5.17 (a)), and after 28 days of degradation in PBS at 37°C (Figure 5.17 (b)). Figure 5.18 shows the SEM micrographs of dip coated and the spray coated UD mat surfaces prior to composite manufacture. The difference between the coating methods can clearly be seen.
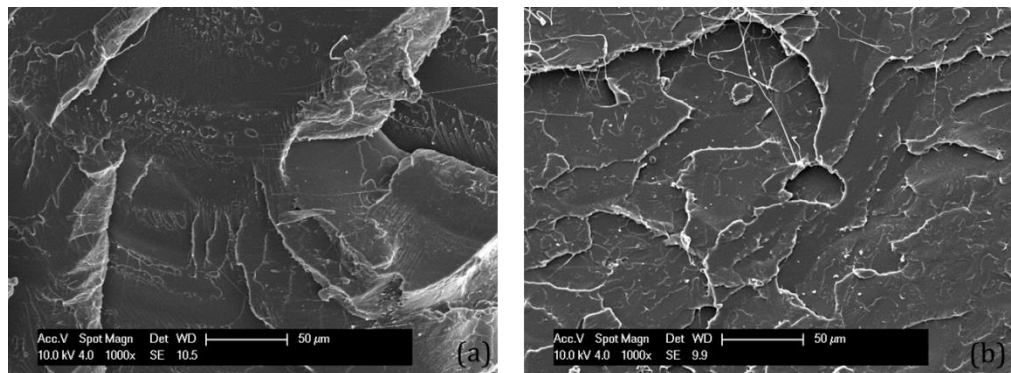
***Figure 5.17:*** *SEM micrographs of a fractured surface of (a) PLA at Day 0 prior to degradation and (b) PLA after 28 days of degradation in PBS at 37°C*
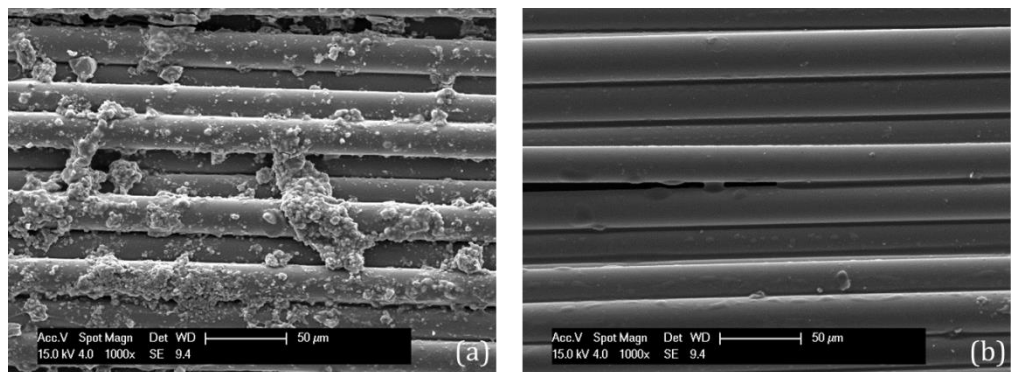


***Figure 5.18:*** *SEM micrographs of a fractured surface of (a) dip coated UD P45 glass fibre mats and (b) spray coated UD P45 glass fibre mats*

The dip coating method (Figure 5.18 (a)) appears to deposit the polymer coupling agent unevenly across the fibre mat whilst the spray coating method (Figure 5.18 (b)) provides a more even application of the coupling agent. Though there did not appear to be a significant difference ($p > 0.05$) between the initial flexural strengths for DC-long and SP-long composites (Figure 5.1), it is likely that the increase in flexural strength seen for DC-long composite samples was due to the roughness of the dip-coated method (Figure 5.18 (a)). During manufacture it is possible that the coating surface acted as a mechanical interlock as well as a coupling agent. As was evident in the results shown in Figure 5.4, the coating method showed no significant difference in the composite interfacial strength.

The retention of transverse strength and resistance to degradation of SP composite samples may be due to the even application of the SP method. An even surface coating may have allowed for a more controlled degradation of the interface. The coupling agent would have protected the fibre surface for a longer period of time. The uneven surface seen in Figure 5.18 (a) may have resulted in sections where the coating was thinner to degrade away more quickly exposing the fibre surface leading to fibre dissolution. This would have caused loss of interface and allowed water easier access to the hydrophilic fibres.

The fractured surfaces for C-long, DC-long and SP-long composites prior to degradation and at 7 and 14 days after immersion in PBS at 37°C are shown in Figure 5.19. Figure 5.19 (a), (b) and (c) represent the samples before degradation, Figure 5.19 (d), (e) and (f) represent the samples after 7 days of degradation and Figure 5.19 (g), (h) and (i) represent the specimen after 14 days of degradation. The fractured surfaces for C-long and DC-long composites at 21 and 28 days after immersion in PBS at 37°C are shown in Figure 5.20. Figure 5.20 (a) and (b) represent the samples after 21 days of degradation, Figure 5.20 (c) and (d) represent the samples after 28 days of degradation.

Figure 5.19 (a), (d) and (g) show short fibre pull-out of C-long samples with the beginning of degradation of the outer surface of the fibres shown in Figure 5.19 (g). The short fibre pull-out is indicative of the degradation of the fibre-matrix interface as seen in Felfel *et al* [2, 39-40]. The fibre degradation observed in Figure 20 (a) and (c) for C-long samples explain the decrease in flexural properties at days 21 and 28. The porous morphology due to fibre dissolution seen in the micrographs at days 21 and 28 also explains the increase in water uptake and mass loss observed for these samples.
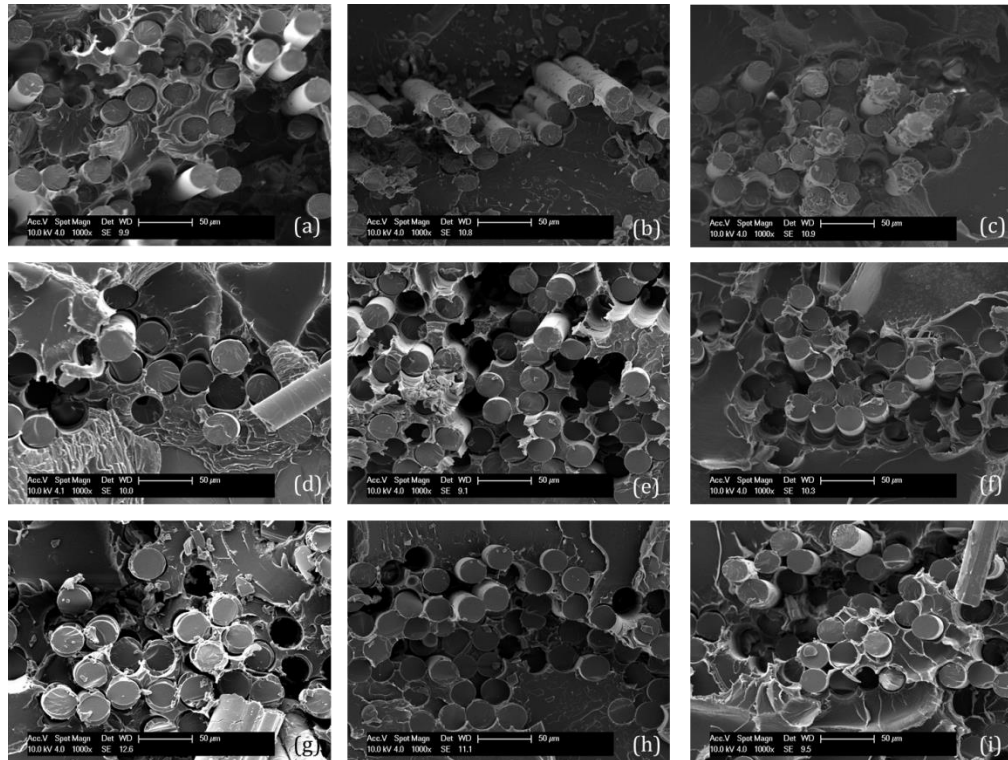
***Figure 5.19:*** *SEM micrographs of a fractured surface of (a) C-long before degradation, (b) DC-long before degradation, (c) SP-long before degradation, (d) C-long after 7 days of degradation in PBS at 37°C , (e) DC-long after 7 days of degradation in PBS at 37°C (f) SP-long after 7 days of degradation in PBS at 37°C, (g) C-long after 14 days of degradation in PBS at 37°C (h) DC-long after 14 days of degradation in PBS at 37°C (i) SP-long after 14 days of degradation in PBS at 37°C.*

Figure 5.19 (b) and (c) show fibres embedded firmly in the matrix. The micrographs taken at day7 and day 14 (Figure 5.19 (e), (f), (h) and (i)) also show that while fibre pull-out can be observed, the fibre-matrix interface is mostly preserved. Fibre dissolution has taken place by day 21 as seen in Figure 5.20 (b) and to a greater extent by day 28. This is, however, not the full dissolution of fibres as was observed by Sharmin [16]. Failure of DC-long composites at day 28 is likely due to the weakened fibre strength as a result of dissolution rather than the loss of interface as observed for C-long samples. In comparison, Hasan *et al.* saw complete interfacial failure in S-PLA coated UD composites after 28 days immersion in PBS [7, 10]. This difference is likely due to the difference in coating concentration between the current study (0.0064 moles) and that conducted by

Hasan *et al.* (0.025 moles) and would have caused an adverse effect as discussed earlier [7, 10].
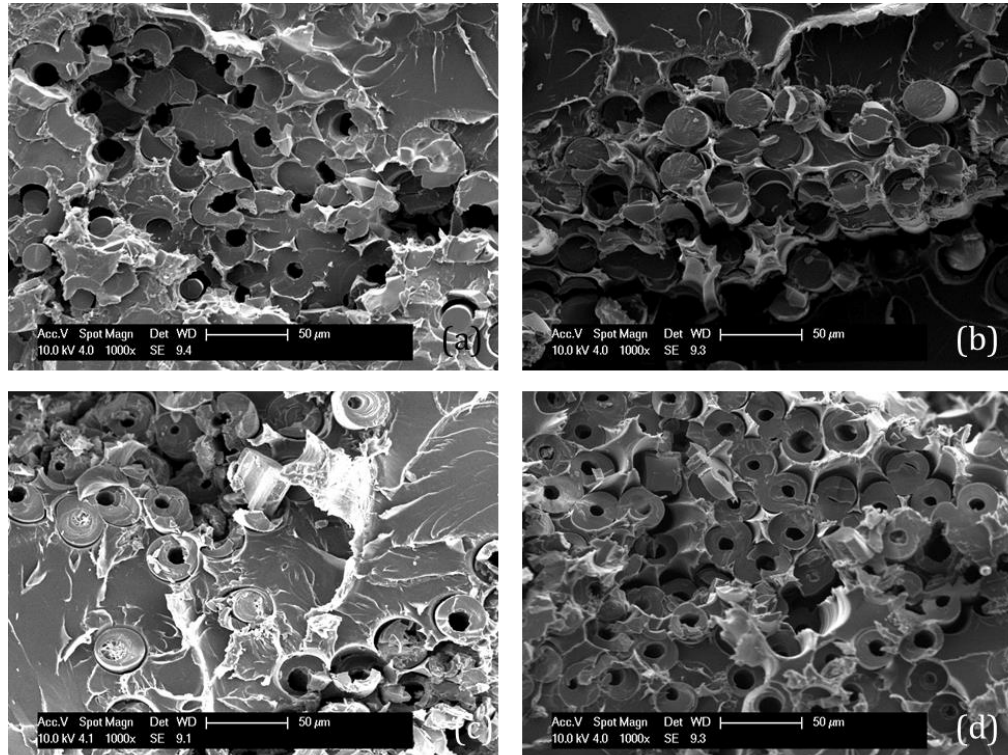


***Figure 5.20:*** *SEM micrographs of a fractured surface of (a) C-long after 21 days of degradation in PBS at 37°C, (b) DC-long after 21 days of degradation in PBS at 37°C, (c) C-long after 28 days of degradation in PBS at 37°C, (d) DC-long after 28 days of degradation in PBS at 37°C.*

The fractured surfaces for C-trans, DC-trans and SP-trans composites prior to degradation and at 7 and 14 days after immersion in PBS at 37°C are shown in Figure 5.21. Figure 5.21 (a), (b) and (c) represent the samples before degradation, Figure 5.21 (d), (e) and (f) represent the samples after 7 days of degradation and Figure 5.21 (g), (h) and (i) represent the specimen after 14 days of degradation. Figure 5.22 shows the fractured surfaces for C-trans and DC-trans composites at 21 and 28 days after immersion in PBS at 37°C. Figure 5.22 (a) and (b) represent the samples after 21 days of degradation, Figure 5.22 (c) and (d) represent the samples after 28 days of degradation.

The micrographs showing composite fracture morphology were investigated to determine the failure mode of the samples: interfacial debonding or matrix failure [11, 23-24]. The fracture surface for C-trans samples, prior to degradation (Figure 5.21 (a)), shows that the sample fractured along the interface. The glass fibres are separated from each other with no matrix material around them [11]. A similar fracture surface morphology is shown for DC-trans and SP-trans samples prior to degradation; however matrix failure can be seen as well. This appears to be consistent with samples with moderate interfacial strength [11].

***Figure 5.21:*** *SEM micrographs of a fractured surface of (a) C-trans before degradation, (b) DC-trans before degradation, (c) SP-trans before degradation, (d) C-trans after 7 days of degradation in PBS at 37°C , (e) DC-trans after 7 days of degradation in PBS at 37°C (f) SP-trans after 7 days of degradation in PBS at 37°C, (g) C-trans after 14 days of degradation in PBS at 37°C (h) DC-trans after 14 days of degradation in PBS at 37°C (i) SP-trans after 14 days of degradation in PBS at 37°C.*

Figure 5.21 (d) and (g) and Figure 5.22 (a) and (c) show the effects of increased immersion in PBS of C-trans composites over time. The more fibre ends exposed to the degradation medium appears to accelerate fibre dissolution leading to weakened fibres [31]. This would have contributed to loss of the fibre-matrix interface and consequently the transverse flexural properties (Figures 5.5 and 5.6). As in the longitudinal samples, S-PLA coated UD composites don't show signs of fibre dissolution up to 14 days of immersion in PBS at 37°C. Failure is shown to be due to a combination of interfacial and matrix failure as seen by Drzal *et al.* for composites with medium interfacial shear stress [11]. SP-trans

samples show increased matrix failure along with interfacial failure (Figure 5.21 (i)). This correlates with the greater interfacial strength observed in SP-trans samples (Figure 5.5).
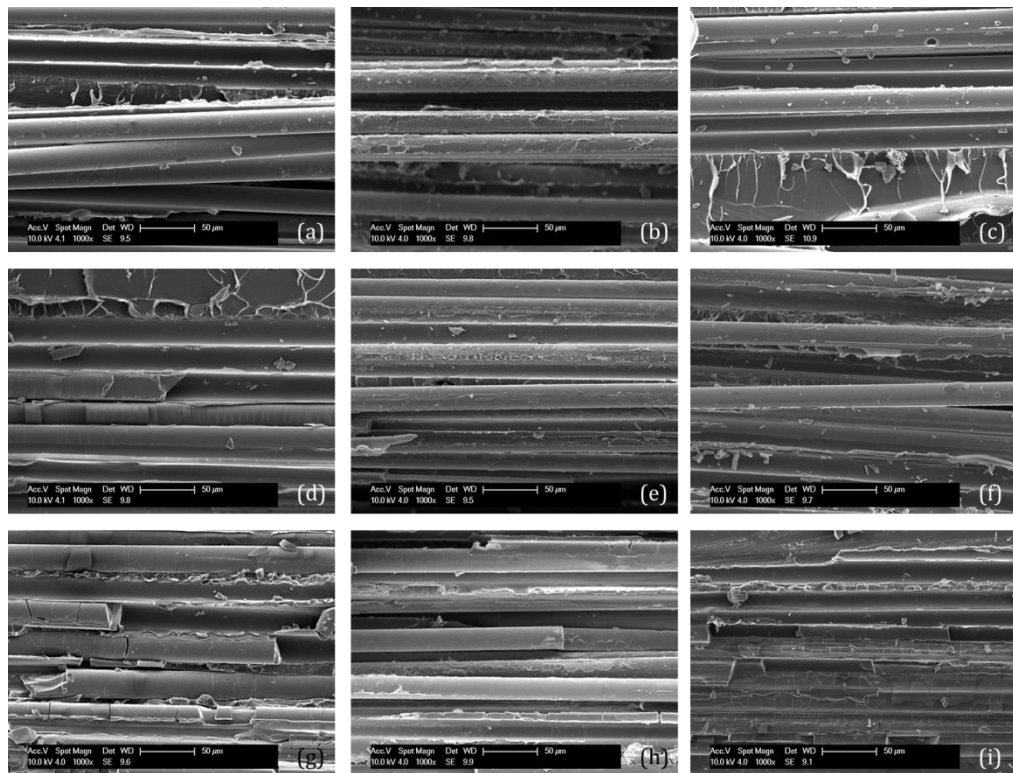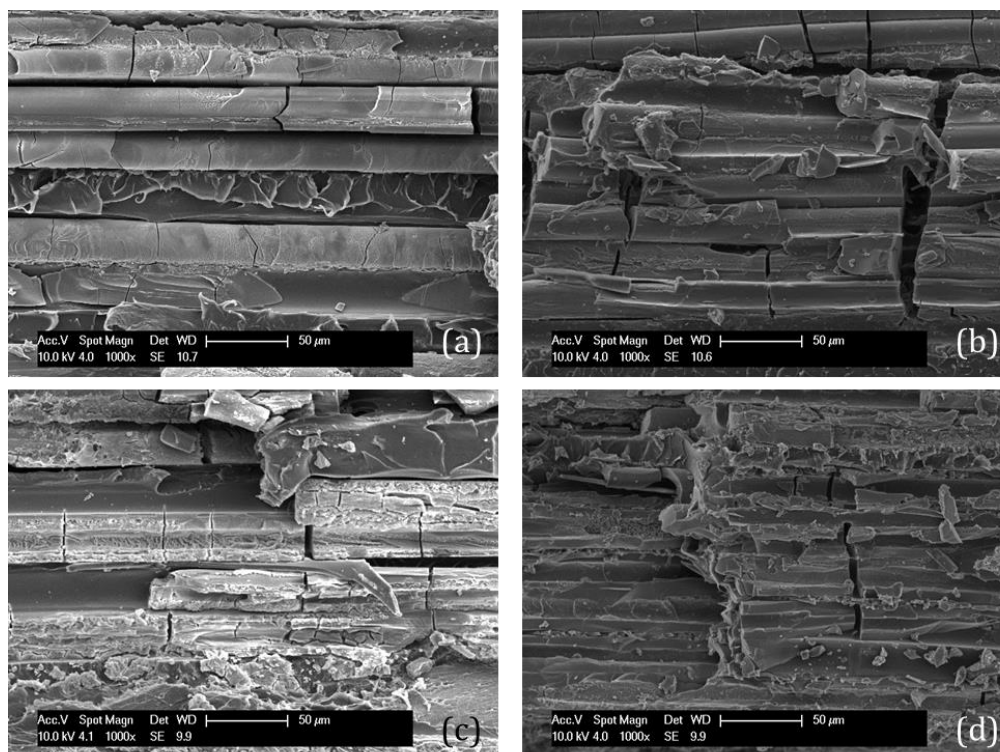


***Figure 5.22:*** *SEM micrographs of a fractured surface of (a) C-trans after 21 days of degradation in PBS at 37°C, (b) DC-trans after 21 days of degradation in PBS at 37°C, (c) C-trans after 28 days of degradation in PBS at 37°C, (d) DC-trans after 28 days of degradation in PBS at 37°C.*

The break down in fibre morphology can be seen for DC-trans samples at days 21 and 28 (Figure 5.22 (b) and (d)) and explains the similarity in flexural strength and modulus between C-trans and DC-trans during the final week of the study. The increased water uptake and mass loss further corroborate the fracture morphology observed in Figure 5.22. It is clear that at this stage, as in the respective longitudinal samples, the dissolution of fibres and corresponding decrease in strength is the main cause for failure over interfacial debonding or matrix failure [31].

It is clear that the S-PLA coating improved interfacial properties and flexural properties up to a certain time point (14 days). Sealing the exposed fibre ends in PGF composite samples from moisture would aide in prolonging the effect of S-PLA coating observed in this study. High strength fibres have been known to lead to fibre reinforced composites with matrix dominated failure [23-24]. Coating higher strength PGF fibres such as those (e.g. P45B5Fe3) studied by Sharmin with S-PLA should be investigated to observe improvements, if any, in interfacial strength. Coating UD mats with longer chain S-PLA is also worth investigating (e.g. S-PLA_l in Chapter 4) as both a binding agent and coupling agent.

## 5.4 CONCLUSIONS

Mechanical and degradation properties were investigated for control and S-PLA coated UD PGF reinforced PLA composites with fibre volume fraction of ~20%. The S-PLA was applied to the UD fibre mats in two different ways: dip coating (DC) and spray coating (SP). DC fibre mats did not negatively affect the fibre alignment during coating or composite production. Composites were investigated with fibres oriented longitudinally and transversely. Initial longitudinal flexural strengths and moduli for S-PLA coated composites were significantly greater than that for control. The initial transverse flexural strengths of the S-PLA coated composites were increased compared to that of control composites. Though insignificant, the increase indicated that the interfacial strengths had improved as well. The coating did not significantly affect the transverse flexural moduli.

The longitudinal properties of all the composite samples decreased significantly during the first week of immersion. DC-long composites had a

higher retention than C-long and SP-long samples. The flexural strength of SP-long composites decreased to that of PLA during the first week. The flexural properties of C-long and DC-long were greater than that of PLA until the end of the study (day 28). The flexural strength and modulus of transverse composites all decreased significantly however SP-trans composites had better retention during the first week. This meant that SP-trans samples had better interfacial strength than the other composites. It was suggested that this was due to the even coating of the coupling agent compared to the uneven one obtained via the DC method.

The water uptake and percentage change in mass remained stable after the initial increase until approximately 2 weeks into the study. A significant increase in water uptake and mass loss was observed for the composites in the last two weeks of the study. This increase coupled with SEM micrographs from these time points confirms that the increase was due the porous morphology created by fibre dissolution. The crystallinity of PLA remained unchanged however all the composite samples had a crystallinity peak at ~16.5°. This was attributed to the formation of a crystalline phase during composite manufacture. The intensity of the crystalline peaks did not change throughout the study indicating that the crystalline phase did not change over the 28 day study. The density analysis confirmed that the crystalline phase did not change in any significant manner.

It was concluded that the S-PLA coated composites managed to retain the mechanical properties and retard degradation for approximately 2 weeks. Overall the coating method did not significantly affect the mechanical properties of the composites. However, the degradation study suggests that SP coating

method may yield a better resistance to moisture. It was suggested that this was, again, due to the even coating compared to the DC coating method.

## 5.5 REFERENCES

1.  I. Ahmed, I.A. Jones, A.J. Parsons, J. Bernard, J. Farmer, C.A. Scotchford, G.S. Walker, and C.D. Rudd, "Composites for bone repair: phosphate glass fibre reinforced PLA with varying fibre architecture", *Journal of Materials Science. Materials in Medicine*, vol. 22, no. 8, pp. 1825-1834, 2011.

2.  R. M. Felfel, I. Ahmed, A. J. Parsons, P. Haque, G. S. Walker, and C. D. Rudd, "Investigation of Crystallinity, Molecular Weight Change, and Mechanical Properties of PLA/PBG Bioresorbable Composites as Bone Fracture Fixation Plates", *Journal of Biomaterials Applications*, vol. 25, no. 7, pp. 756-789, 2012.

3.  N. Han, "Manufacture and Characterisation of Bioresorbable Fibre Reinforced Composite Bone Plates", University of Nottingham, 2013.

4.  J.M.M. de Kok and H.E.H. Meijer, "Deformation, yield and fracture of unidirectional composites in transverse loading 1. Influence of fibre volume fraction and test-temperature", *Composites Part A: Applied Science and Manufacturing*, vol. 30, no. 7, pp. 905-916, 1999.

5.  I. Ahmed, P.S. Cronin, E. Abou Neel, A. J. Parsons, J.C. Knowles, and C.D. Rudd, "Retention of mechanical properties and cytocompatibility of a phosphate-based glass fibre/polylactic acid composite," *Journal of Biomedical Materials Research Part B: Applied biomaterials*, vol. 89, no. 1, pp. 18-27, 2009.

6.  P. Haque, A.J. Parsons, I.A. Barker, I. Ahmed, D.J. Irvine, G.S. Walker and C.D. Rudd, "Interfacial properties of phosphate glass fibres/PLA composites: Effect of the end functionalities of oligomeric PLA coupling agents", *Composites Science and Technology*, vol. 70, no. 13, pp. 1854-1860, 2010.

7. M.S. Hasan, I. Ahmed, A.J. Parsons, G.S. Walker and C.A. Scotchford, "The influence of coupling agents on mechanical property retention and long-term cytocompatibility of phosphate glass fibre reinforced PLA composites", *Journal of the Mechanical Behaviour of Biomedical Materials*, vol. 28, pp. 1-14, 2013.

8. M.C. Zimmerman, H. Alexander, J.R. Parsons and P.K. Bajpai. "The design and analysis of laminated degradable composite bone plates for fracture fixation", In: T.L. Vigo, A.F. Turbak, editors. High tech fibrous materials. Washington: ACS Publications, 1991, pp. 132-148.

9. A.J. Parsons, M.I.K. Niazi, R.R. Habeb, B. Fitzpatrick, G.S. Walker, I.A. Jones and C.D. Rudd, "Mechanical and degradation properties of phosphate based glass fibre/ PLA composites with different fibre treatment regimes", *Science and Engineering of Composite Materials*, vol. 17, no. 4, pp. 243-260, 2010.

10. M.S. Hasan, "Phosphate Glass Fibre Reinforced Composite for Bone Repair Applications: Investigation of Interfacial Integrity Improvements via Chemical Treatments", University of Nottingham, 2012.

11. L.T. Drzal and M. Madhukar, "Fibre-matrix adhesion and its relationship to composite mechanical properties", *Journal of Materials Science*, vol. 28, no. 3, pp. 569-610, 1993.

12. L. T. Drzal, P.J. Herrera-Franco and H. Ho, "Fibre-matrix interface tests", *Comprehensive Composite Materials: Test Methods, Nondestructive Evaluation and Smart Material*,, vol. 5, 2000, pp.71-111.

13. P.J. Herrera-Franco and A. Valadez-Gonzalez, "Mechanical properties of continuous natural fibre-reinforced polymer composites", *Composites Part A: Applied Science and Manufacturing*, vol. 35, no. 3, pp. 339-345, 2004.

14. P. Haque, "Oligomeric PLA coupling agents for phosphate glass/PLA composites", University of Nottingham, 2011.

15. D. Hull and T.W. Clyne, *An Introduction to Composite Materials*, Cambridge University Press: Cambridge, U.K., 1996, Chapter 4, pp. 60-69

16. N. Sharmin, "Preparation and Characterisation of Phosphate Based Glasses, Fibres and Composites: Effect of Boron and Iron Oxide Additions", University of Nottingham, 2014.

17. N. Han, I. Ahmed, A.J. Parsons, L. Harper, C.A. Scotchford, B.E. Scammell and C.D. Rudd, "Influence of screw holes and gamma sterilization on properties of phosphate glass fibre-reinforced composite bone plates", *Journal of Biomaterials Applications*, vol. 27, no. 8, pp. 990-1002, 2011.

18. N. Sharmin, "Preparation and Characterisation of Phosphate Based Glasses, Fibres and Composites: Effect of Boron and Iron Oxide Additions", University of Nottingham, 2014.

19. N. Sharmin, A.J. Parsons, C.D. Rudd and I. Ahmed, "Effect of boron oxide addition on fibre drawing, mechanical properties and dissolution behavior of phosphate-based glass fibres with fixed 40, 45 and 50 mol% $P_2O_5$", *Journal of Biomaterials Applications*, vol. 29, no. 5, pp. 639-653, 2014.

20. I. Ahmed, A.J. Parsons, G. Palmer, J.C. Knowles, G.S. Walker and C.D. Rudd, "Weight loss, ion release and initial mechanical properties of a binary calcium phosphate glass fibre/ PCL composite", *Acta Biomaterialia*, vol. 4, no. 5, pp. 1307-1314, 2008.

21. A.J. Parsons, I. Ahmed, P. Haque, B. Fitzpatrick M.I.K. Niazi, G.S. Walker and C.D. Rudd, "Phosphate glass fibre composites for bone repair", *Journal of Bionic Engineering*, vol. 6, no. 4, pp. 318-323, 2009.

22. I. Ahmed, C.A. Collins, M.P. Lewis, I. Olsen and J.C. Knowles, "Processing, characterisation and biocompatibility of iron-phosphate glass fibres for tissue engineering", *Biomaterials*, vol. 25, no. 16, pp. 3223-3232, 2004.

23. J.M.M. de KoK, "The influence of the interface on the transverse properties of carbon fibre reinforced composites", Eindhoven: Instituut Vervolgopleidingen, Technische Universiteit Eindhoven – III, 1992.

24. J.M.M. de Kok and T. Peijs, "Deformation, yield and fracture of unidirectional composites in transverse loading 2. Influence of fibre-matrix adhesion", *Composites Part A: Applied Science and Manufacturing*, vol. 30, no. 7, pp. 917-932, 1999.

25. T. Norita, I, Matsui and H.S. Matsuda, "Effect of surface treatment of carbon fibre on mechanical properties of CFRP", In: *Composite Interfaces*, Proceedings ICCI-1, Amsterdam: Elsevier, 1986, pp. 123-132.

26. T. Peijs, H.A. Rijsdijk and J.M.M. de Kok, "The role of the interface and fibre anisotropy on controlling the performance of polyethylene fibre reinforced composites", *Composites Science and Technology*, vol. 52, no. 3, pp. 449-466, 1998.

27. L. Onal, S, Cozien-Cazuc, I.A. Jones and C.D. Rudd, "Water absorption properties of phosphate glass fiber-reinforced poly-ε-caprolactone composites for craniofacial bone repair", *Journal of Applied Polymer Science*, vol. 107, no. 6, pp. 3750-3755, 2008.

28. M.A. Slivka and C.C. Chu, "Fibre-matrix interface studies on bioabsorbable composite materials for internal fixation of bone fractures. II. A new method using laser scanning confocal microscopy", *Journal of Biomedical Materials Research*, vol. 37, no. 3, pp. 353-362, 1997.

29. L.V. Lassila, T. Nohrstrom and P.K. Vallitu, "The influence of short term water storage on the flexural properties of unidirectional glass-fibre composites", *Biomaterials*, vol. 23, no. 10, pp. 2221-2229, 2002.

30. Y.Z. Wan, Y.L. Wang, X.H. Xu and Q.Y. Li, "*In vitro* degradation behavior of carbon fibre-reinforced PLA composites and influence of interfacial

adhesion strength", *Journal of Applied Polymer Science Symposium*, vol. 82, no. 1, pp. 150-158, 2001.

31. H. Sekine, K. Shimomura and N. Hamana, "Strength, deterioration and degradation mechanism of glass chopped reinforced plastics in water environment", *JSME International Journal Series 1 – Solid Mechanics Strength of Materials*, vol. 31, no. 3, pp. 619-626, 1988.

32. J.-K. Kim and J.-W. Mai ed., *Engineered interfaces in fibre reinforced composites*, Elsevier, 1998, Chapter 5, pp. 171-237.

33. E.A. Abou Neel, I. Ahmed, J.J. Blaker, A. Bismarck, A.R. Boccaccini, M.P. Lewis, S.N. Nazhat and J.C. Knowles, "Effect of iron on the surface, degradation and ion release properties of phosphate-based glass fibres", *Acta Biomaterlia*, vol. 1, no. 5, pp. 553-563, 2005.

34. L. Shen, H. Yang, J. Ying, F. Qiao and M. Peng, "Preparation and mechanical properties of carbon fiber-reinforced hydroxyapatite/polylactide biocomposites", *Journal of Materials Science: Materials in Medicine*, vol. 20, no. 11, pp. 2259-2265, 2009.

35. S. Iannace, A. Maffezzoli, G. Leo and L. Nicolais, "Influence of crystal and amorphous phase morphology on hydrolytic degradation of PLLA subjected to different processing conditions", *Polymer*, vol. 42, no. 8, pp.3799-3807, 2001.

36. F.J. Buchanan, ed., *Degradation Rate of Bioresorbable Materials Predictions and Evaluation*, ed. C. Press, Woodhead Cambridge, 2008, pp. 320.

37. Z. Zhou, Q. Yi, L. Liu, X. Liu and Q. Liu, "Influence of degradation of Poly-L-lactide on mass loss, mechanical properties and crystallinity in phosphate-buffered solution", *Journal of Macromolecular Science Part B: Physics*, vol. 48, no. 2, pp. 309-317, 2009.

38. R. Zhang and P.X. Ma, "Synthetic nano-fibrillar extracellular matrices with predesigned macroporous architectures", *Journal of Biomedical Materials Research*, vol. 52, no. 2, pp. 430-438, 2000.

39. S. Kajorncheappunngam, R.K. Gupta and H.V.S. Ganga Rao, "Effect of ageing environment on degradation of glass-reinforced epoxy", *Journal of Composites for Construction*, vol. 6, no. 1, pp. 61-69, 2002.

40. K. Liao, C.R. Schultheisz and D.L. Hunston, "Effects of environmental ageing on the properties of pultruded GFRP", *Composites Part B: Engineering*, vol. 30, no. 5, pp. 485-493, 1999.

# CHAPTER 6

# CONCLUSIONS AND FUTURE WORK

## 6.1 CONCLUSIONS

The purpose of this work was to investigate the effect of chain length on the effectiveness of sorbitol-initiated PLA oligomers used to improve the interfacial properties of PGF/PLA composites. Sorbitol-initiated PLA was synthesised to three different chain lengths (S-PLA_s, S-PLA_m and S-PLA_l where s is short, m is medium and l is long). These three coupling agents were then characterised using NMR, GPC, DSC and FTIR in order to confirm conversion, molecular weight and polydispersity, glass transition temperature ($T_g$) and presence of sorbitol on the oligomer chain end. It was found that:

- conversion > 90 % had been reached for all three oligomers

- using poly (methyl methacrylate) (PMMA) standards provided $M_n$ values of 1221, 4972, 25974 for S-PLA_s, S-PLA_m and S-PLA_l, respectively

- PMMA standards were used instead of polystyrene (PS) standards as the chemical structure of PMMA is similar to that of PLA and therefore would give a more accurate $M_n$ value

- $T_g$ increased as the molecular weight of the oligomer increased confirming that the two were related as stated in the theory set out by Flory-Fox and that the $T_g$ can be predicted if the molecular weight of the oligomer is known

- Free hydroxyl groups (OH) are present in S-PLA samples at ~3500 cm$^{-1}$ indicating that sorbitol is in the PLA chain

In work conducted prior to this, it was assumed that the S-PLA oligomer had a single sorbitol chain end. It is now assumed that PLA chains are initiated from

both of the two primary OH groups in sorbitol, causing the sorbitol to lie in the middle of the coupling agent with PLA chains either side. The polydispersity index (PDI) > 1.5 observed for S-PLA_m and S-PLA_l is an indication of this proposed chemical structure.

$40P_2O_5$-$16CaO$-$16Na_2O$-$24MgO$-$4Fe_2O_3$ (P40) fibres were used to conduct an analysis of IFSS on control (uncoated) and S-PLA coated single fibres embedded in a PLA matrix. The coating concentrations used to coat the fibres were dependent on the molecular weight of each coupling agent.

- A low coating concentration had to be used for S-PLA_l as increasing the concentration led to polymer-polymer interactions occurring between the fibres making them difficult to separate.

- The optimum concentration for S-PLA_s was 0.0064 moles with an IFSS value of 24 ± 5 MPa compared to the control IFSS of 12 ± 2 MPa. The IFSS values of S-PLA_s, S-PLA_m and S-PLA_l coated fibres all increased significantly when compared to that of control fibres. It is also likely that the IFSS is limited by the matrix properties.

- Degradation of single fibre composites (SFCs) embedded with S-PLA_s, S-PLA_m and S-PLA_l coated fibres in phosphate buffered saline (PBS) at 37 °C showed that the IFSS increased by 50-60 % IFSS after 7 days compared to the control when calculated with uncorrected Weibull parameters.

- The calculated IFSS of S-PLA_s, S-PLA_m and S-PLA_l coated fibres embedded in PLA using corrected Weibull parameters decreased by 63 %, 67 % and 48 %, respectively, after 7 days compared to the IFSS of control. The decrease in IFSS can be attributed to the loss of interface due

to insufficient bonding and/or due to hydrolysis of the chemical bond between fibre and matrix.

It is difficult to estimate the strength of the fibre embedded in a matrix during degradation and therefore difficult to determine the exact effect of the coupling agents on the IFSS of degraded SFCs. A degradation study of full body composites was required to observe if S-PLA helped to retain the mechanical properties and improve the interfacial properties.

In order to decrease composite production time, cost and material waste, $45P_2O_5$-$16CaO$-$11Na_2O$-$24MgO$-$4Fe_2O_3$ (P45) fibres were used to create unidirectional (UD) fibre mats. The IFSS of embedded control and S-PLA_s coated P45 fibres was compared with that of P40 fibres and it was found that they were statistically similar ($p > 0.05$). This meant that P45 fibres were a suitable substitution for P40 fibres in the manufacture of full body composites. S-PLA_s was selected as it was easier to handle and manufacture.

Control and S-PLA_s coated UD P45 fibre reinforced composites were manufactured with a fibre volume fraction of $\sim$20%. The S-PLA was applied to the UD fibre mats in two different ways: dip coating (DC) and spray coating (SP). Neither coating method negatively affected the fibre alignment during coating or composite production. Composites were prepared with fibres oriented longitudinally (long) and transversely (trans), and mechanical and degradation properties were investigated. Initial longitudinal flexural properties of S-PLA coated composites (DC: 248 ± 16 MPa and 14 ± 1.3 GPa; SP: 212 ± 9 MPa 16 ± 0.4 MPa) were significantly greater than those for control composites (158 ± 23 MPa and 9 ± 1.3 GPa). Initial transverse flexural strengths for S-PLA coated composites also increased though not significantly. The increase did indicate that

the interfacial strengths of the composites had improved. The coating did not significantly affect the transverse flexural moduli.

The longitudinal properties of all of the composites decreased significantly during the first week however DC-long composites had the higher retention. The flexural strength of SP-long composites decreased to that of PLA during the first week. The flexural strength and modulus of transverse composites all decreased significantly however SP-trans composites had better retention during the first week. This meant that SP-trans samples had better interfacial strength than the other composites. It was suggested that this was due to the even coating of the coupling agent compared to the uneven one obtained via the DC method.

The degradation study showed that after the initial increase, water uptake and wet mass change remained stable for 10-14 days. A significant increase in water uptake and wet mass change was observed after this through to the end of the study. This was observed for all composite samples. The increase in water uptake and wet mass together with the corresponding SEM micrographs confirmed that this could be attributed to a porous morphology created by fibre dissolution. DC and SP composites showed better resistance to moisture and retention of mechanical properties than control samples leading to the conclusion that the coupling agent was retarding degradation. The degradation study showed that SP composites had a slightly better resistance to moisture than DC composites. This was attributed, again, to the even coating of the coupling agent compared to the DC method.  SEM micrographs showed that loss of mechanical properties could be attributed to fibre dissolution and not loss of interface in S-PLA coated UD composites.

## 6.2 FUTURE WORK

Based on the conclusions of this project, the following suggestions have been made for future work in the study of the interface of PGF/PLA composites:

- IFSS analysis of other PGF formulations coated with and without S-PLA and conduct an optimisation test to find optimal coating concentration

- Finite Element Analysis of single fibre composites with and without S-PLA coating

- Increase the fibre volume fraction for S-PLA_s coated UD composites to increase the transverse properties and use the in-plane shear stress method along with other off-axis mechanical tests to assess the improvements in macroscopic interfacial properties

- Vary the coating concentration of S-PLA_s, S-PLA_m and S-PLA_l for UD fibre mats, manufacture composites and test the off-axis properties to find the optimum concentration that will yield the maximum transverse strength for interfacial debonding

- Manufacture and assess the mechanical properties of S-PLA coated random mat composites, varying fibre volume fraction, chain length and coating concentration

- Compare the fibre impregnation, mechanical property retention and interfacial properties of composites manufactured via compression moulding, extrusion and *in situ* polymerisation

- Prepare composite samples with fibre ends embedded completely in the matrix to reduce the effect of wicking, retain mechanical properties and maintain the interface